Quaternary of Egypt

12

Mohamed A. Hamdan and Fekri A. Hassan

Contents

Abstract

More than 100 years of continuing research into the Quaternary of Egypt has produced numerous publications. In the last twenty years, Quaternary studies have witnessed great advances in both theories and methodologies, and the pace of archaeological research has accelerated as a new generation of researchers joined in expounding the different dimensions of the Quaternary period of Egypt. We aim in this contribution to provide an up-to-date synthesis of recent research on high-resolution and well-dated paleo-environmental archives of proxy data to understand the emerging picture of the impact of climate change on sediments, paleoenvironments and landscapes in Egypt as a whole.

M. A. Hamdan (✉)
Geology Department, Cairo University, Giza, Egypt
e-mail: hamdanmohamed@hotmail.com

F. A. Hassan
Cultural Heritage Program, French University, Cairo, Egypt

12.1 Introduction

The Quaternary is youngest in a four-cycle division of earth history proposed by G. Arduino in 1759 (Arduino 1760). The term "Quaternary" first used by Raboul (1833), has continued to the present day. Until now, the official status of the Quaternary was that of period/system with a base at 1.8 Ma. The lower boundary of the Quaternary period (i.e. Pliocene-Pleistocene boundary) is varies between 2.5 Ma, based on studies of continental glacial deposits and 1.8 Ma

Z. Hamimi et al. (eds.), *The Geology of Egypt*, Regional Geology Reviews,
https://doi.org/10.1007/978-3-030-15265-9_12

on basis of oceanic oxygen isotope records. The latter age (i.e. 1.8 Ma) is most accepted by Quaternary scientists. The Quaternary Period, originally referred to as the "Ice Age", is now characterized as the geological interval during which the climate of the Earth witnessed spectacular alternations of cold and warm phases, which in Africa corresponded to the interpluvial and pluvial periods, respectively.

More recently, the Anthropocene is a proposed epoch dating from the beginning of significant human impact on the Earth's geology and ecosystems (Waters et al. 2016). As of August 2016, neither the International Commission on Stratigraphy nor the International Union of Geological Sciences has yet officially approved the term as a recognized subdivision of geological time, although the Anthropocene Working Group (AWG) of the Subcommission on Quaternary Stratigraphy (SQS) of the International Commission on Stratigraphy (ICS), voted to proceed towards a formal golden spike (GSSP) proposal to define the Anthropocene epoch in the Geologic Time Scale and presented the recommendation to the International Geological Congress on 29 August 2016. Various different start dates for the Anthropocene have been proposed, ranging from the beginning of the Agricultural Revolution 12–15 kyr BP, to recent.

The most important phenomenon, from a cultural perspective, in the Quaternary is the appearance of humans and from both ecological and anthropological perspectivesit is a period of frequent and often intense climatic fluctuations. Different proxies have therefore been deployed to reconstruct paleoclimatic conditions, paleoenvironmental changes, palaeosols, cultural geography and human evolutionary trajectories. The study of the Quaternary is therefore multidisciplinary par excellence and requires integration of data from different disciplines. One of the most productive developments in the Quaternary studies was the rise of geoarchaeology bringing geology closer to human affairs in the past with its implications for the present and future, especially in the domain of climate change on contemporary societies (see Gladfelter 1977; Hassan 1979a; Rapp and Hill 2006).

Study of Quaternary deposits in Egypt passed through several stages since the beginning of the Twentieth Century (named the foundation, collaboration and integration stages). The foundation stage (first half of the Twentieth Century) includes the seminal work of Blankenhorn (1900) on the Nile Valley; Caton-Thompson and Gardner (1934) in Faiyum and Kharga; Sandford and Arkell (e.g. 1929, 1939) on the Nile-Faiyum divide, Upper Egypt and Red Sea Coast (Sandford 1934) and the work of Ball (1927) and Beadnell (1909) in the Faiyum and Kharga, respectively.

Renewed investigations of the Quaternary in Egypt accompanied the archaeological salvage, exploration and research triggered by the Nubian Salvage campaign. Numerous archaeological expeditions included geologists and geographers. Karl Butzer, who continued to make significant contributions to the Quaternary geology and geography of Egypt, and became one of the leading authorities on ecological study of the Quaternary of Egypt. Butzer (1964, 1982), studied the Pleistocene and Holocene geology of the Nile Valley from Sudanese border to Kom Ombo plain (Butzer and Hansen 1968). De Heinzelin (1968) examined the Quaternary sediment in Sudanese Nile Valley, while that of the prehistory and Holocene geology of Lower Nubia were examined by Combined Prehistroic Expedition led by Fred Wendorf. The Combined Prehistoric Expedition was by far the most dedicated to the continuation of prehistoric and geoarchaeological studies in Egypt after the building of the Aswan High Dam. They began their investigations immediately after the completion of work in Nubia on the prehistory and geoarchaeology of Esna, Dandara, and Dishna sectors of Upper Egypt (Wendorf and Schild 1976). During these investigations, they closely collaborated with Egyptian geologists of the caliber of Rushdi Said and Bahay Issawi then associated with the Geological Survey of Egypt. As such they engaged numerous young Egyptian geologists from the Geological Survey in their geological investigations. Fekri Hassan, at the time a teaching assistant in the Department of Geology at Ain Shams University, joined the Prehistoric Combined Expedition in the archaeological and geological survey of the area between Dandara and Sohag. Combining his academic training both as a geologist and an archaeologist, he obtained his Ph.D. with Fred Wendorf at Southern Methodist University, USA. He led numerous expeditions as a Principal Investigators in Siwa, Bahariya, Naqada, East Delta and undertook geoarchaeological work in the Faiyum, Farafra and other sites during the next stage of Quaternary studies in Egypt, beginning in the 1980s. Over the long years of working first along the Nile and later in the Eastern Sahara, significant contributions to the Quaternary geology of Egypt were made by Vance Haynes as a collaborator with the Prehistoric Combined Expedition (Wendorf and Schild 1976) and with fellow geologists and geochronology specialists.

The integration stage is characterized by the application of chronometry to archaeological sites and sediments. Detailed paleoenvironmental studies using paleontological (pollen, ostracods, diatoms…etc.) and geochemical (trace metals, rare earth elements and stable isotope) proxies and associated detailed investigations of archaeological and bioarcheological materials (lithic artifacts, pottery, and charcoal) were made. Integration of dating technologies (^{14}C, OSL, TL and recently ESR) with paleoenvironmental proxies draw a clearer picture of paleoclimatic variation during the Quaternary that correlate well with the global climatic framework. Finally, the integration stage is

represented by the work of Wendorf and Schild in Nabta playa, Bir Tarfawi and in Wadi Kubbaniya (Wendorf and Schild 1986, 1989) and by Daniel Stanley and his coworkers (Stanley 1988; 1990) by their intensive coring programs in the Nile Delta. It also includes work by Fekri Hassan and his coworkers in the Nile Valley, Farafra and the Faiyum (Hassan 1986, 2007a, b, 2010; Hassan et al. 2001, 2012, 2017; Flower et al. 2012, 2013; Hamdan et al. 2016a; 2019). Hassan also initiated a research trend modeling the link between climate change and origins of agriculture in Egypt (Hassan 1986) and the relationships between Nile floods and the course of Egyptian civilization (e.g. Hassan 1997). This work extended research into the relevance of geoarchaeology to contemporary social affairs including the impact of climate change on food security and droughts in Africa. During this period, Rudolf Kuper and his coworkers began their survey of the Eastern Sahara from Siwa to Gilf Kebir (e.g. Kuper and Kröpelein 2006). At this time research in the Egyptian Sahara included studies of Kharga and Dakhla Oases (Smith et al. 2004).

12.2 Nile Sediments in the Nile Valley, Nile Delta and Faiyum

The Main Nile in Egypt is the northern extension of the course of the Nile starting in the Sudan as a result of the confluence of the Ethiopian tributaries, mainly the Blue Nile, and the White Nile draining a large area in Equatorial Africa (Fig. 12.1a). The river basin spans 35° of latitude (4° S to 31° N) encompassing a wide variety of climates, river regimes, biomes and terrains from the Equatorial lakes plateau of the White Nile headwaters to the delta complex in the Eastern Mediterranean Sea. It is unique among the large rivers of the world in that it flows for ca. 2700 km through the Sahara Desert without any significant perennial tributary inputs. Of all the world's rivers with catchments greater than 1 million km^2, the Nile has the lowest specific discharge, 0.98 L s^{-1} km^2 at Aswan (Shahin 1985). Geologic evolution of River Nile during Quaternary is controlled by major tectonic phenomena-including the rifting of East Africa—climatic changes and other factors (Said 1981, 1993; Butzer 1997; Woodward et al. 2007). According to Said (1981), the Nile Basin includes five major regions that differ from one another in structure and geological history (Fig. 12.1b). These are: (1) The Equatorial lake plateau, (2) The Sudd region and central Sudan with low gradient floodplains and extensive swamplands, (3) The Ethiopian Highlands forming the headwaters of the Blue Nile and the Atbara, (4) The great bends and cataracts of the desert Nile and (5) The Egyptian region including the low gradient delta complex.

12.2.1 The Nile Valley

12.2.1.1 Nile Early Origins (Pre-quaternary)

There is a substantial literature debating the geological history of the River Nile, based on different geological and geomorphological proxies (Macgregor 2012). There are two main theories about the early origin of the Nile River in Egypt: the Egyptian ancestor Nile and the African ancestor Nile.

The Egyptian ancestor Nile theory (Butzer and Hansen 1968; De Heinzelin 1968; Wendorf and Schild 1976; Said 1981; Issawi and McCauley 1993) proposes that the early ancestors of River Nile were Egyptian Rivers that drained from Egyptian territories. Evidence of this theory includes landform, radar and mineralogical data indicating a diminishing contribution from Ethiopian volcanic sources with increased age. The second theory, the African ancestor Nile (McDougall et al. 1975; Pik et al. 2003; Ebinger 2005; Underwood et al. 2013, Fielding et al. 2017, 2018) indicates that the Egyptian Nile was fed by waters originating from the Blue Nile and other Ethiopian tributaries during the Oligocene onward. Abdelkareem et al. (2012) proposed that the Nile formed during subsequent stages and lengthened as Africa drifted northward relative to the Earth's equator; i.e. it is probable that during the late Eocene or Oligocene, the Earth's Equator was located at the present-day latitudes of Chad and Sudan. That paleogeographic position of the Equator would have produced pluvial conditions throughout North Africa. They also suggest an easterly river course in Egypt during the Oligo-Miocene along the Qena Valley but others favored a more westerly course. Evidence presented by the second theory includes the large sediment volumes in the Nile which are proposed to be inconsistent with a purely Egyptian hinterland. More recently, Fielding et al. (2018) demonstrated the presence of Ethiopian Cenozoic Continental Flood Basalt (CFB) detritus in the Nile delta beginning ca. 31 Ma. They show that the Nile River was established as a river of continental proportions by Oligocene times with there was no significant input from Archaean cratons, supplied directly via the White Nile to the Nile Delta. Whilst there are subtle differences between the Nile delta samples from the Oligocene and Pliocene compared to those from the Miocene and Pleistocene, the overall stability of the Ethiopian signal throughout the delta record and its similarity to the modern Nile signature, indicates no major change in the Nile's drainage from Oligocene to the present day (Fielding et al. 2017, 2018).

The Egyptian ancestor Nile theory comprises two hypotheses: a single-master-stream and a multi master stream hypotheses. The former is based on the study of drill cores in the Nile Valley and the delta, which suggest that the Nile Valley started as a single-master-stream initiated since the late Miocene (Said 1981). This hypothesis does not take

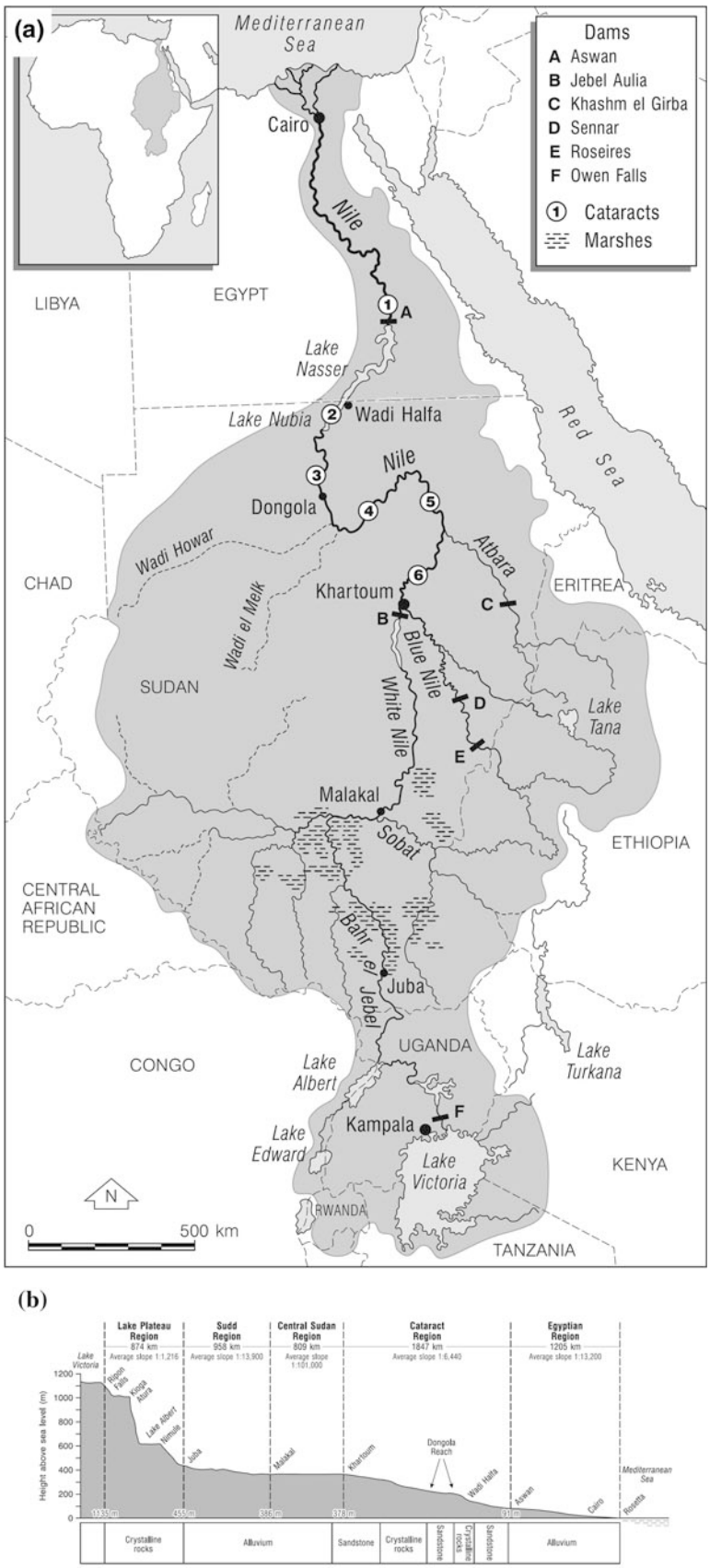

Fig. 12.1 **a** Map of the Nile Basin showing the drainage network, basin states, and major dams (*Source* Woodward et al. 2007). **b** Long profile of the Nile from the White Nile headwaters to the Mediterranean Sea (*Source* Said 1993)

into account any fluvial activity during the widespread northward regression of the Tethys Sea over Egypt (late Eocene-Oligocene). Five successive units of fluvial sediments were distinguished (Said 1993). Each one of these units has characteristic features referring to deposition by different rivers. These are from oldest to youngest: Eonile, Paleonile, Protonile, Prenile and Neonile. The last three river systems are dated to the Quaternary and are discussed in detail in following sections.

The second hypothesis is based on extensive field geological and geoarchaeological proxies as well as remote sensing technology (e.g. Issawi and McCauley 1993; Issawi and Osman 2008; Abotalib and Mohamed 2013). It attempts to avoid the major problems caused by the single-master-stream concept and described the evolution of river systems in Egypt from the late Eocene regression of the Tethys Sea to the Recent (Fig. 12.2). During the Cenozoic, Egypt was drained not only by a single master stream, but by several major drainage systems (Issawi and McCauley 1993). The first stage, called the Gilf system (ca. 40 to 24 million years), consisted of a northward flowing consequent stream river that followed aretreating Tethys Sea, creating newly emergent land in Egypt (Fig. 12.2a). It also includes streams that formed on the flanks of the Red Sea region towards the end of the Eocene.

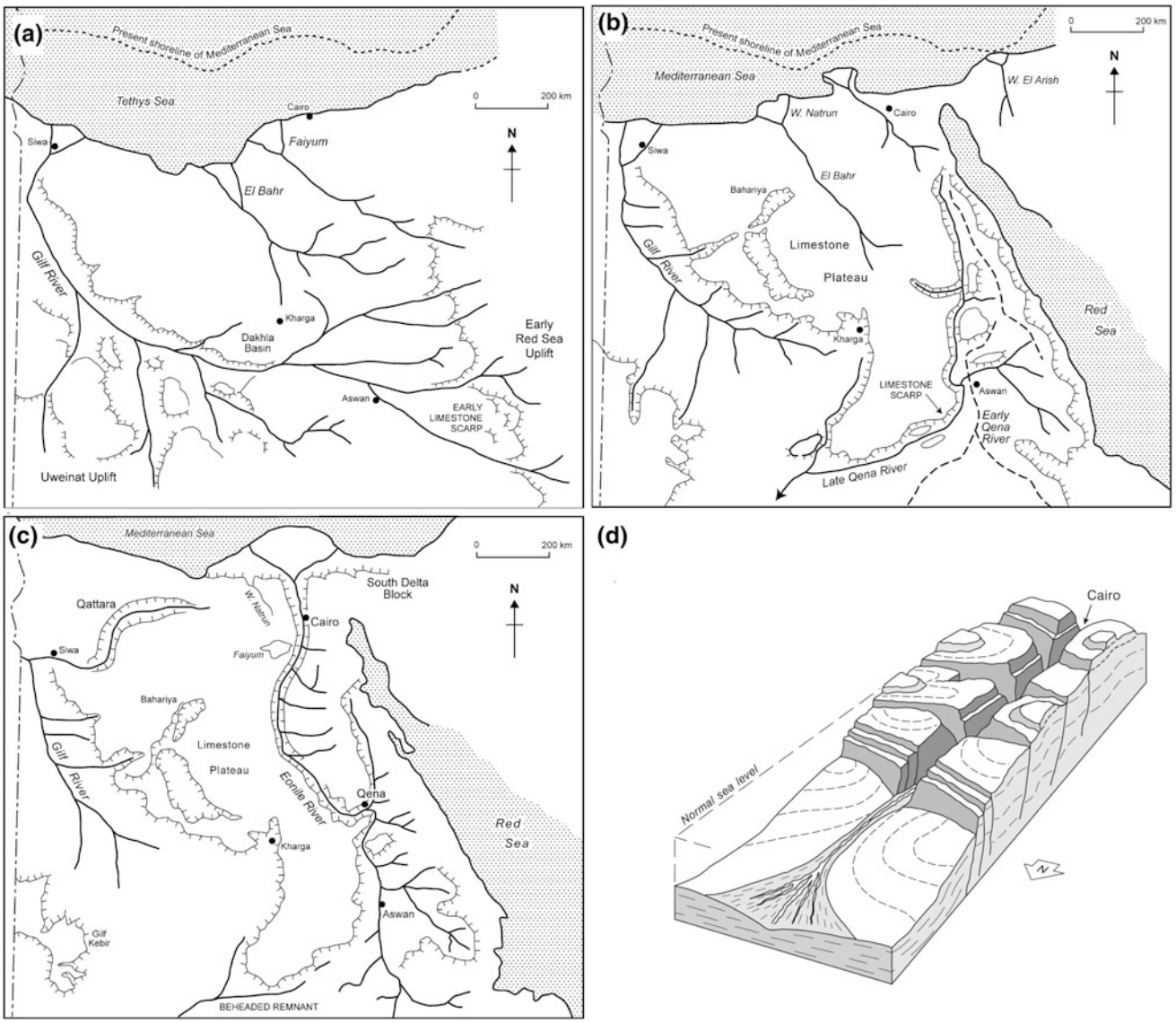

Fig. 12.2 **a** Sketch showing the Gilf system (System I) at the approximate end of the Oligocene; **b** Sketch showing the Qena system (System II) in approximately the middle Miocene; **c** Sketch showing the Nile system (System III), which resulted from a major drop in Mediterranean sea level in the Messinian (about 6 Ma) (*Source* Goudie 2005, modified from Issawi and McCauley 1992). **d** Schematic reconstruction of the Nile Canyon showing the main channel and tributary gorges cut by the Egyptian Nile drainage during the late Miocene (Messinian) salinity crisis (*Source* Said 1981)

The Gilf System involves three major rivers: the Gilf River, the Ur-Nil River and the Bown-Kraus River (Issawi and McCauley 1993). These rivers deposited their sediment load in delta systems along the shore of the late Eocene- Oligocene seas, located on what is known today as the Western Eocene Limestone Plateau. It seems that before the formation of the Nile Canyon, this plateau was continuous with its extension in the Eastern Desert (Abotalib and Mohamed 2013). The Bown Kraus River was a major river running NW and fanning in the northern part of Faiyum Depression. The Ur-Nile ran parallel to the Bown-Kraus River and built its delta in Bahariya Depression (Issawi and Osman 2008). The Gilf River ran northward from the Gilf Kebir Plateau to Siwa Depression. This river system is represented by deltaic deposits of the Gebel Qatrani Formation, which crops out in the Faiyum Depression and elsewhere in north-central Egypt. However, Underwood et al. (2013), believe that these delta sediments were deposited by a continental-scale, northerly drainage pattern draining waters from the Turkana region of East Africa during late Eocene-Oligocene.

The second stage, termed the Qena system (Miocene times), was caused by major tectonic activity in the Red Sea area (Fig. 12.2b). This caused a reversal of drainage to occur with a large river flowing southwards towards Aswan and the Sudan. Qena system consists of two major rivers: the Qena River and the Allaqi River. The Qena River flowed southward from the Red Sea Hills, while the Allaqi River flowed northward from southernmost hills as Gebel Gerf and Gebel Elba. These two rivers likely met along the present course of the Nile south of Aswan. Subsequently, the Qena River captured the Allaqi River and continued to flow southwestward at the foot slope of Gebel Kalabsha (Issawi and Osman 2008). On the other hand, Abdelkareem and El-Baz (2015) belief that the earlier Wadi Qena probably hosted the master river course prior to the present Nile River and had followed the general northward slope of Egypt prior to the Red Sea tectonics. It was at this time that catastrophic flooding may have created some major erosional flutes and gravel spreads in the Western Desert (Brookes 2001).

Abotalib and Mohamed (2013) introduced a new concept to river systems evolution in Egypt. It involves the existence of a new river system which flowed northward during late Miocene times: the North Egypt River. This river was separated from the oldest southern Qena System by a natural dam (E-W faulted block) between Nag Hammadi and Wadi El-Assuiti. The North Egypt River flowed first from the mouth of Wadi El-Assuiti and then, flowed northward to join the waters drained from the Tarfa and Sannur drainage basins befor terminating in the Miocene Wadi Natrun Delta.

The third stage, termed the Nile system (Fig. 12.2c), was associated with base level changes in the Mediterranean basin. In Messinian time (ca. 6 Ma.), the Mediterranean dried up for about 600,000 years (Hsu et al. 1973) because of closure of the Straits of Gibraltar. Base level dropped by 1000 m or more. Down cutting and headward erosion became dominant processes forming the Eonile Canyon (Fig. 12.2d), an incised deep gorge four times larger than the Grand Canyon of the Colorado in the USA. Because of its gradient advantage, it captured the south-flowing Qena system and became the first north-flowing river system that extended the length of Egypt to the Mediterranean. Further downstream, the late Miocene Nile created a series of fans in the region of the North Delta Embayment (Nile Cone) and evaporites accumulated in the distal areas of these fan complexes under arid climatic conditions.

Higher sea levels during the Pliocene resulted in the creation of a long narrow marine gulf in the Nile Valley that reached as far south as Aswan (Pliocene Gulf; Said 1981). The marine gulf is represented by a fossil cliff-line of an early Pliocene transgression on the escarpments bordering the Giza Pyramids Plateau (Aigner 1983). Moreover, the plateau formed a "peninsula" within the Pliocene gulf invading the "Eonile canyon". Marine Pliocene sediment is represented by the Kom el Shullul Formation exposed in the eastern foot slope of the Giza Pyramid Plateau and in the Shakhlouf area, north east of the Faiyum Depression (Said 1981; Hamdan 1993). The marine sediments of the early Pliocene filled about one third of the depth of the Messinian canyon. The late Pliocene Nile saw a shift from marine to brackish conditions with a load of fine-grained sediments derived from local wadi systems (Paleonile; Said 1981). This period saw the complete infilling of the Eonile canyon (Said 1981) as the freshwater zone moved northwards towards the modern Mediterranean coastline. These late Pliocene sediments are represented by the Helwan Formation exposed in the mouth of Wadi Garawi and contain brackish water microfossils (Said 1981; Hamdan 1993). The Paleonile sediments are also represented by the Qaret El-Muluk Formation; these are composed of friable sands, mudstones, shale and minor limestone with combined total thickness of approximately 50 m (El-Shahat et al. 1997). The fossil content consists of fresh and brackish water elements: charophytes, ostracods, gastropods, oysters and benthonic foraminifera. Planktonic forams which suggest marine influence have been also recorded. The terrestrial and aquatic continental vertebrate fauna includes mammals, reptiles, fish and aves (El-Shahat et al. 1997).

12.2.1.2 Early Pleistocene Nile

In Egypt, the early Pleistocene was generally arid, however, there were two short humid episodes (i.e. the Edfu and Armant formations; Said 1981) (Fig. 12.3). The Armant Formation is made up of alternating beds of locally derived gravels and fine-grained clastic rocks. The gravels are cemented by tufaceous material and the pebbles are subangular and poorly sorted. The formation abuts the sides of wadis draining into the Nile.

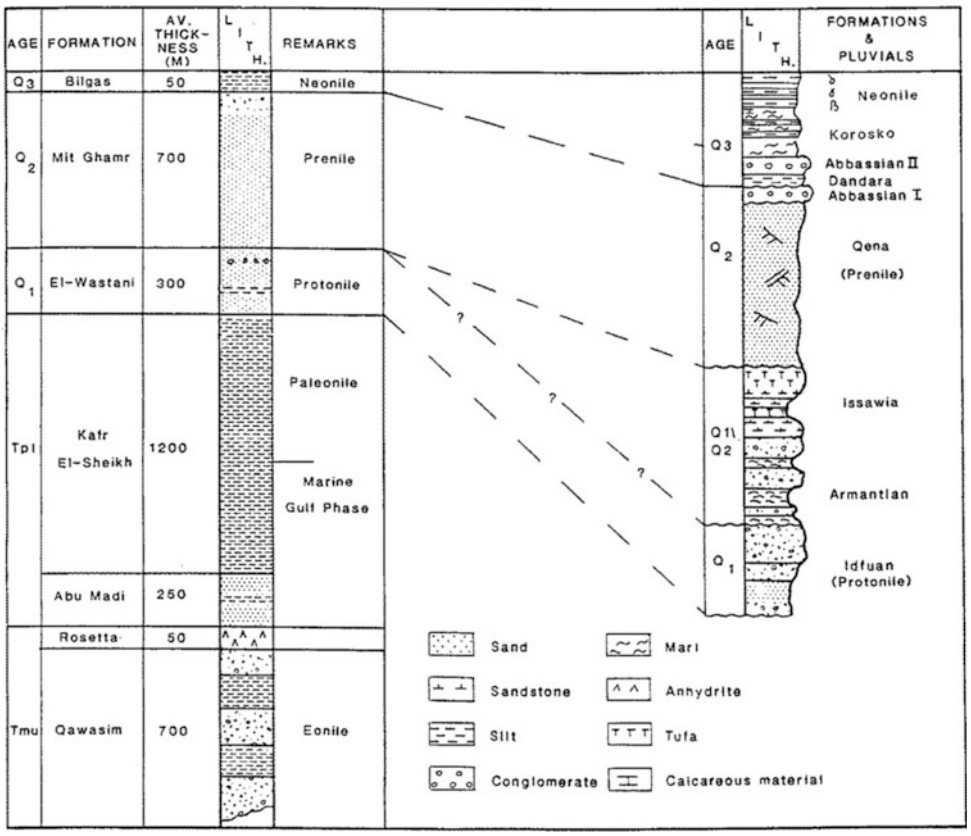

Fig. 12.3 Nile sediments in the Nile Valley and Nile Delta (*Source* Said 1993)

In the area between Esna and Manfalut, the Issawia Formation (Said 1981) is made up of 16 m of chocolate brown clays, followed by a 7 m thick tufaceous hard limestone bed below 22 m of red limestone breccia. The breccia contains a hard cemented bed in the higher levels known as brocatelli limestone (see Butzer 1980; Ahmed 1993). The Idfu Formation (Said 1981) is composed of more than 15 m of fluviatile gravels and sands embedded in red-brown silt matrix. The coarse sands and gravels consist mostly of rounded flint and are covered with a red-brown soil.

The early Pleistocene is well developed in a sand quarry near Mena House hotel on the Giza Pyramid Plateau and attains ca. 30 m in thickness, consisting of cross bedded gravelly quartzose sand. These deposits were deposited by a low sinuosity braided river. The early Pleistocene sediments are also exposed in a sand quarry at Qasr el Basil area, west Nile-Faiyum Divide (Hamdan 1993). They form a long, narrow and highly desiccated terrace ca. 70–80 above sea level, consisting of cross bedded pebbly coarse to medium grain quartzose sand occupying a channel 10–15 km west of the modern Nile floodplain.

12.2.1.3 Middle Pleistocene Nile

During middle Pleistocene, a powerful river with a distant source reached Egypt. This river, the Prenile, drew its waters from Ethiopia when the Atbara and possibly the Blue Nile pushed their way into Egypt across the Nubian swell by a series of cataracts (Said 1981, 1993). The Prenile (Qena Formation) is composed of alternating, cross-bedded, occasionally consolidated, coarse-grained sands and thin beds of grits, and gravels, with casts of fresh water shells and attains a thickness of 20 m (Fig. 12.3). The oldest Nile aggregation- also called "Alpha" aggregation (Said 1993) consists of two gravel formation (Abbasia "I" and Abbasia "II"), in between there is thick floodplain silt (Dandara Formation; Said 1993). The Dandara Formation is approximately 15 m in thickness and is composed of a grey, loose and fine sandy silt bed at the base, followed by brown silts with thin carbonate interbeds and occasional lenses of gravel and capped by a distinct red soil. It was dated more than 39–40 kyr B.P (Wendorf and Schild 1976). However, recent work shows that the Dandara silt is dated to late Acheulean ($\geq$ 200 kyr BP, see Deino et al. 2018).

The Abbasia Formation (Said 1981) is composed of massive, loosely consolidated gravels of polygenetic origin. The pebbles are rounded to subround. They were derived from the uncovered basement of the Eastern Desert. The Abbassia "I" gravels are archeologically sterile while as Abbasia "II" gravels are rich in archeological material of early Paleolithic (late Acheulean) tradition. These sediments are dated to 600–350 kyr BP (see Deino et al. 2018). According to the recent dates of artifacts in the Abbasia/Dandara complex, we consider these river systems

are dated to middle Pleistocene rather than late Pleistocene as mentioned previously by Said (1993).

12.2.1.4 Late Pleistocene Nile

The late Pleistocene history of River Nile is very complex and mainly controlled by different geological and climatic factors. Both local climatic conditions and those in the Nile headwaters have played an important role in late Pleistocene history of the River Nile. Local climatic conditions add more water to the river through run off from local wadis during wetter climate and accumulate dune sand on the western bank of the river during arid conditions. Indeed, the study of late Pleistocene Nile sediments is crucial not only for understanding the Nile behavior and paleoclimatic variation but also for understanding the early *Homo* species migrations out of Africa. It is now accepted that during late Pleistocene, the Nile Valley was a vegetated corridor through which the exodus of *Homo sapiens* out of Africa and into Eurasia occurred between ~50 and 120 kyr BP (see Timmermann and Friedrich 2016). Early Human migrated from northeastern Africa into the Arabian Peninsula and the Levant and expanding further into Eurasia and beyond.

Based on ^{14}C dating and associated archaeology, two late Pleistocene aggradations (i.e. "Beta" and "Gama" aggradations; Said 1993) are distinguished, i.e. middle and late Paleolithic floodplains. Middle Paleolithic silt is represented by the Dibeira-Jer Formation (De Heinzelin 1968). The Dibeira-Jer Formation forms terraces about 36 m above the modern flood plain in Nubia and about 8 m above the modern flood plain in Upper Egypt (Said 1981). It has been divided into several aggradations episodes (floodplain silt) separated by periods of regression (dune sands). It has an estimated thickness of more than 8 m. These silts include no archaeology at Kom Ombo, but in Nubia they include sites with middle Paleolithic artifacts (Wendorf et al. 1989). Another middle Paleolithic aggregation is recorded, the Makhadma Formation which consists of sheet wash gravels, pebbles, and boulders with middle Paleolithic artifacts (Wendorf and Schild 1976). They rest unconformable over Dandara Formation or Prenile sands (Said 1993) and overlain by sediments carrying fresh, late Paleolithic artifacts. In Wadi Kubbaniya (west Aswan), two overbank silts are interbedded with dune sands; the lowest and oldest parts of the silts lie beyond the range of radiocarbon dating; they could well be as old as 70 kyr BP (Butzer 1997). The topmost and youngest parts, on the other hand, ended well before 30 kyr BP (Wendorf et al. 1989).

Another middle Paleolithic silt is represented by the Ikhtiariya Formation (Said 1981), which is made up of well-sorted, massive, dune sands, with a thickness of 4–6 m. It contains middle Paleolithic artifacts and a few mammal bones. The Formation overlies eroded bedrock, the Dandara Formation, and is conformably overlain by the Masmas-Ballana Formation and fluvial sands. The Formation is assumed to represent aeolian deposits contemporaneous with the Mousterian-Aterian pluvial dated at 80–40 kyr BP (Said 1993). More recently, the age of the Aterian has dated to ca. 150–40 kyr BP (Campmas 2017). The middle/late Paleolithic boundary is characterized by deep cracking vertisols and the Nile entrenched its channel by at least 20–25 m and middle Paleolithic silts were deflated (Butzer 1997). Renewed aggradations ("Gamma" Neonile floodplain silt; Said 1993) within a more restricted valley is primarily recorded near Kom Ombo by channel complexes that range from channel beds and point-bar sequences to levee and overbank silts (Butzer 1997).

Late Paleolithic floodplain silt is represented by the Masmas-Ballana Formation which composed of dune sands intercalated with silts and capped by a podzol soil (Said 1981). The top of the dune deposits is rich in late Paleolithic artifacts. Butzer and Hansen (1968) introduced the name Masmas Formation for silts and channel beds in the Kom Ombo area in Upper Egypt with thickness more than 43 m and contain a mollusk fauna. De Heinzelin (1968) applied the name Ballana Formation to dune sands which interfinger the upper part of the Dibeira-Jer silts in the Egyptian Nubia. The Deir El-Fakhuri Formation (Wendorf and Schild 1976) is represented by diatomite and pond sediments interrupted by silt units, which overlie the Ballana Formation, and underlie the Sahaba Formation. This Formation has an estimated thickness of more than 6 m at Esna and Toshkka in Egyptian Nubia. Pollen and diatom analyses of the sediments of the Ballana and Deir El-Fakhuri Formations suggest an arid grassland environment (Wendorf and Schild 1976).

The Sahaba-Darau Formation (Said 1981) consists mainly of floodplain silts. It has a thickness of more than 6 m. The formation overlies the recessional pond deposits of the Deir El-Fakhuri Formation. The Sahaba-Darau Formation is equivalent to the Gebel Silsila Formation of Butzer and Hansen (1968) in the Kom Ombo area. The Sahaba Formation as described by De Heinzelin (1968) was divided into two aggradation units separated by an episode of down-cutting (Deir El-Fakhuri Formation). The Sahaba Formation yielded typical Sebilian assemblages characterized by abundant Levallois artifacts.

12.2.1.5 Holocene Nile

The Holocene aggragation in the Egyption Nile Valley floodplain (delta Neonile; Said (1993) is subdivided into several formations, i.e. Dishna-Ineiba, Arkin and El-Kab formations. The Dishna Formation, dated to 10–9 kyr BP, is represented by a succession of playa deposits and Nile silt with interbeds of gravels and pebble sheets. It is coeval with the Malki Member of Butzer and Hansen (1968), and slope-wash debris of the Birbet Formation of De Heizenlin (1968). This Formation overlies the Sahaba Formation which

is overlain by the Arkin Formation. The Ineiba Formation, 9–7 kyr BP, was introduced by Butzer and Hansen (1968) as a widespread wadi accumulation with a lower conglomeratic bed (Malki Member) and brown clays in the upper part (Sinqari Member). The Dishna-Ineiba Formation represents deposits which formed during the recession following the Sahaba-Darau aggradation. The playa deposits accumulated behind the natural levees and abandoned channels of the Sahaba-Darau aggradation (Said 1981).

The Arkin Formation (Said 1981) is made up of ca. 6 m of silts and fine-grained micaceous sands. It overlies the Dishna Formation and underlies post- Arkin sediments. Its age is assumed to be 9.2–7.2 kyr BP, based on radiocarbon dates (Said 1981). The Arkin Formation is coeval with the Arminna Member of the Gebel Silsila Formation of Butzer and Hansen (1968) in the Kom Ombo area. The El-Kab Formation is made up of a series of Nile sediments, now under cultivation, on the east bank of the Nile River, from El-Kilh (about 15 km north of Idfu) at the Old Kingdom fortress of El-Kab. Radiocarbon dates on charcoals yielded ages between 6.4 and 5.98 kyr BP.

Recent subsurface studies in Saqqara-Memphis floodplain (Fig. 12.4a) reveals a complex fluvial history of both aggradation and degradation events corresponding to magnitudes of Nile floods and paleoclimatic conditions in the African Nile headwaters (Hamdan 2000a; Hassan et al. 2017, Hamdan et al. 2016a, 2019). The sequence began with a unit of late Pleistocene fluvial sand and gravel and relics of early Holocene fluvial sediments (Fig. 13.4b). Middle Holocene is represented by period of high Nile flows associated with steep sea level rises and the floodplain occupied by swamps and anastomosing channels. After the Old Kingdom, the River Nile changed to a more stable meandering channel with well-developed levees and flood basins. Middle Kingdom is represented by a widespread layer of alluvial silt and sand, indicating high Nile floods, which agrees with historical records. Normal floods with several lows and highs prevailed during the last two thousand years. The Holocene floodplain sequence exhibits several discontinuities in sedimentation, particularly at 8.2 cal kyr BP between early Holocene and Predynastic period, at 5.4 cal kyr cal BP; between Predynastic and Old kingdom; at 4.2 cal kyr BP corresponding to First Intermediate Period; at 2.4 cal kyr BP between late Period and Ptolemaic, and at 0.8 cal kyr BP (Fig. 12.4c). These are extremely significant in linking major changes in Nile floods to global climatic events. These five events are recognized as events of global cooling, often abrupt, and associated with areas directly or indirectly affected by monsoonal rain and changes in the ITCZ. They are also evident in the drop of African lake levels in the Nile headwaters and a reduction in the level of the nearby Faiyum Lake (Hamdan et al. 2019).

12.2.1.6 Dramatic Events in the Geologic History of River Nile

The sedimentary history of the Nile River in Egypt bears witness to a number of dramatic events that occurred during the late Pleistocene-Holocene due to severe changes in global climatic conditions. The late Glacial Maximum (LGM), the Wild Nile pluvial period and several climatic events during the Holocene (e.g. the 4.2 dry event) all had great impacts on the hydrology and sedimentology of the river. In turn these events affected or interacted in a variety of ways with human activities.

Blocking of the Nile Valley During the LGM

Behavior of the Nile during the late Pleistocene was a matter of debate between the scientists working in the Egyptian Nile Valley. A model of the river during LGM indicates that the Nile Valley was occupied by series of braided channels with total discharge much less than today, at 10–20% of its modern volume (Wendorf and Schild 1976; Schild and Wendorf 1989; Hassan et al. 2017). The lack of vertical accretion of braided coarse siliciclastic sedimentation in Upper Egypt and lack of late Paleolithic sites in Lower Egypt, make a braided model unlikely. Another model of the LGM Nile Valley environments was proposed by Vermeersch and Van Neer (2015). These authors believe that a series of lakes occupied Nile Valley due to sand dunes blocking the Nile Valley at Naga Hammadi and other places in Upper Egypt during the LGM. The presence of lakes in the Nile Valley during the LGM could offer humans excellent possibilities for food exploitation in otherwise very harsh climatic and environmentally challenging conditions (Vermeersch, and Van Neer 2015). The damming of lakes occurred at different elevations above the present floodplain and in turn there is little correlation with cultural identities. Indeed, the existence of lakes within Nile Valley of upper Egypt was previously mentioned by Vignard (1923), who discovered sequence of late Paleolithic sites on the shores of a progressively shrinking lake fed by local wadi systems, which had been dammed up behind Gebel Silsila. The model of Vermeersch and Van Neer (2015) is plausible but needs to be supported by description of proper lacustrine sediment facies with diatom analysis.

The Wild Nile

The onset of post-glacial warming (after LGM) was marked by an upsurge of exceptionally high Nile floods at 13–11 cal kyr BP, an event labeled as the “Wild Nile”. The event indicates increased rainfall in the source areas of the Nile in Equatorial Africa and Ethiopia (Williams et al. 2010, 2015) and heralds the initial step in the establishment of the current Nile regime, which was well established by 11.5 cal kyr BP following a recessional episode from 13 to 11.5 cal kyr BP. In Wadi Kubbaniya wild Nile event was identified a

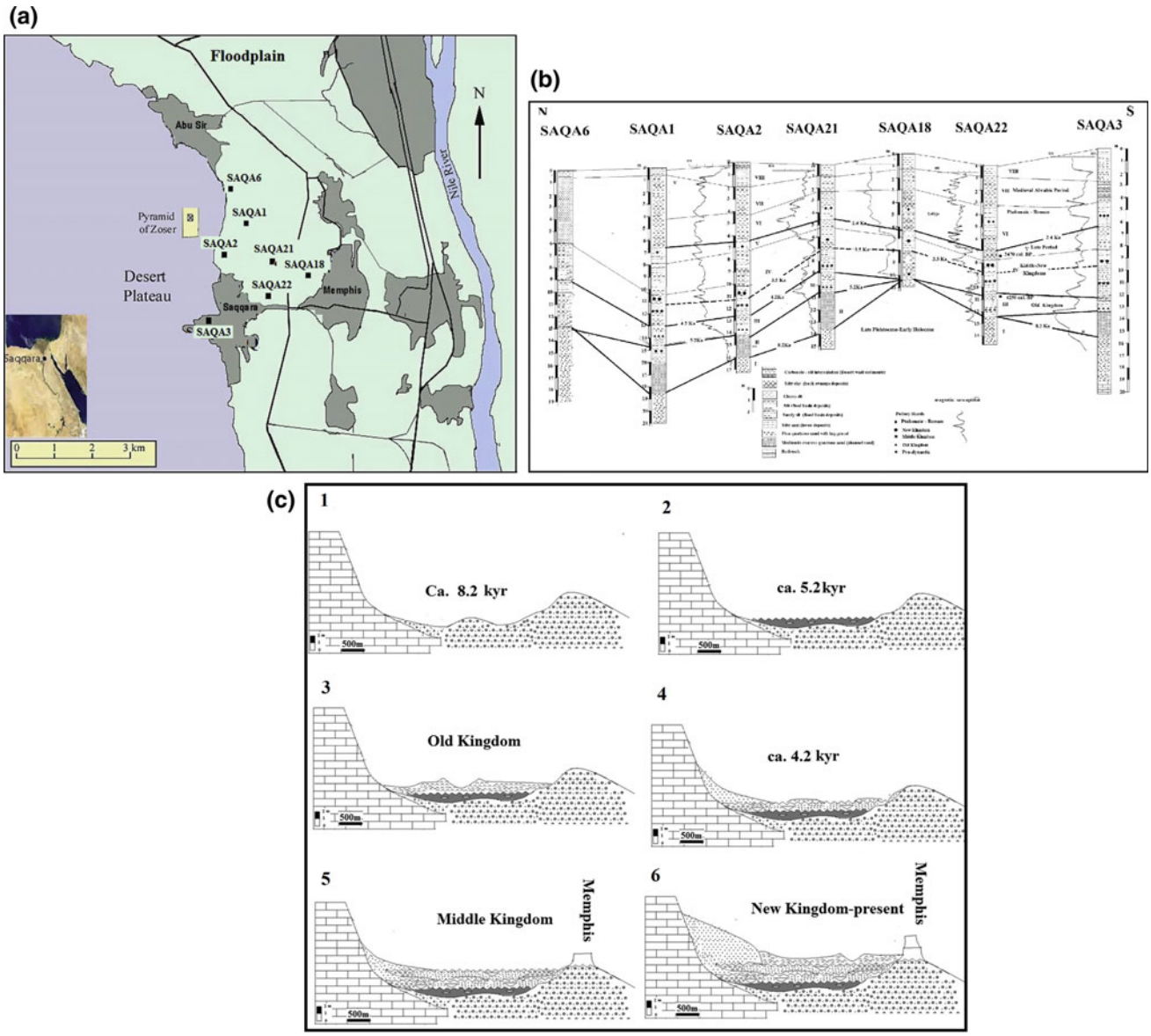

Fig. 12.4 Alluvial history of the Saqqara-Memphis Floodplain during the middle Holocene; **a** Google Earth image of the Saqqara-Memphis floodplain with core locations; **b** Lithostratigraphy of Holocene sediment in the Saqqara-Memphis floodplain; **c** Evolution of Saqqara-Memphis floodplain through the Holocene; (1) degradation of the floodplain during the 8.2 cal kyr BP arid event; (2) degradation of the floodplain during 5.2 cal kyr BP; (3) aggradation of the floodplain during the early Dynastic-Old Kingdom (5–4.2 cal kyr BP); (4) degradation of the floodplain during the First Intermediate Period (4.2 cal kyr BP); (5) aggradation of the floodplain during the extremely high middle Kingdom floods; (6) aggradation of the floodplain from New Kingdom to present (*Source* Hassan et al. 2017)

comparably rapid rise of Nile flood deposits from 111 to 118 m between about 12.6 and 12.3 cal kyr BP; exceptionally high flood waters entered far up the wadi but left only 50 cm of thin-bedded silts and marls (+25 to 26 m) (Schild and Wendorf 1989).

12.2.2 Dry Event (Collapse of Old Kingdom)

The collapse of the Egyptian Old Kingdom was triggered by low Nile floods, combined with a decentralization of political power and weakening of the central administration (Hassan 1997, 2007b; Hamdan et al. 2016b, 2019). The 4.2 cal kyr BP climatic event is clearly manifested in the geological record at Saqqara as an erosional event, recorded at the top Old Kingdom sediments. Hamdan et al. (2016b, 2019) used sedimentological, mineralogical, and geochemical proxies as well as pollen analysis to study sediments coeval to this event through drilled cores in Faiyum and Saqqara regions. The pollen diagram of these sediments shows that Asteraceae tubuliflorae pollen exceeded 50% and Amaranthaceae, Liguliflorae, small quantities of *Rumex* and

other ruderals as well as *Acacia* were present (Hamdan et al. 2019). These pollens indicate onset of desert conditions during the 4.2 dry event. This period spanned a 100 years or less, and Nile floodplain converted to dry desert conditions. The heavy minerals assemblage reflects mixing of Nile floodplain and desert wind-blown environments (Hamdan 2000a). The high zirconium content of these sediments also indicates high aridity and sand storms, which led to sand encroachment from the Western Desert to the Nile Valley (Hamdan et al. 2018). The latter is supported by an ancient eye witness account: "Ipuwer" who mentioned to his son Lo that "the desert claims the land and the lands are injured" (Hassan 2007b). XRF data for the 4.2 cal kyr BP event shows low ratios of both diagnostic Blue and White Nile elements (Fe/Al; Ti/Al; Sr/Al) and together with the high content of zirconium (Hamdan et al. 2019), which indicates reduced effects of Ethiopian flood water. Contemporary with this dry event, several lakes in the Nile catchment record water level declines at this time (Adamson 1982).

12.2.2.1 Shifting of Nile channel

Shifting of the Nile channels in the Nile floodplain has been substantial in the alluvial landscape, which fundamentally affected the structural and functional development of the ancient Egyptian civilization (Hassan et al. 2017). Detection of river shift in the Nile Valley is based on the relationship between the elevations above sea level of ancient settlements along the older courses of the Nile (Jeffreys 2008; Jeffreys and Tavares 1994; Bunbury et al. 2008, 2017). Hassan et al. (2017) proposed a model of channel shifting based on geoarchaeological investigations using drill core data to consider the relationship between settlement depths and sedimentological characteristics and the interpretation of Landsat and Google imagery (Fig. 12.5). The model supposes that there was a main Nile (on the eastern side of the Nile Valley) and secondary Nile distributary channels closer to the western plateau. During Old Kingdom there was an eastwards shift of the western Nile branch and a westward shift of the main Nile channel. In fact, these secondary branches migrated much faster than the main channel because they were situated at a relatively higher elevation and would have dried out in mid-winter during low Nile water flow. There are different estimates for the rate of Nile channel movement during the Old Kingdom; Hillier et al. (2006), measured a rate of eastwards shifting in some areas of the Nile floodplain to be about 9 km per 1000 years, mainly by island production and capture. Lutley and Bunbury (2008) also claimed that the River Nile had moved at a rate of 9 m/yr. Hawass (1997) estimated the migratin rate of the Bahr el-Lebeini, an Old Kingdom secondary channel near the Giza Plateau, to be about 3.58 m per year. Hassan et al. (2017) calculated a rate of 3.2 m per year for the eastern movement of the secondary channel (1.64 km the distance between the early Old settlement and late Old Kingdom settlement, over 500 years).

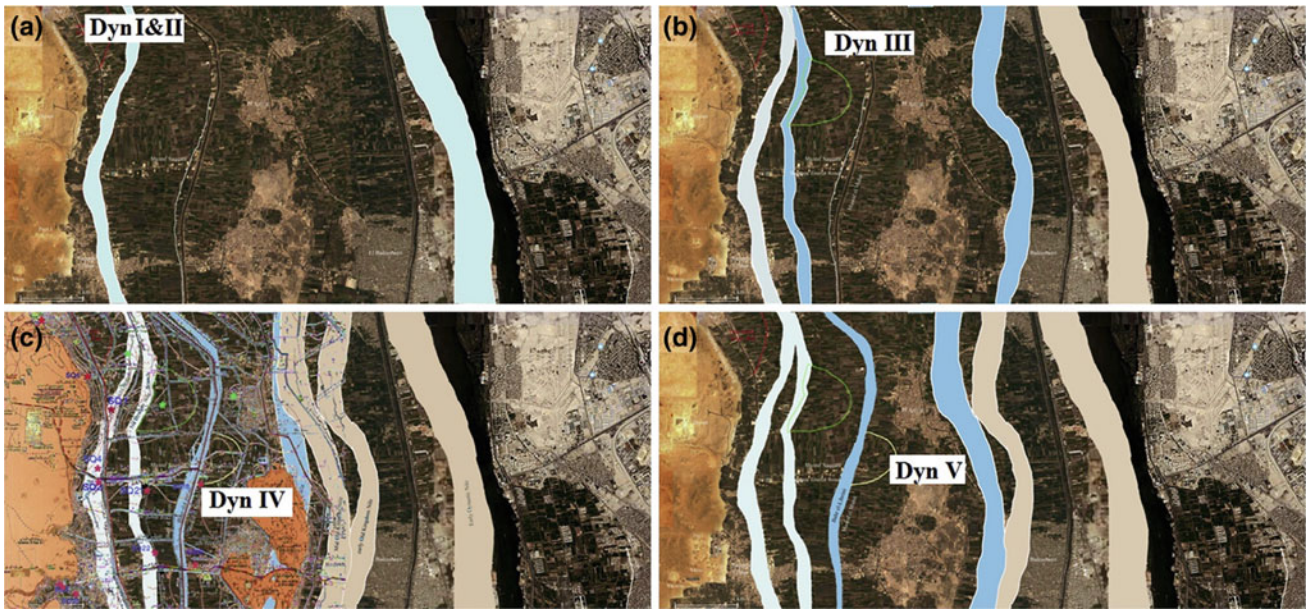

Fig. 12.5 Interpretive model of the Saqqara-Memphis floodplain: **a** location of a principal lateral channel running close to the escarpment of the Western plateau with the main branch of the Nile running along the eastern side of the modern floodplain; **b** during the Dynasty III, when the Djoser pyramid was built, the early Dynastic channel migrated eastward to the location now occupied by the Shebrament Canal; **c** continuous westward and eastward migration of the main channel and western channel, respectively and emergence of Memphis as a island between these two channels; **d** at the time of Unas (end of Dynasty V, 4.356–4.323 kyr BP) the ancient western channel in this location is currently occupied by the Bahr Libeini which parallels the Miheit Drain (*Source* Hassan 2017)

12.2.3 Nile Delta

The Nile Delta, one of the largest deltas in the world, occupies an area of ca. 25,000 km^2 and is bounded by desert to both the east and west. Its apex is located at Cairo, where the river divides into two main distributaries: the Rosetta and Damietta; these discharge over the triangular-shaped alluvial plain and flow north into the Mediterranean. The sedimentary succession in the Nile Delta attains thickness of ca. 4000 m and composed of sand and gravel overlain by a thin layer of alluvial clay. The geologic history of Nile Delta is complex, goes back to late Miocene, and includes five delta phases; Eonile Delta; Paleonile Delta; Protonile Delta; Prenile Delta and NeoNile Delta (Fig. 12.3). A large amount of research has been undertaken on the Pleistocene and earlier history of the Nile Delta, mainly as a result of oil exploration (e.g. Rizzini et al. 1978).

Eonile Delta was formed during the late Miocene and represented by the Quasiam Formation (Fig. 12.3). This Formation attains ca. 700 m in thickness and represented by coarse sand and gravel intercalated with thick shale beds. It is evident that the Quasiam formation has been deposited in the form of coalescing fans in front of an E-W active fault scarp. Quasiam Formation is overlain by ca. 50 m thick unit of evaporite rocks (Rosetta Formation). The Paleonile Delta phase (Pliocene Gulf) is represented by two formations; Abu Madi and Kafr el Sheikh. Abu Madi Formation attains about ca. 250 m of sand with a thin shale unit in the middle part of the section. Kafr el Sheikh Formation (late Pliocene), attains ca. 1200 m in thickness and consists of shale with marine fossils in the lower part and brackish and freshwater fossils in the upper part. Protonile Delta (early Pleistocene) is represented by El Wastani Formation (ca. 300 m) composed of coarse sand with few shale and gravel interbeds. The Prenile delta (middle Pleistocene) is represented by the Mit Ghamr Formation (ca. 700 m) and consists of coarse sand and gravel from Ethiopian sources. Finaly, Neonile delta phase (late Pleistocene-Holocene) is represented by the Bilqass Formation, which is made up of alternating fine and medium-grained sands, interbedded with clays rich in pelecypod, gastropod and ostracod fragments, plant material, and peat layers.

Late Quaternary sediments of Nile Delta were intensively investigated in the last three decades, based on archaeological excavations, drilling of shallow cores and radiocarbon dating. A survey of the published literature provided 1640 relevant core records within the fluvial zone of the delta (Pennington et al. 2017). These studies provide much evidence for the changing patterns of Nile behavior as well as for global sea level changes. In the coastal region of Nile Delta, late Quaternary sediments comprise three sedimentary sequences (Stanley and Warne 1993a). Sequence "I" (late Pleistocene—ca. 38–12 kyr BP), is represented by iron-stained quartz-rich sands and stiff mud, deposited by braided channels associate with a drop in sea level and the coastline was located further north of its modern position. Sequence "II" is represented by transgressive sand with a shallow marine fauna dated to mid-Holocene (ca. 8 cal kyr BP; Stanley and Warne 1993a). Sequence "III" (ca. 7.5 cal kyr BP onwards), is represented by a variety of lithologies of marine, semi-terrestrial, coastal, estuarine, lagoonal and in some cases fluvial deltaic environments.

In the fluvial-dominated region of the Nile Delta, late Quaternary succession is subdivided into three Sequences; Sequence "I", Transgressive Sand and Sequence "II" from older to younger. Indeed, for simplicity and preventing confusion with previous nomenclature, we used "Sequence" rather than "Formation" as originally used by Pennington et al. (2017). Figure 12.6 shows summary cross-sections of previous studied geoarchaeological/geological areas in the Nile Delta, reinterpreted within the stratigraphic divisions of the synthesis of Pennington et al. (2017). The Sequence "I" comprises medium-coarse quartzose sands, with pebbles of quartzite, chert and dolomite and is subdivided into two units; Zagazig and Minuf units, from older to younger, respectively. The Zagazig unit is generally, massive to laminated or cross-stratified; yellow fine to medium grained sands (De Wit and van Stralen 1988; Hamdan 2003a; Rowland and Hamdan 2012). Mineral composition includes iron oxides (magnetite, hematite and ilmenite), hornblende, augite and epidote (Hamdan 2003a; Pennington et al. 2017). Minuf unit consists of fine grained micaceous sand with stiff or compact clayey lenses (Butzer 1997; Sandford and Arkell 1939). The Transgressive Sand Sequence (early Holocene), is composed of coarse, poorly-sorted, olive-grey to yellowish-brown quartzose sands which contain a high percentage of heavy minerals, as well as mollusk and echinoderm fragments (Chen et al. 1992; Coutellier and Stanley 1987; Stanley et al. 1992). These deposits are probably originally fluvial sediments that incorporated a littoral signature during retrogradation of the shoreline and major reworking by waves and other coastal processes between ca. 15 and 8 cal kyr BP.

Sequence "II" is made up the "alluvial mud" of the delta plain and is divided into three units from base to top; Sequence "IIa", Sequence "IIb" and aeolian sand (Pennington et al. 2017). Sequence "IIa", is made up of bluish-black silty-clay to clayey silt containing a high percentage of organic matter and peat layers. Sequence "IIb" is generally brown-grey in color, less rich in organic material, and very predictable in the lateral variation of its grain size. This later unit represents overtopping of levees and the development of a wide floodplain during the late Holocene. The sequence of the fluvial-dominated delta is ended by a modern aeolian Member (Pennington et al. 2017).

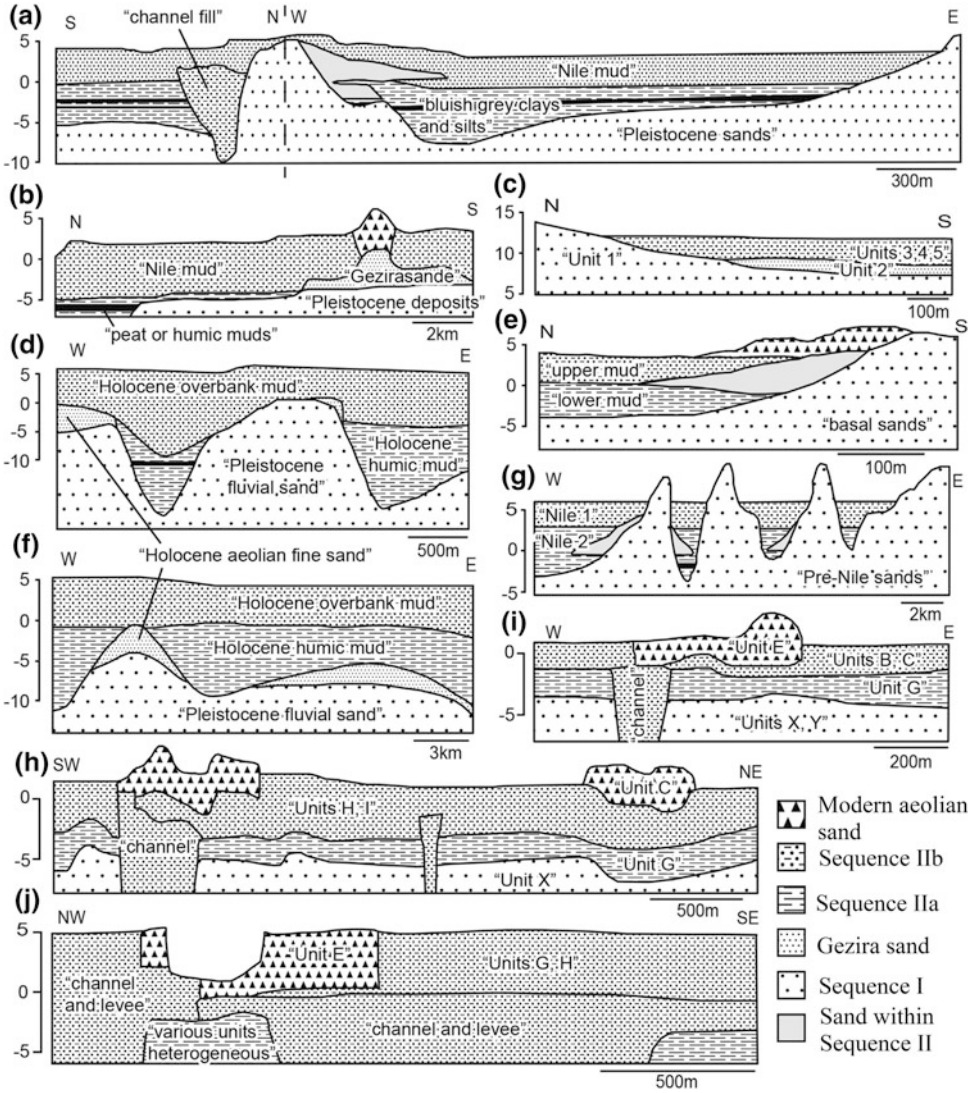

Fig. 12.6 Summary cross-sections of previously published geoarchaeological/geological works in the Nile Delta: **a** Minshat Abu Omar, adapted from Andres and Wunderlich (1992); **b** Kafr Hassan Dawood (Hamdan 2003a); **c** Quesna, adapted from Rowland and Hamdan (2012); **d** Sais, adapted from El-Shahat et al. (2005); **e** Kafr Hassan Dawood, adapted from Hamdan (2003a); **f** MUWDS, adapted from El-Awady (2009). **g** AUSE, adapted from Andres and Wunderlich (1992); **h** Kom al-Ahmer/Kom Wasit; **i** Tell Mutubis; **j** Kom Geif (Pennington et al. 2017). The names of the units given in quotation marks are those from the published literature; the key shows their reinterpretation within the framework of the current synthesis (*Source* Pennington et al. 2017)

12.2.4 Significant Geological Features in the Nile Delta

12.2.4.1 Nile Cone

Nile Cone is a largest Mediterranean deep sea fan and has a complex history related to large scale tectonics in the East Mediterranean basin and evolution of the Nile River which has served as its major sediment source (Stanley and Maldonado 1977). The cyclic nature of Nile Cone sediments record modifications of eustatic sea level and paleoclimatic conditions at the Nile headwaters. It also reflects changes in the physical oceanography of the coastal area, including current patterns and stratification, and biogenic productivity. The cone consists of six sediments types; turbidite sand and silt, turbiditic mud, hemiplegic mud, calcareous ooze, organic ooze and sapropels.

12.2.4.2 Sapropels

Sapropel is a dark-colored organogenic sediments that is rich in organic matter intercalated with the offshore Nile cone sediments since mid-Miocene times (Mourik et al. 2010). Their formation in the Mediterranean is relate to increasing amounts of freshwater reaching the basin by a combination of various factors including increased precipitation versus evaporation, discharge from the Nile and other bordering rivers. The large amounts of fresh water delivered by the Nile have led to increased nutrient supply and anoxia promoted by stratification of the water column (Krom et al. 2002; Fielding et al. 2018). Sapropels occur (quasi-) periodically in sedimentary sequences of the last 13.5 million years, and exist both in the eastern and western Mediterranean sub-basins (Rohling et al. 2015). Extensive study, based on records from both short (conventional) and long

(Ocean Drilling Program) sediment cores, and from a wide variety of uplifted marine sediment sequences on the basin margins and islands. The sapropels are important in paleo-climatic studies, especially monsoon intensity in the Nile headwaters.

12.2.4.3 Sea Level Change in the Nile Delta coast

Intensive coring programs in the delta plain have reveal that the Mediterranean Sea was some 100 m lower than the present level during late Pleistocene and fluvial and deltaic environments extended out 40–50 km beyond the modern coast (Butzer 1997). In response, the Nile channel and distributaries were entrenched up to 30 m below the present surface into older Pleistocene sands and gravels. During post-glacial warming, global temperature rise melted the ice-caps causing sea level to rise and, at the same time, rainfall increased in the catchment area of the Blue Nile (Woodward et al. 2007). The sea level rose rapidly by several meters per millennium at the shelf-edge of the Nile Delta between 10–7 cal kyr BP (Stanley and Warne 1994). Moreover, Fairbanks (1989) noted that the ending of the last ice age led to a global sea-level rise of 120 m. Assuming that the current floodplain gradient of ca. 1 m/km, this sea-level rise could potentially produce a marine transgression of a similar extent (Bunbury and Jeffreys 2011). Due to high rates of sea-level rise and river sediment loads high rates of flood basin aggradation took place. Subsequently, the delta plain was dominated by a swampy, wetland landscape with the formation of anastomosing rivers and crevasse splays (Pennington et al. 2017).

During the late Holocene period, a gentle sea level rise of 1.0 m per millennium occurred until the present lower rates. Subsequently, the in-channel aggradation rates decreased and the crevassing and avulsion became relatively less dominant processes in landscape formation. The channels would have migrated across their floodplain primarily via lateral channel migration and point bar deposition. The resulting landscape has been referred to as a "meandering" deltaic environment (Pennington et al. 2016).

12.2.4.4 Ancient Delta Branches

Since the end of the last ice age, global temperature rise melted the ice-caps causing sea level to rise and, at the same time, increased rainfall in the Nile Headwaters (Woodward et al. 2007). Rising sea level and increasing Nile flow both push the river towards the production of more distributaries and will also shift the delta head southward. According to Stanley and Warne (1993b), the number of distributaries reached a maximum around 6000 years ago and since then has gradually declined. In the present time, there are only two Nile channels bifurcates ca. 20 km north of Cairo; Rosetta and Damietta branches. However, there were seven branches during the pre-dynastic period that were reduced to five branches during the Paranoiac times (Tousson 1922). There were two branches in west delta as sub-branches of current Rosetta Branch, i.e. Canopic and Bolebetic. In west delta, there were five branches; Sebennitic, Bucolic, sub-branches of Damietta Branch; Mendesian, Tanitic and Peluciac. During early Holocene, probably the branches are more and mainly in the form of anastomosic channels associated with rapid sea level rise (Pennington et al. 2017). The concentration of former distributaries (Four major ones) in the northeastern part of the delta was partly due to the rapid subsidence (Stanley 1988). According to Said (1990), the disappearance of the ancient branches occurred during low-flood years, when deposition exceeded erosion. On the other hand, Sneh et al. (1986) concluded that the degeneration of the lower reaches of the Pelusaic Branch was due to the silting up of the mouth of the distributary by the prevailing W-E long-shore current.

12.2.4.5 Delta Subsidence

The subsidence of the Nile Delta received much attention from the scientific community and extensive coverage by the media in the last decades (Becker and Sultan 2009). Numerous studies have attempted to measure rate of subsidence along Nile Delta. The techniques used have included in situ observations (Marriner et al. 2012; Stanley and Warne 1993a; Warne and Stanley 1993) as well as remote sensing techniques (Aly et al. 2009, 2012; Becker and Sultan 2009). These studies have recorded differential subsidence velocities on the Nile Delta that range from slightly emergent to subsidence rates as high as approximately 10 mm/yr.

Early studies provided estimates of vertical motion from slightly emergent to subsidence of just over 4 mm a year. The maximum rates of subsidence occur east of the Damietta promontory. A zone containing the highest rate of subsidence was attributed to the major eastern Mediterranean fault system with accelerated velocities attributed to the thick belt of Holocene sediments in the north. The thick Holocene sediment layer is presumed to form a hinge line marking its southern edge (Stanley and Warne 1993a). A later study reported subsidence velocities ranging from 0.0 to 5.0 mm/yr across the northern Nile Delta (Marriner et al. 2012). Buried and submerged archaeological sites have also been used to date subsurface horizons (Warne and Stanley 1993). This information was then used to calculate rates of subsidence that range from 0.9 to 5 mm/yr (Stanley 2012; Stanley and Toscano 2009; Warne and Stanley 1993).

An alternative approach to sediment core studies has been to use radar satellite data to measure subsidence on the Nile Delta. One study used 34 descending ERS-1 and ERS-2 satellite data images spanning 8 years and beginning from 1993 to 2000 to measure average subsidence rates of 7 mm/yr. The study proposed that subsidence within the study area was influenced by groundwater extraction, tectonics, and possibly the subway system running under the

city (Aly et al. 2009). Another study conducted by Becker and Sultan (2009) used 14 ascending ERS-1 and ERS-2 satellite radar images spanning just over 7 years from 1992 to 1999. The maximum subsidence velocities measured by the study range from 6 to 8 mm/yr on the north-western portion of the delta.

Generally, all studies concluded that a combination of factors have been responsible for the Delta subsidence, including tectonic readjustment of strata at depth, sediment compaction, growth faulting and soft sediment deformations under large anthropogenic structures, possibly triggered by earthquakes, tsunamis. These studies show very clearly that the delta has ceased to increase in altitude relative to sea level. Although, tsunamis are relatively rare in the Mediterranean Sea, their potential risk cannot be neglected. Alexandria City was not affected by a major earthquake or tsunami in recent years (Jelínek et al. 2009). However, historical events show that approximately 5,000 people died and 50,000 houses were destroyed in the city after the earthquake in 21 July 365 AD. The Roman historian Ammianus Marcellinus wrote about the impact of this event in Alexandria: "*The solidity of the whole earth was made to shake and shudder, and the sea was driven away. The huge mass of waters was return when least expected killed many thousands by drowning. Huge ships perched on the roofs of houses and others were hurled nearly 3 km from the shore*". The last tsunami to hit the eastern Mediterranean occurred on August 8, 1303 AD. It destroyed the great lighthouse of Alexandria, one of the seven wonders of the ancient world (Jelínek et al. 2009).

12.2.4.6 Turtle-Backs

In the eastern Delta, geoarchaeological investigations showed the existence of scattered small or large ridges of Pleistocene coarse sand (turtle backs) (De Wit 1993; De Wit and Van Straten 1988; Andres and Wunderlich 1992; Hamdan 2003a; Rowland and Hamdan 2012). Turtle-backs are deposits of sand, sandy clay, and impure silt, yellow in color and forming higher longitudinal hummocks over the Delta surface. They appear as yellowish islands in the green fields of the Delta, rising some 10–12 m above the surface; some may rise only one meter above the surface. Four of these turtle-backs are found near Quweisna (see Rowland and Hamdan 2012), two between Banha and Qalyub, one near Fagus, and five near Manzala, occupying an average area of 2 km^2 each. Sandford and Arkell (1939) consider these turtle-backs as relics of middle Paleolithic silts analogous to deposits on the lateral margins of the delta.

12.2.5 Faiyum

The Faiyum Depression is encircled by a northern escarpment and for much of its past it contained a large lake (Lake Moeris) fed by Nile run-off through the Bar Yussef (Fig. 12.7a). Fluctuations in Nile flooding directly controlled the levels of the lake which, in turn affected ancient settlement patterns in the Faiyum (Hassan 1986). A series of ridges along the western edge of the depression define paleo-shorelines at 44–42, 34–39, 28–32, and 23–24 m ASL equivalent to heights of 71, 61–66, 55–59, and 50–51 m of the floodplain at Beni Suef in the Nile Valley (Hamdan 1993).

The Faiyum region has been widely investigated as early as the 19th and early 20th centuries by several geologists (Schweinfurth 1886; Brown 1892; Ball 1939). This interest arose due to the abundance of rich archaeological sites and extensive documentary records (see Brown 1892). However, these early archaeological investigations were inconsistent concerning the role of the lake and the first systematic investigation, performed by Caton–Thompson and Gardner (1929, 1934), confirmed that modern Lake Qarun is a remnant of the former great lake, Lake Moeris. Further studies were carried out by Sandford and Arkell (1929); Little (1936) and Wendorf and Schild (1976). Reviews by Hassan (1986) and Butzer (1997) have shown that past fluctuations in water availability, due to climate and human changes, caused major variations in the level of Lake Qarun during the Holocene. From the early Holocene until the Greece-Roman period, the basin received Nile water principally controlled by climate with lake levels fluctuating according to Blue Nile flow from monsoonal rainfall in Ethiopia and, to a lesser degree, to central east African rainfall via the White Nile. Since the middle Kingdom, Nile inflow has been more or less regulated by hydrological modifications

The Holocene Faiyum sedimentary sequence was investigated in surface exposures of ancient beaches, archaeological sites (Wendorf and Schild 1976; Hassan 1986; Butzer 1997, 1982; Hassan et al. 2012) and more recently in cores from modern Lake Qarun (Flower et al. 2006, 2012, 2013; Hamdan et al. 2016b; Marks et al. 2018). The early Holocene sediments of the former great lake are well known from subsurface and surface sections in the northern part of the lake (Wendorf and Schild 1976). They are related to several successive lakes called Paleomoeris (13 m ASL), Premoeris (19–24 m ASL) and Protomoeris (19–24 m ASL). Each of these lake units are separated by episodes of low stand lakes. The sediments of Paleomoeris stage are recorded only in the northern Faiyum and are represented by fluvial sands, shore facies and shallow lake bed facies of diatomite and diatomite marls, ca. 13 m ASL (Kozlowski 1983). These sediments are dated to 9948–10233 cal BP. The upper diatomite unit possesses deep fossil desiccation cracks, indicating episodes of low lake level. The deposits represent the Premoeris stage of Wendorf and Schild (1976) and consist of sand intercalated with dark grayish brown friable sediments. They obtained a date of

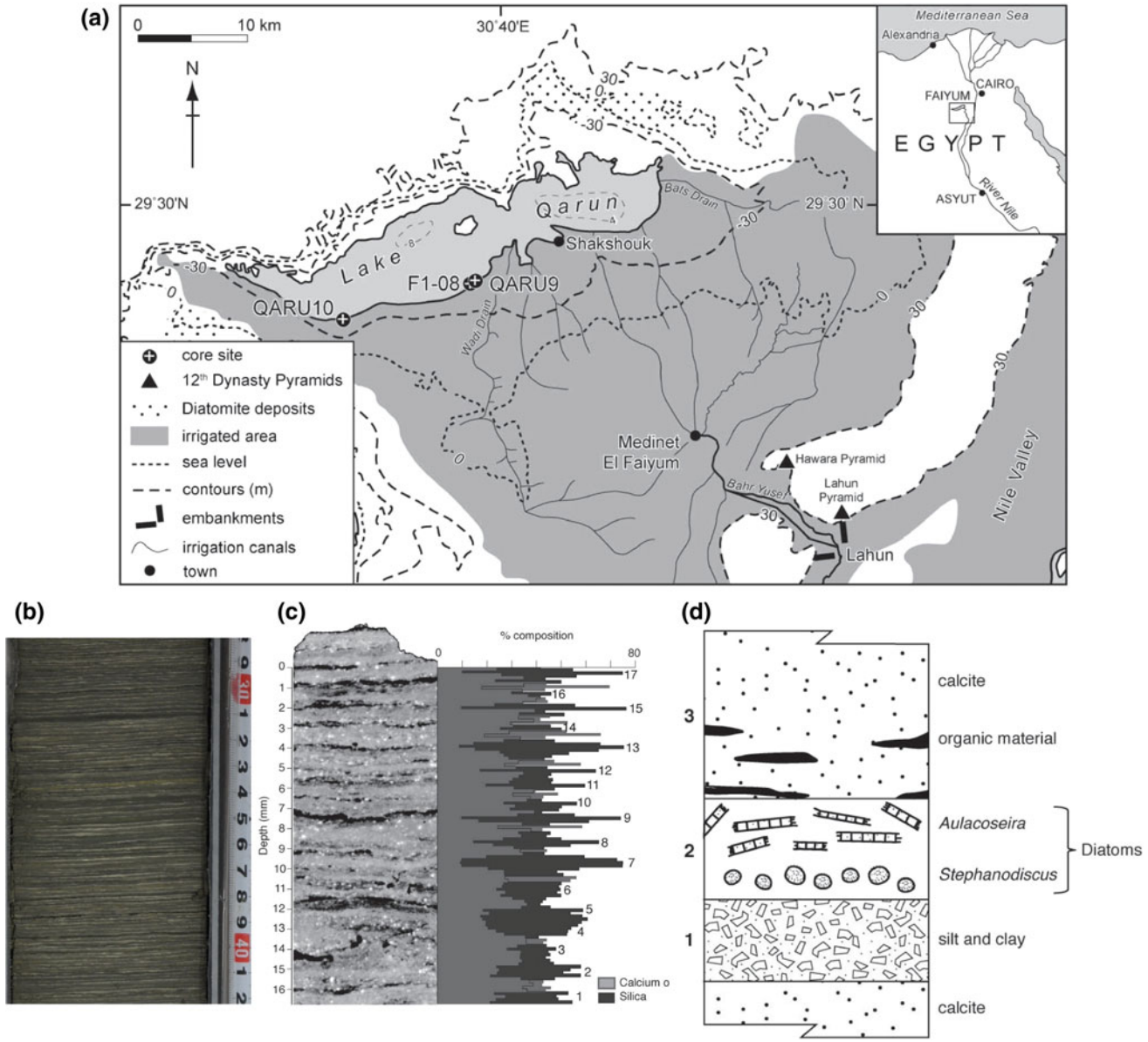

Fig. 12.7 **a** Faiyum Depression; **b** Early Holocene, non-glacial varves sub-sectionfrom a sediment core; **c** Microprobe elemental analysis of a thin section of Faiyum varve sediments showing the correspondence between the proportions of Si and Ca; **d** Diagrammatic representation of a typical varve structure in finely laminated sediment of Faiyum. See text for detail (*Source* Flower et al. 2013)

9450–8634 cal BP from charcoal obtained at an elevation of 19 m ASL, contemporaneous with a mat of swamp deposits. In Western Faiyum, deposits of Premoeris stage are banked against the eastern face of the Gisr el Hadid storm beach ridge and represented by of intercalations of beach sand and gravel with freshwater shells (Hassan 1986, Hassan et al. 2012). Terminal Paleolithic artifacts (Qarunian) were found in association with the Premoeris deposits and dated to 9064–9355 cal BP and 8445–8572 cal. BP. The sediments of Protomoeries stage consist of sand and sandy silt intercalated with dark swamp layers (19–24 m ASL) and dated to 8188–7699 cal BP.

In cores drilled at the margin and within Lake Qarun (Fig. 12.7a), the early Holocene sediments (ca. 10–8.2 cal kyr BP) is represented by varved sediments (Fig. 12.7b) corresponding to seasonal Nile flood water influx to Faiyum Lake via Howara channel (Flower et al. 2012, 2013; Hamdan et al. 2016b; Marks et al. 2018). The early Holocene varves (non-glacial) were formed in a deep lake with an absence of benthic bioturbation and with deep water anoxia (Flower et al. 2012). The varves consist of mm and sub-mm laminated sediment of calcareous clay with dark allogenic clayey silt (deposited during late summer Nile floods) time (Flower et al. 2012; Hamdan et al. 2016b). Elemental

analysis of the thin section in the varve sediments using microprobe techniques demonstrated clear geochemical differences between the laminae (Fig. 12.7c). Detailed microscopic, geochemical and micropaleontology reveal that the Faiyum varves generally consist of three laminae (Fig. 12.7d); (1) terrigenous laminae composed of angular clastic silt grains and clays indicate material of fluvial origin and could mark the effects of Nile flood (late summer); (2) a white authogenic diatom layer usually comprised of *Stephanodiscus* and then *Aulacoseira* valves formed late August or September after flood time, and (3) an endogenic calcite (micrite) layer deposited during the following summer season and ofteninter-calated with organic matter. Diatom and pollen data of early Holocene sediments in a long core from Tersa (middle of Faiyum Depression) also show abundant planktonic taxa, (e.g. *Cyclostephanos, Aulacoseira*) and high aquatic/terrestrial pollen ratios also indicating deep, open lake conditions (Hamdan et al. 2016b).

Hassan et al. (2012) studied stable isotopes of oxygen and carbon in freshwater mollusk shells from a sequence of dated paleolake deposits in the Faiyum Depression and provided an outline record of lake development during the Holocene. During early Holocene, the freshwater shells yielded more negative $\delta^{18}O$ and $\delta^{13}C$ ratios than did middle and late Holocene shells, suggesting high Faiyum lake levels and less evaporation compatible with high Nile discharge. The he isotopic composition of accretionary layers in the single *Unio* shell indicated two periods of low $\delta^{18}O$ values corresponding to two periods of water supply to the lake; Nile waters during summer flood and other due to runoff from local sources during winter rainy periods (Hassan et al. 2012). Study of the isotope composition of the accretionary layers of one *Unio* shell, indicated the existence of a short rainy season during winter time.

The middle-Holocene sediments represent the lower part of the Lake Moeris stage and are represented, in northern Faiyum, by pale brown sands, unconformably overlying older lacustrine sediments (e.g., Neolithic site Kom "W"; Caton-Thompson and Gardner 1929, 1934; Wendorf and Schild 1976). The dates associated with the Neolithic sites occupations are: 6897–6324 cal BP at 17 m ASL and 6957–6407 cal BP at 15 m ASL (Hassan et al. 2012). In southeast and southwest Faiyum, a middle Holocene beach forms a curved elongated ridge c. 20 km long from Edwa Village (16 m ASL) to Ezbet el Gebel Village in the southwest of the Faiyum (14 m ASL). The Edwa ridge dates to the Neolithic i.e. ca. 7150–5950 cal BP and extends in an E-W direction rising up to 18–14 m ASL; (Caton-Thompson and Gardner 1934; Hassan 1986; Hassan and Hamdan 2008, Hassan et al. 2012). In subsurface, middle Holocene lacustrine sediments are represented mainly by two different facies. The early middle Holocene (ca. 8–6.2 cal kyr BP) is represented by alternating homogenites layers and varve packets. The homogenite layers consist of a massive mud layer up to one cm in thickness resting on the eroded top of a laminated packet. The latter are generally thicker than the homogenite layers (several cm in thickness) and consist of horizontal mm-scale white and dark grey laminae. Subtle seismicity layers are recorded in the varve layers with clear microfolds and microfaults (Hamdan et al. 2016a). These sedimentological characteristics reflect a large deep lake. Late middle Holocene sediments (ca. 6.2–4.2 cal kyr BP), are represented by massive stiff clay with white carbonate and iron oxide layers, indicating drop in lake level. Isotope data show increasing ^{18}O enrichment and increasing benthic diatoms at end of the Holocene indicate lowering in lake level and increase aridity (Hassan et al. 2012).

Late Holocene lacustrine deposits occur at 35 m below sea level (Hassan et al. 2012). Based on the elevation, stratigraphic position and archaeological context, it is likely that lacustrine sediments in this area date to a time interval from the pharonic late Period to the Roman period; i.e. from ca. 3000 to 1600 cal BP (Caton-Thompson and Gardner 1934; Wendorf and Schild 1976; Hassan et al. 2012). Late Holocene sediments consist of 9 m of beach sand intercalated with scattered diatomaceous deposits. In subsurface, late Holocene lacustrine sediments (4-0 cal kyr BP), are represented by massive highly bioturbated, semi-soft silty clay, few diatoms, and becoming more sandy upwards with red potsherds near the top.

The analyses of the Faiyum cores reveal intersecting results about fluctuations in lake level, which reflect variation in the Nile floods and the climatic conditions on the African Nile headwaters. The lake was high large fresh water lake during early Holocene and then subjected to an abrupt drop the level at 8.2 cal kyr BP. before rising again from 8 to 6.2 cal kyr BP. From 6.2 to 6 cal kyr BP, the lake level dropped markedly and thin laminate sedimentation ended permanently. During 6–4.5 cal kyr BP, the lake became small and its level oscillated between 10 and 0 m ASL. At 4.5–4.2 cal kyr BP, the lake show great drop in lake and most parts of the lake were almost desiccated. Ancient modifications to regulate inflow to the Faiyum basin were notably introduced during the 12th Dynasty to compensate for fluctuations in water availability caused by variations in the Nile floods (Hassan and Hamdan 2008). Later, more hydrological modifications were introduced during Ptolamic time, to extend and regulate agricultural lands in the Faiyum (Hassan 1986).

12.3 Quaternary Sediments and Landforms Related to Humid Climate

Sediments related to humid periods commonly occur in the present day hyper-arid Egyptian deserts; they are represented by lacustrine, alluvial, solution and karstic features

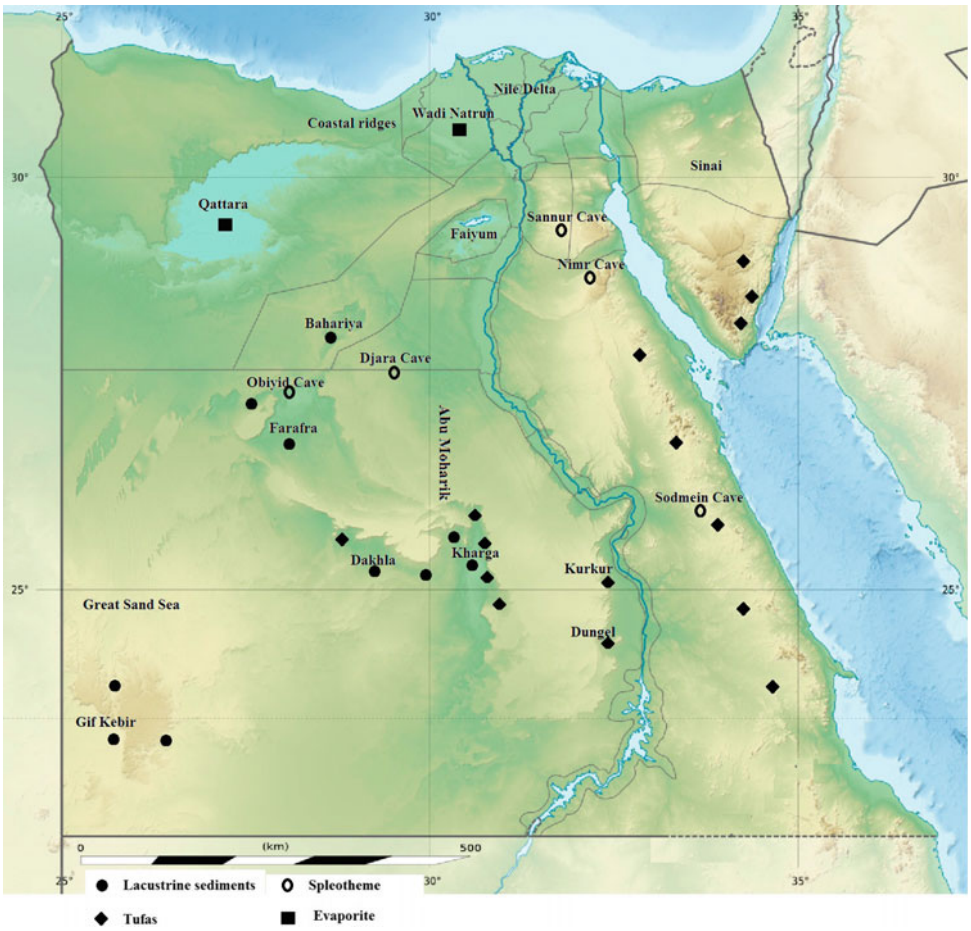

Fig. 12.8 Distribution of Quaternary sediments in the Western Desert of Egypt

(tufa and speleothem deposits) (Fig. 12.8). These deposits are well dated and associated with archaeological material indicate wetter conditions during Quaternary. Some of these landforms (i.e. karst, caves and alluvial) are inherited from a previous wetter climate but in many areas still dominate despite a major drying of climate. The hyperaridity has preserved these landforms and landscapes, which in wetter areas would have been totally eroded.

12.3.1 Lacustrine (Playa) Sediments

A playa is a Spanish term meaning a shore or beach; it is typically a dry, vegetation-free, flat area at the lowest part of an internally drained desert basin where ephemeral lakes form during wet periods. They are underlain by stratified clay, silt, and sand, and commonly, by soluble salts. Playas occur in intermontane basins throughout the arid lands. Indeed, these are many confusing definition in terms playa, playa lake and sabkha. To eliminate these confusions, Briere (2000) proposed that: (1) playa is a discharging intercontinental basin with a negative water balance, remaining dry 75% of the year, and often associated with evaporates; (2) Playa lake: a transitional category between playas and lakes, essentially a flooded playa; (3) Sabkha: a shallow basin limited to marginal marine settings and associated with several percent gypsum or gypsum, partly laminae due to preferential halite dissolution during flooding. Generally, playas have four characteristics (Motts 1969): (1) an area occupying a basin or topographic valley of interior drainage; (2) a smooth barren surface that is extremely flat and has a low gradient; (3) an area infrequently containing water that occurs in a region of low rainfall where evaporation exceeds precipitation, and (4) is an area of fairly large size (generally more than 600–1000 m in diameter).

The term playa was first used in Egypt to describe certain Quaternary sediments in Kharga and Dakhla Depressions (Beadnell 1909). Investigations of playa deposits intensified since the 1970s in conjunction with archaeological investigations of the middle Pleistocene and Holocene prehistory of the eastern Sahara. The playas occur as basin-fill deposits ranging in size from a few hundred m^2 to over a hundred km^2. The depth of the playa basin does not exceed several meters; 2.5–8 m deep in Farafra (Hassan et al. 2001); about 3–4 m in south Farafra (Embabi 1999); up to >10 in Nabta playa (Wendorf and Schild 1980). The playa basins have

five origins; (1) karstic e.g. Farafra Depression (Hassan et al. 2001; Hamdan and Lucarini 2013; (2) wind deflation e.g. Bir Kesiba playa (Wendorf and Schild 1980); (3) damming blockage of the wadis by sand dunes e.g. Gilf Kebir Plateau (Kröpelein 1987); (4) interdunal troughs e.g. Nabta playa (Wendorf and Schild 1980) and (5) ponding of irrigation waters, e.g. Kharga and Dakhla (Caton-Thompson 1952). Playa sediments consist of several meters of stratified, fine-grained silt intercalated with sand and occasionally gravel that either appear as flat areas with scarce or no vegetation or as fields of yardangs. They exhibit several sedimentary structures of fluvial environments, e.g. normal grading, mud drapes and cut and fill structures. Past lacustrine environments are indicated by e.g. flat laminated sand silt intercalation and beach gravels. Aeolian sand is often intercalated with the playa silt.

The playas are distributed from Siwa in the north to the southern limits of Egypt, as at Nabta, and lie mostly at the foot slopes of escarpments at the edge of depressions in the Western Desert. Here there are more than 100 playas whose areas exceed 2 km^2 (Embabi 1999). Of these, there are 25 in Dakhla Depression (Brookes 1989 and 1993), 21 in Kharga Depression (Hamdan 1987) and 24 in Farafra Depression (Hassan et al. 2001; Hamdan and Lucarini 2013). Other playas smaller than 2 km^2 are spread. Occur not only in the large depressions, but also in small ones on the plateaus and in the southern plains.

The current amount of rainfall in the southern part of Egypt is insufficient to sustain playas. However, occasional heavy rainstorm in the depressions of the Western Desert can create small pools and puddles. In the northern part of the Egypt, where rainfall is limited to 50–100 mm/year, winter rains over the El-Diffa (Marmarica) Plateau along the Mediterranean Coast create shallow pools in small karstic depressions. Some of those pools often last for about a month. The saline lakes in the Siwa Depression today are not playas in the sense used to describe the Holocene playas of the Western Desert. The Siwa lakes, such as Siwa, Aghourmi, Zaytoun, and Maa'ser are fed by limited groundwater discharges from along fault lines. With very limited influx of rainwater and a high rate of evaporation the lakes are saline. Accordingly, their influx salts levels fluctuate seasonally depending on the seasonal differences in evaporation rates. Salt deposits are found both at the bottom of these lakes and along their shorelines. The Holocene playas of the Western Desert are also different from the Wadi el-Naturn lakes (see below), which are fed by seepage from Nile water, and are enriched in sodium carbonate, bicarbonates and chloride. Playas are also distinguished from Birket Qarun in the Faiyum Depression, which is now fed, like the newly created Wadi Rayan Lake, by irrigation drainage water.

The playas were favorable places for human habitation during Holocene as attested by the abundance of artifacts in association with playa sediments compared to their paucity or total absence elsewhere. Those playas fed by surface runoff and/or by spring water would have been hospitable places for people, especially during episodes of dry climate and dry seasons of the year. Moreover, playas are a main target of modern national agriculture reclamation projects in the western Desert because of their lithological characterizes and low salinity soils. Subsequently, however, these projects represent great threats to the prehistoric archaeological sites. Indeed, the threats are very high in Bahariya, Dakhla and Kharga areas where almost all playas are disappearing.

Chronologically, there are two playa generations in Egypt, based on dating techniques and associated archaeological materials. The first is Pleistocene and lakes are mainly large, permanent and mainly fed by ground water with little surface water. In contrast, Holocene playas are typically smaller, temporary and mainly formed by surface discharge (few were fed by ground water).

12.3.1.1 Pleistocene Lacustrine Sediments

During the middle Pleistocene, several large lakes existed in central and southern Egypt. The Bir Tarfawi/Bir Sahara region contains sediments recording a series of discrete lake phases ca. 230–60 kyr BP (Wendorf et al. 1993). In the Bir Tarfawi Depression, Pleistocene sediment records significant climatic and environmental changes during the last half million years (Blackwell et al. 2017) with distinct three playa generations. The older existed at the periphery of the depression at an elevation of 247 m ASL associated with Acheulean artifacts. The second playa (White Lake), existed in the north-central part of the depression, and dated to 248 ± 28 and 218 ± 27 kyr BP (Hill and Schild 2017). The third generation (Grey-Green Lake) at an elevation of 242 m ASL and dated to 105 ± 15 to 141 ± 3 kyr BP (Blackwell et al. 2017).

In the last two decades, there are several hypotheses connecting the depressions of southwestern Egypt with several mega-lakes. Maxwell et al. (2010) used digital elevation models- but did not take into account deflation during arid periods- to assume the existence of intensive middle Pleistocene lakes in the Tarfawi-Kiseiba-Toshka region of southern Egypt. Moreover, another mega-lake would have covered an area extending from the Sudanese border north to the Kharga and Dakhla Oases during the late Pleistocene (Issawi and Osman 2008; Maxwell et al. 2010). Detailed investigations of exposed sections of these mega-lakes show different lithological characteristics which may indicate local lakes rather than one mega-lake (see Hill and Schild 2017). The only evidence supporting a late Pleistocene mega-lake is represented by bones of Nilotic fish (Van Neer 1993). These fossils are also used as an indication of an ancient channel transporting Nile waters to Tarfawi-Kiseiba Depression (Van Neer 1993; Issawi and Osman 2008).

Dakhla Depression also hosted several large Pleistocene lakes (and perhaps, at times, one very large lake; Smith 2012), with a potential combined area of ca. 1700 km^2 (Brookes 1993; Ashour et al. 2005; Kieniewicz and Smith 2009; Smith 2012). They are preserved in two basins in the Dakhla Piedmont and represented by two facies: Facies A and Facies B (Brookes 1993). Facies A comprises horizontal, parallel-stratified turbidite beds; more sandy in lower part and more muddy in the upper bed. Most of the sediments were reworked mainly from Dakhla shale. Facies B comprises two sub-facies; sub-Facies B1, comprises thin couplets of large-crystal gypsum and clastics and includes 10–20 cm beds of biogenic lacustrine marl, which indicate deposited in saline lakes (Brookes 1993). Sub-Facies B2 consist of massive, pale-brown muddy sand. An exceptional event associated with the Dakhla playa, is a mid-Pleistocene catastrophic meteoritic impact event which scattered 'Dakhla Glass' around the depression surface (Osinski et al. 2007, 2008). The Dakhla Glass has been found embedded in the pale lake beds and in lags on eroded outcrops around the depression. The ages of Dakhla Glass average at 145 ± 19 kyr BP by 39Ar/40Ar so constraining the age for deposition of the lacustrine units bearing the glass (Renne et al. 2010).

At Um Dabadib, in the north Kharga Depression, remnants playa sediments are heavily dissected and associated with middle Paleolithic artifacts. They are represented by a 11.5 m thick section filling a trough eroded into the lower pediment (Hamdan 1987). The section begins with layer of about 80 cm of very pale brown aeolian sand; then overlain by about 200 cm of thin laminated playa silt with abundant shale flake and brown aeolian sand. The rest of the section (about 8 m) is represented by thick layers of brown massive playa silt and clayey silt with abundant shale flakes and desiccation cracks and Dikika structure. The top part of the playa sediments may be eroded and shows the development of a brown palaeosol which has been truncated and is now overlain by a gypseous crust with dark patinated sandstone slabs. The formation of gypseous deposits suggests high ground water and an arid climate during the late Pleistocene (Hamdan 1987). At Abu el Agl playa, three OSL dates were given for middle Paleolithic playa sediments; 79 ± 20; 67.6 ± 10.7 and 110 ± 18 kyr BP. One ^{14}C date on aostrich eggshell at the top of the middle Paleolithic playa sediments yielded a date of 20,580 + 280 BP (Ashour et al. 2005; Donner et al. 2015).

In the Eastern Desert, the Sodmein Playa (ca. 40 km north-northwest of the Quseir) is one of the rare Pleistocene playas with Pleistocene human occupation (Kindermann et al. 2018). Based on the associated artifacts, the playa is dated to early phases of MIS 5 (i.e. 118 ± 8 kyr BP). The playa sequence consists of the following units from base to top: (1) thick aeolian sandy unit with very thin silt laminae and lag gravels, indicating slight water events; (2) laminated sandy silts with gravel layers, indicating fluvio-lacustrine sedimentation during wetter climate conditions; (3) thick and massive, calcareous silts, representing an ephemeral lake; (4) miixture of gravels, sand and some silt accumulations. Small mollusks were found in several sections of the entire profile. Similar playa was described by Hamdan (2000b) at Esh Malaha area, north Eastern Desert, with sequence of intercalated calcareous silt, sand and gravel and dated by U/Th dating to 45–65 kyr BP.

In Sinai, thick section of Pleistocene fresh water lake sediments was recorded in environs of Wadi Feiran and Tarfat (Gladfelter 1988, 1990). The lakes were developed at different levels, impounded by dykes who formed barriers across the major wadi system and also acted as aquicludes (Issar and Bruins 1983). The lacustrine sediments of Wadi Feiran consist of interbedded alluvial, palustrine and colluvial sediments. A major portion of the original sequence has been eroded away and badland terrain occurs where extensive remnants of the beds are found. A complete stratigraphic section of aggragation is not preserved at a single location, but within Wadi Abu Nashre, an unusually thick occurrence of these deposits is preserved and associated with the Upper Paleolithic sites (Gladfelter 1990). Marl in the Pleistocene contains mollusk, ostracods and charophytes, species from habitats of freshwater ponds that existed in shallow depressions on alluvial bottoms (Gladfelter 1992). The mollusk assemblages as well as fish bones recovered archaeologically indicate that the ponds were perennial features. Radiocarbon assays obtained from certain marl units establish the late Pleistocene age of these deposits (i.e. 29,100 ± 460 BP (SMU 1845); 18,910 ± 200 BP).

Pleistocene playa sediments are also recorded at Northern Sinai (Sneh 1982; Goldberg 1984; Kusky and El-Baz 2000; Embabi 2017). The Pleistocene lakes occur in wadis and low areas between hills and mountains (Kusky and El-Baz 2000) and sometimes formed behind sand dune dams (Sneh 1982). In the Quseima area, one of the tributaries of Wadi El Arish, the sediment begins with early middle Paleolithic gravels (90–65 kyr BP), overlain by unit of sands, clays and silts dated to ca. 33.8 kyr BP (Embabi 2017). Some of the fine-grained sediments are interpreted as lake deposits, although many of them probably existed for a short period only. Other lakes may have persisted for longer periods, as indicated by the presence of clays with ostracods, inter-bedded with horizontal silt and sand layers of Upper Paleolithic (Kusky and El-Baz 2000).

Abu-Bakr et al. (2013) summarize the geomorphic evolution of the paleodrainge and paleolakes in North Sinai. They mapped the ancestral course of Wadi El-Arish by integrating a Radarsat-1 image with SRTM data in synergy with optical images and field investigations. A segment of the former drainage course with a length of 109 km and a width of 0.5–3 km was discovered beneath the sand dunes

west of Gabel Halal. The former course of Wadi El-Arish was dammed as a result of recent structural uplifting (anticlinal fold) at Wadi Abu Suwera. This structural high blocked the NW pathway, and forced the flow direction to deviate to the NE through the gorges of Talet El-Badan and Gabel Halal, respectively. Three major paleolakes have been identified along the main course of Wadi El-Arish within structurally controlled depressions formed due to the anticlinal ridges of the Syrian Arc System in North Sinai. These paleolakes were most likely developed behind the folded hills in two main stages, interrupted by the deviation of the river course. During the first stage, the southern paleolake developed from excess rainfall in the upper reaches of Wadi El-Arish, where the river was probably blocked and failed to reach the Mediterranean Sea. The central and northern paleolakes were formed in the post-deviation stage and the latter are estimated to be the largest of the three paleolakes (about 337 km^2).

Another controversial playa called "armored playas" (Said 1990), are extensive sheets of playa deposits which are veneered by a layer of white nodular chalcedony cobbles up to 15 cm in diameter embedded in a reddish brown matrix. Issawi (1971) considered that these playas were related to doming movements and structure lines. Other studies (e.g. Haynes 1980), however, has shown that the chalcedony cobbles seem to have been formed in standing bodies of water, rich in sodium carbonate and silica having a pH of 9.5 or higher (Said 1990). The age of these playas is not known, but they are certainly older than Neolithic (i.e. Pleistocene).

12.3.1.2 Holocene Playas

Holocene playas are the most widespread landforms in the lowland of the Western Desert of Egypt and primarily associated with Neolithic sites. Generally, from the early to mid-Holocene (ca. 11,500–5000 calBP), playa sediments of the Western Desert indicate a vivid climatic change, from hyperaridity to semi-aridity and back to its present hyperarid state (Hoelzmann 2002). It seems that, playa deposition started in mountainous areas much earlier than in the lowlands and stable conditions were established soon after the regional rise in groundwater. By 8 cal kyr BP, optimum conditions prevailed throughout Western Desert as documented by playa sediments which prove the existence of stable freshwater lakes. The decline of the wet phase started earlier in the north (ca. 7.5 cal kyr BP) and later in the south (ca. 6 cal kyr BP). The end of playa sedimentation in Western Desert can only be placed tentatively around 5 cal kyr BP.

The lacustrine deposits at Nabta Playa have a direct stratigraphic relationship with many archaeological sites associated with the early Neolithic and range in age from ca. 9.3 to 7.3 cal kyr BP. These are El Adam, El Ghorab, El Nabta, and Al Jerar (Wendorf and Schild 1980). The base of the playa sequence is represented by phytogenic dunes which developed before the formation of the earliest lacustrine silts. The dune sands are overlain by beach sands containing freshwater gastropods which, in turn, are overlain by reddish brown playa silts with blocky structure. Based on pollen, diatom, and geochemical data, the lakes water level began to rise at ca. 8.4 cal kyr BP, reaching a maximum at ca. 8 cal kyr BP and persisted until ca. 7 kyr BP, around 6.2 kyr BP, the modern phase of hyperaridity began in the Eastern Sahara and the area was abandoned.

In Dakhla Depression, Brookes (1989) identified three sets of Holocene playa deposits. The first consists of playa sand, in places with redeposited carbonate sand and overlying gravelly slope wash andthen with reddish brown aeolian sand. This section identified from Locality A, is dated to $\geq$8.7 cal kyr BP. In another locality (Area B), 8 m thick playa sandy silt, capped by a halite-rich crust and overlain by massive, angular limestone gravel. The playa deposits of this setion are dated to => 8270 BP. In another area (Locality C), playa deposits consist of pale brown silty sand with gypsum encrustations dated to 7.8–7.1 cal kyr BP, or younger. The top of Area C shows inactive springs. Brookes attributed much of the variability to local differences within the depression.

Two generations of playa exist at Um Dabadib; early and middle Holocene playas (Hamdan 1987). The early Holocene playa is ca.7 m section of massive playa silt at the base with a thick unit of aeolian sand-thin playa silt intercalation in the middle and thick scree of large limestone boulders and reddish brown palaeosol at the top. It is associated with terminal Paleolithic artifacts which date to the early Holocene. In the Abu Tartur basin, playa sediments yield OSL dates ca. 9.4 cal kyr BP to about >ca. 7.93 cal kyr BP and associated with several temporary occupations of hunter gatherers associated (Bubenzer et al. 2007). One OSL date yielded 9.1 + 1.6 cal kyr BP in the Abu el Agl playa basin (Ashour et al. 2005; Donner et al. 2015). Middle Holocene playa exposures in the center of the Umm el Dabadib basin are represented by a massive homogeneous lacustrine deposit and associated Neolithic artifacts. One ^{14}C dating on ostrich eggshell associated with younger playa sediment at Umm el Dabadib yielded 7220 $\pm$ 150 cal BP (Hamdan 1987); a corresponding playa deposit in the Abu Tartur basin is dated to about 7200–6300 cal BP (Bubenzer et al. 2007). Playa dates of 6230 $\pm$ 90 BP and 5980 $\pm$ 90 BP were recorded at Abu el Agl playa (Ashour et al. 2005; Donner et al. 2015).

Several Holocene playa generations are evident in Farafra Depression (Barich and Hassan 1987; Hassan et al. 2001; Hamdan and Lucarini 2013). Early Holocene playa deposits are represented by massive mud with thin, gypsum crusts and iron oxide stains, suggesting deposition under warm, arid conditions and short wet periods sufficient to form shallow temporary lakes (Hassan et al. 2014). The deposits from the next moist episode in Farafra are recorded at Ain Raml where

they are dated to 9650 ± 190 cal BP. At Wadi Obeiyid, the playa deposits are exposed in a series of yardangs, consisting of a sequence of mostly white to very pale brown playa mud interbedded with cross-bedded sand and fluvial gravel in the lower unit (8080 ± 60 cal BP). The middle unit of this sequence is dated on in situ charcoal 7725 ± 60 to 7320 ± 110 cal BP. (Hamdan and Lucarini 2013; Hamdan 2014a, b). The youngest deposits at Wadi Obeiyid Playa are preserved at a rock shelter and consist of a intercalation of white, angular, chalk rubble in a friable, calcareous loam yielding a radiocarbon age of 6050 ± 75 cal BP (Hamdan and Lucarini 2013; Hamdan 2014a, b).

In Bir Obeiyid, Farafra Depression (Fig. 12.9a), three Holocene playa generations were described by Hamdan and Lucarini (2013), P_I, P_{II}, P_{III} (Fig. 12.9b). The early Holocene playa (P_I) sediments occupy a closed basin in the higher reaches of the Bir El-Obeiyid Depression (ca. 90 m ASL). One ^{14}C dating of 10,721 ± 325 cal BP is given to this basal Playa "P_I" (Hamdan and Lucarini 2013). The playa sequence begins with aeolian sand and then intercalates upward with thin laminae of white calcareous playa mud with desiccation cracks. The topmost of playa "P_I" sequence is represented by thick limestone rubbles mixed with gypsum and aeolian sand. The early Holocene playa is truncated by white subangular chalk rubble, grading vertically into the underlying bedrock chalk and horizontally to the playa deposits, probably indicating severe mechanical weathering under subaerial conditions during deposition. Temperature variations coupled with freezing of moisture trapped in fissures would have been sufficient to produce angular clasts and limestone blocks. The white color of the deposits indicates that temperature and rainfall were sufficiently low to mobilize iron oxides (Hassan et al. 2001). This phase of rubble formation is dated to 8079 ± 107 cal. BP and therefore related to the global 8.2 cal kyr BP cold phase (Hamdan and Lucarini 2013).

The middle Holocene playa "P_{II}" occupies the deepest part of the Bir El-Obeiyid Depression (ca.75 m ASL) and is mainly eroded into yardangs (up to 3.0 m above the surrounding depression). The sediments of playa "P_{II}" overlythe deflated surface of the limestone rubble of Playa "P_I" and are dated to 7510 ± 107–6407 ± 84 cal. BP. They consist of mainly of fine sand, silty sand and silt, deposited

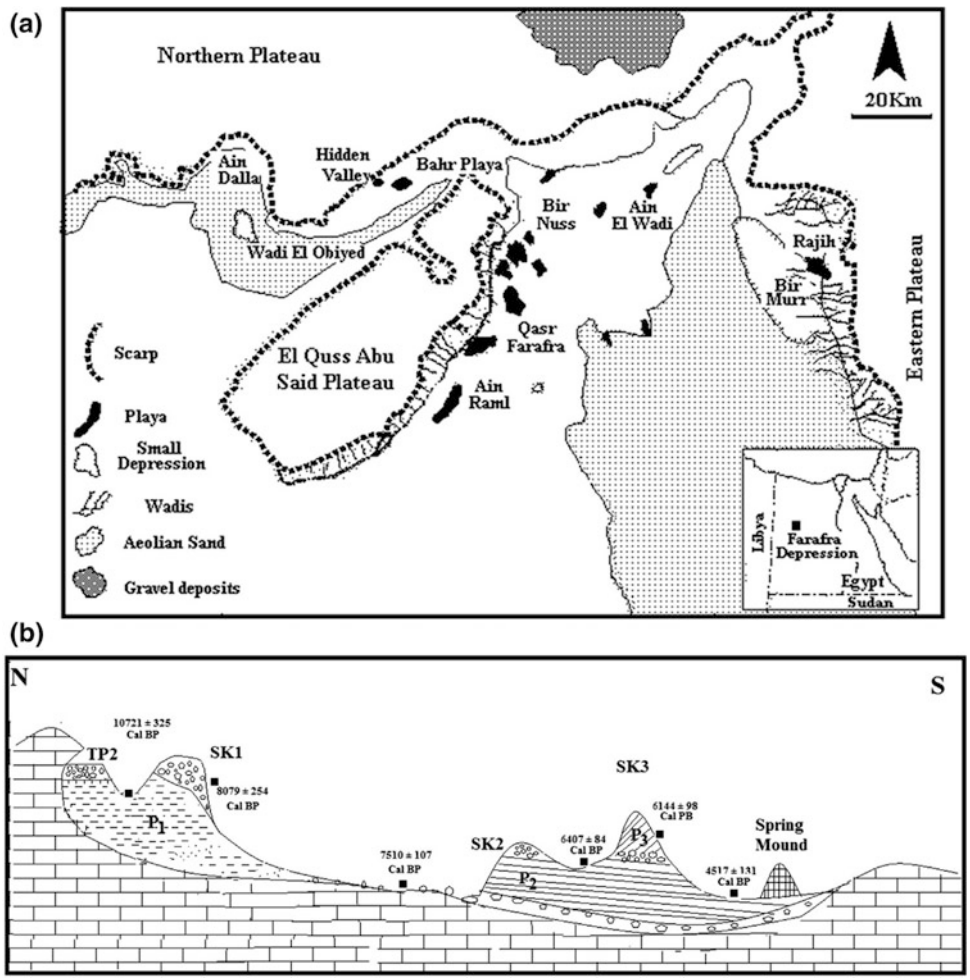

Fig. 12.9 **a** A map of the Farafra Depression showing locations of Sheikh El-Obeiyid area and other playa deposits in the Farafra Depression: **b** N-S geological cross section at the Bir El-Obeiyid Playa, showing that early Holocene; **c** middle Holocene playas "PII" and "PIII" (*Source* Hamdan and Lucarini 2013)

by two water sources. The calcareous playa sand and silt are cemented by freshwater carbonate and contains thin laminae of algal tufa, indicating a groundwatersource. The continuous sedimentation and absence of aeolian sand layers probably reflect stable, wetter conditions. The last phase of "P_{II}" is marked by a layer of grain-supported angular limestone rubble, indicative of a short dry and cold episode.

Late middle Holocene playa "P_{III}" is separated from "P_{II}" by thin limestone rubbles and consists of thin layers of playa silt intercalated with thick aeolian sand. One ^{14}C date of 6144 ± 98 cal. BP. is given for playa "P_{III}". The existence of several aeolian sand layers and a highly desiccated playa silt layer indicate that the climate was highly episodic during the deposition of playa "P_{III}". The last stage of the evolution of the Bir El-Obeiyid playa basin is represented by spring activity. The spring mounds exist in the deepest part of the basin and attain a height of about 10.0 m above the deflated level of the Holocene playa. This spring fed water to the playa in the late Holocene (4517 ± 131 cal BP).

Holocene playa deposits in Siwa consist of yellow and brownish yellow sand to loamy sand followed upward by very pale brown to yellow loamy silt. Granulometric analysis and X-ray diffraction analysis of the clays reveal a change through time toward greater surface runoff under gentle rainfall as suggested by an increase in the silt-clay content and kaolinite (Hassan 1976). This phase is dated to ca. 8.6–8.1 cal kyr BP and is correlated with the Nabta Phase I (8.6–8.2 cal kyr BP). In Bahariya Oasis, investigations at El-Heiz reveal mud pan deposits dated to c. 6.9–6.3 cal kyr BP (Hassan 1979b). They consist of a basal unit of aeolian sand with salt crusts followed by playa silt topped by aeolian sand.

Holocene playa sediments existed around Djara Cave region (see below), with a maximum thickness of 2 m (Kindermann et al. 2006). They consist of reddish sand and silt and capped with limestone scree and burned stones from hearth mounds (Bubenzer and Hilgers 2003). Luminescence dates of the playa sediments range between 6.8 ± 0.5 and 8.67 ± 0.5 cal kyr BP (OSL) and show that the entire playa sediments accumulated during the early and mid-Holocene (Bubenzer and Hilgers 2003).

In Gilf Kebir, Holocene playas are developed by blockage of wadis by sand dunes (Maxwell 1980; Pachur and Röper 1984; Kröpelein 1987). In Wadi Bakht, more than 10 m of inter-layered lake and aeolian deposits were deposited upstream from a dune dam (Maxwell 1980; Kröpelein 1987). The age of these playa sediments varies between 8200 ± 500 and 6080 ± 420 cal BP (Kröpelein 1987). Based on sedimentary analyses and archaeological context, the Gilf Kebir experienced wet climate between 9.5 and 6 cal kyr BP; between 6 and 5 cal kyr BP, the climatic conditions shift toward moderate aridity with the maximum rainfall of 100–150 mm (Kröpelein 1993).

12.3.2 Alluvial Deposits

Gravel terraces along wadi margins in the Egyptian deserts record relatively short distance fluvial transport of sediments off the high plateaus and mountainous areas (Caton-Thompson 1952; Brookes 1993). External drainage of many desert wadis is covered with Holocene alluvial and aeolian sand dunes which seem to have accumulated in response to the rising sea leve. Records of earlier deposits and terraces are known along many of wadis. In Western Desert, fluvial sediments are difficult to recognize, they either eroded away or modified and hidden by dune sands. In the present review, two types of Quaternary alluvial sediment are describe these are buried radar rivers and inverted wadis.

12.3.2.1 Radar Rivers

The term "Radar Rivers" refers to almost fully aggraded Tertiary basins and valleys that lie beneath the sand sheet in southern Egypt and northern Sudan. These features were first recognized when radar images produced by the imaging radar (SIR-A) experiment aboard the November, 1981 flight of the space shuttle Columbia (McCauley et al. 1982). Radar Rivers have been described under different synonymy; e.g. Radar Rivers and Subsurface Valleys (McCauley et al. 1982, 1986; Ghoneim et al. 2007); Paleo-rivers (McHugh et al. 1988); Paleo-drainages (McCauley et al. 1986; Schaber et al. 1997) and Paleo-channels (El-Baz et al. 1998).

Three types of "Radar Rivers" have been recognized in the SIR-coverage of the Eastern Sahara (McCauley et al. 1986): (1) a Radar River (RR-1) is a broad, aggraded valley or basin with stubby tributaries, 10 to 30 km wide and up to hundreds of kilometers long. Wadi Arid is the type area in Egypt. The RR-1 valleys as seen on SIR-A images are strikingly similar in scale and overall appearance to the Nile River Valley some 300 km to the east (McCauley et al. 1982). These broad valleys are now almost completely aggraded with fluvial deposits that underlie regional aeolian sand sheets; (2) Radar River RR-2 type (braided channels inset in the RR-1 valleys), consists of groups of narrow, 0.5- to 2-km-wide. The type area for these braided stream complexes is Wadi Safsaf. The islands are formed of RR-1 valley fill, which consists of sand and fine pebble alluvium cemented by secondary calcium carbonate. Nodules of $CaCO_3$ are commonly disseminated in the upper 2 to 3 m of the valley fill; (3) Radar River (RR-3) (narrow, long, bedrock-incised channels), are partly visible on the ground and on Landsat in areas where the sand sheet is patchy. They are conspicuous on SIR because the dark response of their unconsolidated channel fills contrasts with the brighter response of surrounding bedrock.

The Radar Rivers are relics of a Tertiary system that drained the Eastern Sahara before the onset of general aridity in the early Quaternary and again by intermittent running

water during the Quaternary pluvial episodes (McCauley et al. 1986). Red Sea Mountains are the main source of water for these valleys (Issawi and McCauley 1993). Three major paleo-drainage systems developed in response to tectonic uplift and sea level changes from late Eocene to late Pleistocene. They represent a part of a regional Tertiary system called "the Trans-African Drainage System" (Issawi and McCauley 1993). These systems are named as the Gilf system, the Qena system, and the Nile system (See Sect. 2.1.1). McHugh et al. (1988) have shown that at least the upper 40 m of these ancient valleys (which are hundreds of meters deep) are now filled with late Pleistocene alluvium, mainly sand and fine gravels. These sediments became cemented by calcium carbonate deposited under fluctuating groundwater conditions. The widespread alluvium and ubiquitous carbonated deposits imply climatic conditions with annual rainfall approaching 400–600 mm (McHugh et al. 1988). The last stages of aggradation are archaeologically dated by the Acheulean remains incorporated within the alluvium. Uranium-series age determinations on 25 carbonates samples have yielded modal dates for episodes of carbonate formation: >300, 212, 141 kyr BP and 45 kyr BP.

SIR-C data in the southern part of the Western Desert and Northern Sudan reveal the existence of four major drainage lines formed by the Toshka Hydro-System and drained internally in a basin into the Selima Sand Sheet (El-Baz et al. 1998). Ghoneim et al. (2007) used SRTM data to reveal wide paleo-river courses emerging from the Gilf Kebir plateau to the south, and draining towards the east (Fig. 12.10). These channels represent the upper stream area of a large paleo-drainage system and are believed to be responsible for the groundwater resources that supply productive agricultural farms in East Uweinat area of south-western Egypt. The shape of the derived SRTM contour lines around the exits of these channels along the mountain front suggests the existence of a broad, sloping depositional landscape caused by the coalescing of a number of alluvial fans to form a large Bajada (Ghoneim et al. 2007).

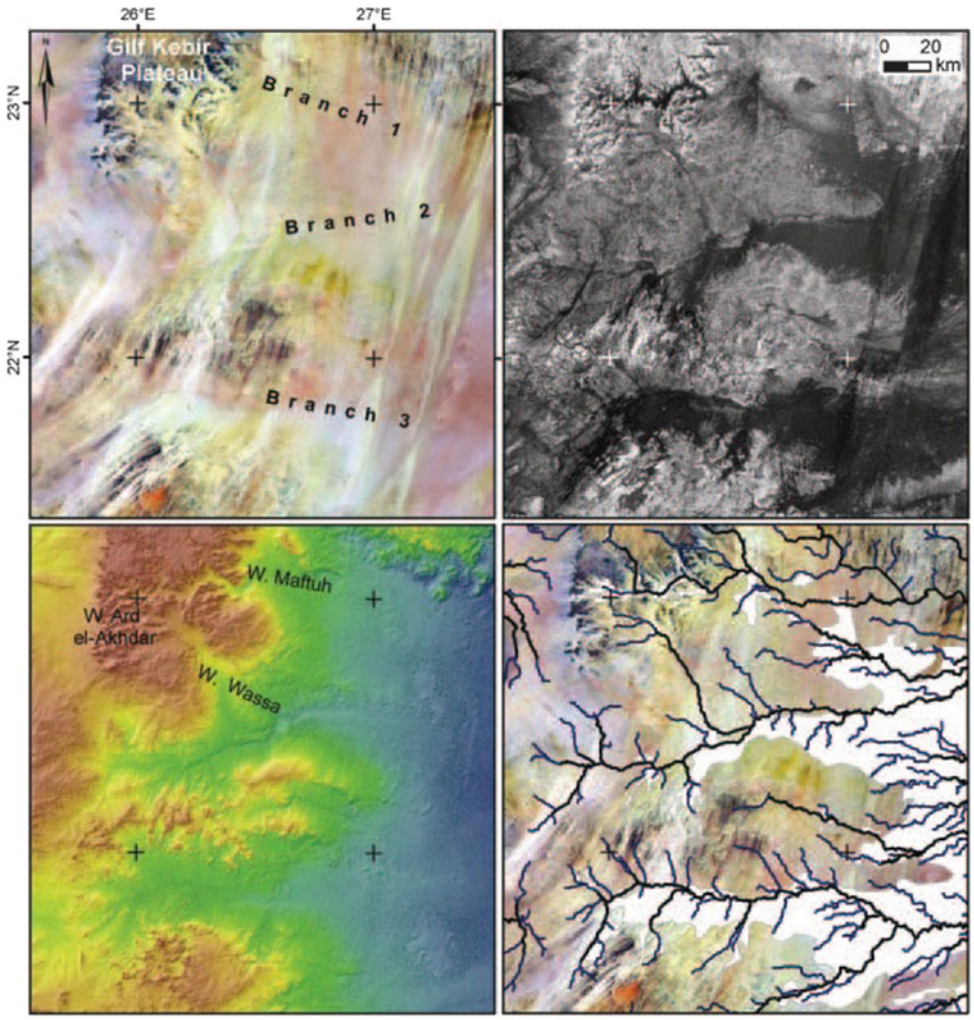

Fig. 12.10 **a** the ETM + image of the three wadi branches of the Gilf Kebir area; **b** Radarsat-1 image of these drainage networks; **c** SRTM data of Gilf Kiber area; **d** The digitized radar-dark feature (white spaces) with the SRTM-derived channels (dark lines) overlain (*Source* Ghoneim et al. 2007)

12.3.2.2 Inverted Wadis

Inverted wadis are elongated, sinuous and sometimes branching gravel ridges which stand out above the rock cut surfaces (Giegengack 1968). They were first noted by Knetsch (1954), who described one gravel-capped sinuous ridge in Egyptian Nubia and called it as a "pseudo-esker", by analogy with glacial deposits on the plains of northern Europe (Zaki and Giegengack 2016). Inverted wadis in SE Egypt form a rectangular pattern, with an average length extending for about 10 km, maximum width not exceeding 300 m, and height of as much as 20 m (Fig. 12.11). Inverted wadis developed via cementation of minerals causing surface armoring (Giegengack 1968). The minerals, which cause the cementation, are calcium carbonate, hematite, silicon dioxide, and iron oxide.

Inverted wadis occur throughout the Lake Nasser region area, on both sides of the Nile. Because blown sand covers much of the ground surface in the Western Desert, inverted wadis appear on air photos as dark traces in a sea of pale sand. Inverted wadis in the Eastern Desert, east of the Nile, are also abundant, but, since they represent dark traces on dark bedrock, they are not as easily identified from air photos as those in the Western Desert (Zaki and Giegengack 2016). Sediments of inverted wadis consist of indurated poorly sorted gravel and coarse sand deposits with abundant rolled Acheulean artifacts (Giegengack 1968). The gravels are mostly dark brown limestone and chert. They range in size from pebbles, poorly sorted, rounded to sub-rounded and sometimes discodial in shape embedded in pale brown sandy matrix. The stratigraphic framework of the formation of thse inverted wadis include three gravel units; (1) Early Nile Gravel deposited in Nile flood-plain gravel with Acheulean artifacts; (2) Wadi Conglomerate topographically inverted to form sinuous ridges after deposition of early Nile gravel; and (3) Late Nile Sediments (ca. 27–5 kyr BP) with late Paleolithic artifacts (Giegengack and Zaki 2017).

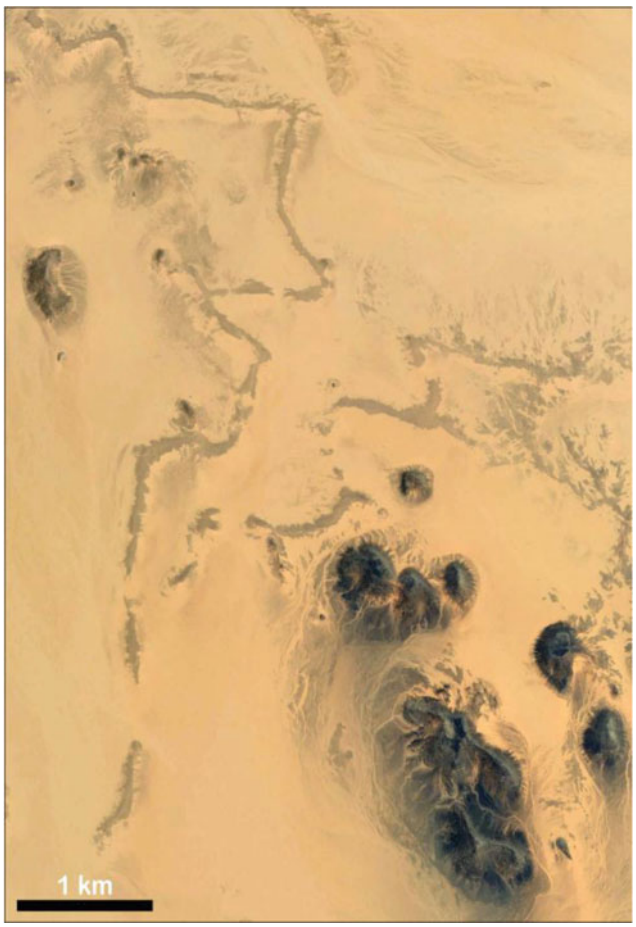

Fig. 12.11 Rectangular pattern of an inverted channel at 22°56′ N, 32°07′ E, 7 km in length, maximum width is about 80 m, and the height is about 7 m (*Source* Zaki et al. 2018)

More recently, Zaki et al. (2018) studied inverted wadis in seven sites in the Western Desert and compared them with similar features in Mars. East of the Bahariya Depression, fifty-nine bodies of mostly dendritic inverted channel features have been described with 761 m; 60 m; 7 m average length, width and height, respectively. 53 spell out sinuous inverted-channel bodies have been delineated in the area west of Ghard Abu Moharik with, with average length, width and height as 1.896 km, 91 m and 13 m, respectively. In the plateau east of Kharga Depression, fifty-nine inverted channel bodies are described, with 2.184 km, 104 m and 12 m asaverage length, width and length respectively. In the Nile Valley, west of Esna city, fifty-five inverted channels were recorded with average length width and height of 1.324 km; 49 m and 17 m, respectively. In addition, Zaki et al. (2018) mentioned poorly define inverted forms in the Nile-Faiyum Divide, previously described by Sandford and Arkell (1929) and dated them to Pliocene age. Another abnormal inverted features in Dakhla Depression, was described by Brookes (2003) as meander scrolls in the sandstone of the Taref Formation (Turonian). Indeed, most of these inverted channels are likely related to ancient river systems described by Issawi and McCauley (1993). However, some features relate to middle Pleistocene Nile hydrology, especially, those of Lake Nasser (Giegengack and Zaki 2017).

The formation of inverted wadis is essentially based on two criteria. Most of the channel fill is represented by bed-load gravel, sometimes of boulder size, such as those in the south-eastern part of the Western Desert. These materials exhibit high porosity and most likely are filled by secondary minerals e.g. iron oxides calcium carbonate and silica. The cemented bed load sediments become more resistant to erosion relative to the soft bedrock. A Few inverted features consist of sand and silt armored by lag gravel and caliche was recorded in the Sheikh Obeiyid playa, Farafra Depression (Hamdan and Lucarini 2013). These inverted features represent fluvial channels that fed the middle Paleolithic lakes.

The nature of inverted wadis reflects the different climatic conditions prevailing in the Western Desert, probably since the Oligocene. During wetter climatic conditions, rivers deposited their sediments, especially bed load gravels and successive wetter periods not only fed water to new channels but were also responsible for depositing secondary cementing materials in the older fluvial bed load gravels. This led to lithification of the ancient fluvial sediments and made them more resistant to erosion. We believe that most inverted topography is related to the hyperarid climatic conditions of the middle and late Pleistocene and late Holocene.

12.3.3 Solution and Karstic Features (Tufa and Spleothem Deposits)

12.3.3.1 Karstic Landforms

Karst is terrain with distinctive hydrology and landforms arising from the combination of high rock solubility and well-developed solution channel (secondary) porosity and permeability underground. Aqueous dissolution is the key process. It creates the secondary porosity and permeability may be largely or wholly responsible for a given surface landform (Gunn 2004). Karst landforms are inherited from past humid climates and have been exposed to modifications during their long history of development (El-Aref et al. 1987). Karst is a dominant feature in the limestone plateaus of Egypt and is represented by different landforms such as doline and uvala depressions, rock-towers, cone-karst, and blind valleys (El-Aref et al. 1987; Embabi 2017). It is important to note that the karstic activity in Egypt took place under wet tropical to subtropical conditions and are somewhat different from those of seasonally wet Mediterranean highlands karst region. The tropical karst regions are characterized by higher surface limestone solution than temperate karst because of the great amounts of surface runoff aided by vegetal and biological activity. The initial corrosive action of tropical waters occurs close to the surface where they become rapidly saturated. This may explain the typical temperate karst features such as large cave systems. Caves in tropical karst tend to be a network of tunnels and of solution dolines. Moreover, temperate karsts of dolines, uvalas and poljes form where solution is evenly spaced over the area. The depressions of tropical environments, the "cockpits" form because water goes rapidly underground without being saturated, thus promoting depth.

The most famous karstic features of the Western Desert are extraordinary chalk pillars, towers and rounded blocks in the "White Desert" artistic chalk of the Farafra Depression. The White Desert National protected area was declared in 1983 to protect the spectacular karst landscapes and associated erosional features. Among the 52 potential sites in the Bahariya—Farafra territory, about nineteen have been selected as potential geomorphosites (El-Aref et al. 2017a). These geomorphosites reveal great geodiversity reflecting high scientific, aesthetic and management values for various activities, not least geotourism (El-Aref et al. 2017a).

About sixteen fields of various karst landforms in the Bahariya-Farafra Plateau were described and mapped for first time by El-Aref et al. (2017b). Among these, karst fields, karst wadi, karst depressions, polygonal karst landforms and Qaret El Sheikh Abdalla Uvala (Denuded and Rejuvenated Karst Landforms). The latter explain well stages of karstication process since post Eocene major paleokarst formation until the final stage of denudation and paneplantion. The Eocene limestone plateau northwest of Assiut also contains karstic shafts infilled with solution breccias and reddish terra rossa (Mostafa 2013). The morphology of these shafts and their infillings suggest that they developed in vadose zones at the base of epi-karst limits. The Giza Pyramid Plateau contains surface karstic features (e.g. karrens, rain pits, rounded rims and solution basins) as well as subsurface features (e.g. karst ridges, shallow holes and dolines) (El-Aref and Refai 1987).

El-Aref et al. (1987) believe that karst and karstification processes were initiated since the late Cretaceous and adapted term "paleokarst" for the older landforms and attributed the Quaternary age to the last stage of karst landforms. A paleokarst is an inert landform and should be distinguished from fossil karst and relict karst. Fossil karst is used to describe karst features that are not in equilibrium with modern landscape process, but is not inert from a karst perspective. Relict karst is isolated from the karst excavation processes that formed it, but still is subject to modification for example by weathering, breakdown, and spleothem deposition. However, the terms paleokarst and fossil karst are often used interchangeably (Gunn 2004). In Egypt, the current hyperarid climate is not suitable for formation of karst landforms; therefore terms paleokarst and fossil karst are adequate.

The karst landforms of the Western Desert exist on three erosion surfaces. Each is characterized by its geomorphic, lithological and archaeological characteristics (El-Aref et al. 1987; Hamdan and Lucarini 2013): (a) Erosion surface "S_1" at the Paleocene/lower Eocene contact in the Farafra formation is characterized by low relief, eroded shallow karst depressions of different sizes; there are also abundant Egyptian alabaster and silcrete deposits and including a sharp pedestal-like hill rising about 40 m above the level of the surrounding plateau (Hamdan and Lucarini 2013); (b) Erosion surface "S_2" at the contact between the Tarawan and Ain Dalla formations is characterized by a rough surface and abundant silcrete duricrust and caverns; (c) Erosion surface "S_3" form the main depressions of the Western Desert.

Three erosional surfaces were also described by Philip et al. (1991) in the Nile Valley at Gebel Homret Shibun. The oldest (highest, "S_1") attains an elevation of 340 m ASL and

is represented by convex top hills with a free face of duricrust and debris slope of 30°. Duricrust profile consists, from base to top: (a) a lower horizon of cavernous and brecciated bedrock; (b) a middle horizon of limestone breccia fragments either cemented by gravitational and blocky calcite or embedded in residual terra rossa; (c) an upper hard cap calcrete, cementing highly subdued and fragmented limestone. The intermediate erosional surface "S_2" attains an elevation of 200–300 m ASL and is covered by terra rossa mixed with calcrete and a thin veneer of silcrete. The surfacial silcrete grades downward into highly cavernous and silicified limestone. The karst profile of surface "S_2" is subdivided into three horizons: (1) An upper horizon corresponding to the infiltration upper vadose zone covered by a thick terra rose and calcrete, (2) A subsoil horizon, where the rock horizon has been affected by intensive karstification resulting in sculpturing, dissolution, alteration of the limestone bedrock, and the formation of surface and subsurface solution features, subsurface caves and inter-karstic deposits. Solution features includes sinkholes and tabular and or funnel dolines. Subsurface solution features includes vertical or inclined solution cavities and horizontal solution cavities formed along bedding planes. Intra-karstic deposits are represented by dolines and cave fill. The lower horizon is represented by partially altered bedrock. The third erosion surface, at an elevation of 70–160 m ASL, is a plain surface characterized by undulating relief interrupted by residual duricrust of the cone-hills and ridges. The "S_3" surface is usually truncated by small and very small drainage basins with dendritic to subdendiritic patterns.

Absolute dating of the karstification in Egypt is not possible. U/Th dating of spleothem deposits in the caves (see below) gives only the age of last stage of karstic processes. However, the age of initial karst stages are given from terrestrial fossils associated with terra rossa in solution cavities in both the Western and Eastern Deserts. The karstic shafts in the limestone of Bahariya-Farafra Depressions contain small vertebrate fossils dated back to late Miocene (Pickford et al. 2006; Mein and Pickford 2010). In Khasm El-Raqaba limestone quarry (Eastern Desert), small fossil vertebrates representing snakes, rodents and bats, have been recovered from karst fissure-fill deposits intrusive into the Eocene limestone (Gunnell et al. 2016). These fossil assemblages indicate mixed subtropical and more arid microhabitats and dated to late middle Miocene.

Evaporite karst

The term "evaporite karst" is normally employed to denote karst in more soluble salts, most commonly in gypsum and halite. Under normal conditions, the solubility of gypsum is up to three orders of magnitude greater than that of calcite, but the solubility of rock salt is roughly 140 times greater than the solubility of gypsum (Gunn 2004). In the Red Sea Coast, the carbonates and the evaporites have been subjected to intensive karstification processes, dominated by surface and subsurface solution features (El-Aref et al. 1986). Isolated cone hills and karst ridges with surface depressions and subsurface caves characterize the carbonate rocks while cone-karst and cockpits characterize the evaporites. Formation of alabastrine gypsum, silicification, dolomitization and dedolomitization are the main wall rock alterations affecting bedrocks during karstification. The development of hard capping duricrusts is certainly the result of precipitation and evaporation during arid to semiarid climatic periods. Brecciation, collapsing and recementation of the duricrust indicate effectively drier and wetter oscillations condition during karstification. El-Aref et al. (1986) concluded that the karstification probably prevailed during the Pliocene or Pleistocene. In addition to paleoclimate, the tectonic setting of the Red Sea coastal zone and the lithology of the country rocks are considered to be the fundamental factors controlling the formation and the distribution of the Red Sea karst landforms.

Economic Importants and Geohazards of Karst Landforms

Several studies reveal that karstification processes were responsible for the formation of many economic ores. Oxides and sulphides of iron, lead and zinc and barite are also found in association with the Red Sea karst (El-Aref 1993; El-Aref et al. 1986). The types of ore minerals and their distributions are controlled by the physico-chemical conditions of the karst water induced during evolution of the karst. The barite and the oxide minerals, together with the final deposition of $CaCO_3$ and the silicification processes, characterize the percolation zone of the mature karst system. The sulphides must be deposited under reducing conditions which characterize the general inhibition zone of the karst system (El-Aref 1993). Iron and manganese ores in Bahariya and Umm Bogma, Sinai, respectively, are most likely related to paleokarst processes (e.g. El-Aref and Lotfy 1985; El-Sharkawi et al. 1990).

Several geohazard problems are associated with karst landforms since they are often underlain by cavernous carbonate and/or evaporite rocks. Impacts and problems associated with karst are rapidly increasing as development expands upon the karst landforms. This has led to an escalation of karst-related environmental and engineering problems such as landslides developed on rock cuts/slopes weakened by karstification features. Youssef et al. (2018) studied the effects of karstification and sinkholes on the stability of the rock cuts/slopes along some desert highways in middle Egypt. They concluded that there is a crucial impact of the karst features on slope instability; many sections of the rock cuts along these highways are not stable and

may endanger the traffic safety. Different karst features contribute to slope stability problems such as differential erosions, open joints, empty cavities, filled sinkholes, and weathering effect along discontinuities.

12.3.3.2 Speleothem (Cave) Deposits

Caves are the most important karstic feature that exists along the limestone plateaus of Eastern and Western Deserts as well as Sinai. Caves can be subdivided into different types according to their geological, geomorphological, archaeological significance, e.g. caves with speleothems, paleontology caves, historical and archaeological caves.

(1) **Caves with Speleothem deposits**

The largest known caves, with speleothem deposits in Egypt are represented by the Sannur and Djara caves, which are characterized by their internal speleothems and flow-stones (Embabi 2017). The Djara cave is an important site in Egypt, located in hyperarid terrain between Assiut and Farafra Oasis. It is a dissolution cave, consisting mostly of a single large chamber approximately 19 × 10 m, and is typically 6 m high (Brook et al. 2002). The main entrance leads to a steep slope initially on rock, and past a series of wall flow stones, stalactites and columns. The floor of the large chamber is covered by ca. 6 m of aeolian sand (Kuper 1996). The cave contains numerous large stalactites, columns (>15 m in diameter and >6 m high), flowstones and sporadic stalagmites (Brook et al. 2002). Helictites have grown from the roof and walls in several parts of the cave, and locally are present as smaller deposits on larger stalactites and columns. Collapse blocks of limestone and broken formations are common near the entrance. Younger speleothem of Djara cave yielded U/Th ages of 140 ± 16, 201 ± 2 and 233 ± 24, 221 ± 34, and 283 ± 56 cal kyr BP (Brook et al. 2002).

Sannur cave is the most important and beautiful Egyptian cave- assigned as a National Protected Area in 1998. It is found in low rolling hills of middle Eocene limestone (Philip et al. 1991). Its entrance is located near the bottom of a pit-like quarry 50 m deep where Egyptian alabaster (calcareous thermal spring deposits) is quarried. Basically, the cave consists of a flat-floored curving chamber, crescentic in plan-view and 275 m long and ca. 20 m high. Massive speleothems and curving walls characterize the eastern and western galleries (Günay et al. 1997). The roof of the cave is almost horizontal at the inner wall, it then curves downward to meet the cave floor by as much as 12 m (Halliday 2003). The speleothem deposits of Sannur Cave have a very fresh, glistening appearance and may have been deposited or enlarged very recently (Halliday 2003). They range from towering stalactitic columns and subaqueous mammillaries to glistening thickets of intricate crystalline "popcorn" and tiny glassy helictites. Stalactites vary from soda-straw forms to large tapered types (Philip et al. 1991). The dates of the speleothem of Wadi Sannur range between 140 ± 16 cal kyr BP and 283 ± 56 cal kyr BP (Dabous and Osmond 2000). However, these dates represent the U mobilization and the last phase in speleothem deposition. Rifai (2007) dated six laminae in the Wadi Sannur stalactite; they range from 188-36 kyr BP and suggested that these laminae were deposited over a period of ca. 52 kyr BP. The estimated growth rates of Sannur's stalactite are variable and range from 0.12 to 9.30 μm/year. The stalactite began to grow with deposition rate of 3.7 μm/year (between 188 and 175 kyr BP), with non-deposition phase between 175 and 160 kyr BP, and increase rapidly around 145.35 kyr BP, (9.3 μm/year). By the end of the growth period it has decreased by about 4.1 μm/year.

(2) **Paleontogical "Nimir" Cave**

Nimir Cave is a large solution cave on the northern slope of the southern Galala plateau, ca. 40 km southwest of St. Anthony monastery. The main chamber is 36 m long, 18 m wide and 11 m high. The floor consists of aeolian sand and limestone talus. A large stalagmitic column dominates the far end of the main chamber (Halliday 2003). This cave is especially important for paleoecological studies, which revealed a radically different Holocene ecology (Goodman et al. 1992). Excavation of the cave revealed numerous finds representing remains of at least 29 individuals of leopards (Goodman et al. 1992). These materials seem derived from animals that visited, lived and died in the cave throughout the Holocene; radiocarbon dates of leopard tissue indicate that the species was present in the Epi-Paleolithic, Neolithic, Predynastic and Second Intermediate period (ca. 7–3.65 cal kyr BP). The cave has archaeological significance; rock art is represented by a group of leopards being chased by several men armed with spears (Hobbs and Goodman 1995).

(3) **Caves with archaeological significance**

Obeiyid and Sodmein caves are examples. Obeiyid Cave, with rock art, is located in Wadi Obeiyid, Farafra Depression (Hamdan et al. 2014). The cave is located about 50 m above the floor of the wadi and can be entered through a 2 × 2 m square opening extended in a N-S direction (Fig. 12.12a). The walls are sharp and straight and run parallel to the dominant joint trends. The opening has an unusual appearance and does not resemble other fracture bounded cavities. It may have been artificially enlarged and consists of three adjoining circular chambers connected to form an elongated cavity (Fig. 12.12b). They were termed Front (southwestern), middle and Back (northeastern) Galleries. The wall of the front and back galleries shows four big and five small solution hollows (niches), of diameters range from 5 to

50 cm. The ceilings are rounded off and in some places show dripstone stalactite and stalagmite deposits. The cavern is about 13 m in length, while its height varies from 1.5 m at the opening to 6 m in the back Gallery (Fig. 12.12c).

The Southern chamber attains 5.5 m, 4.5 m and 3.5 m in length, width and height, respectively. The middle chamber is 2.8 m in length and width and 2.4 m in height. The Northern chamber attains 3.5 m in length and width and 6 m in height. There are allogenic clastics in the floor of the eastern chamber, flow-stones in the floor of western chamber; rimestones and dripstones occur along the walls. Small stalagmites exist outside the cave. Two spleothem samples from Wadi Obeyed Cave were dated using U/Th dating to 45 ± 2 and 287 ± 67 kyr BP corresponding to flowstone and dripstone samples, respectively (Hamdan et al. 2014c).

The cave is very important for its wealth of rock art, displayed at various heights on the limestone walls. The lack of archaeological materials in the cave may, however, be due to its use as a ritual place. Paintings and engravings are located on two 'registers' (or levels) on the walls of the three rooms. Rock art in the Obeyed Cave is represented by carbonized negative human hand prints, depictions of animals (goats, giraffes), boats and lion paws; all are dated to middle Holocene occupation (Barich 2014).

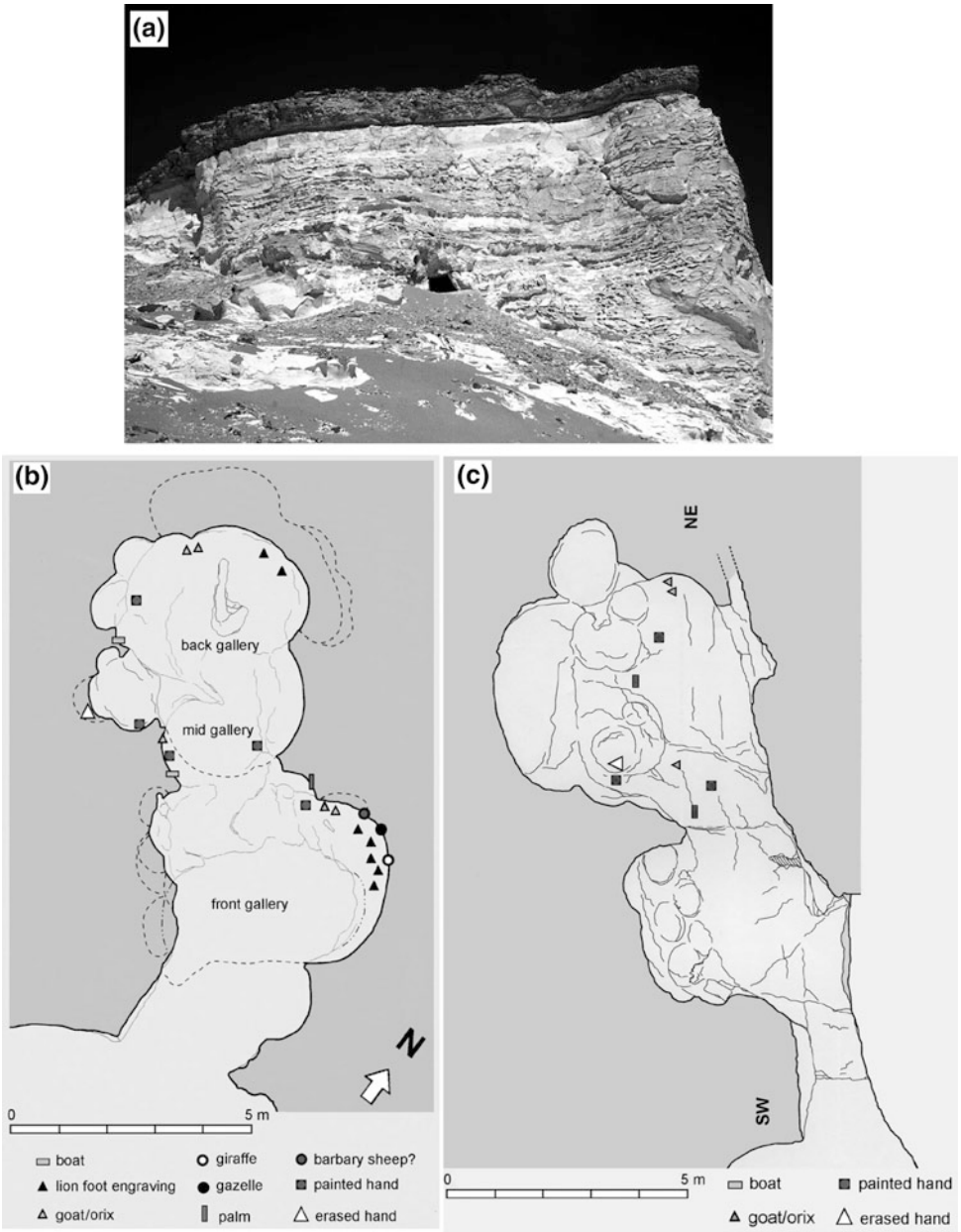

Fig. 12.12 **a** Farafra, Wadi Obeiyid. Cave 1, view of the cave which opens onto the southern slope of the Northern Plateau; **b** planimetry of the cave showing the three adjoining chambers which form the elongated cavity. Symbols indicate the position of rock art works; **b** planimetry of the cave showing the three adjoining chambers which form the elongated cavity. Symbols indicate the position of the rock art works; **c** cross-section of the cave along the NE-SW axis (*Source* Barich 2014)

Sodmein is a large but quite shallow cave standing at the base of a limestone cliff. It is developed within a system of microfaults on the Thebes Formation of Wadi Sodmein, 40 km NNW of the seaport of Quseir, Red Sea (Vermeersch et al. 1994). It was formed by both karstic and physical breakdown processes of the limestone bedrock (Moeyersons et al. 2002). Sodmein Cave has very important geologic and archaeological features. Geological importance of the cave is represented by ca. 4 m of stratified cave sediment dated to the late Quaternary. These sediments contain cryptotephra in two ca.50 cm layers at 25–30 cm and 150–155 cm (Barton et al. 2015). The upper cryptotephra is dated to late Pleistocene/early Holocene with a homogeneous calc-alkaline composition, most likely derived from central Anatolian volcanism. The lower cryptotephra has a dominant Na-rich trachyte component and dates to the late Pleistocene and an unknown volcanic eruption (Barton et al. 2015). Paleontologically, the cave sediments yield several organic units, containing herbivore dung, mammal (sometimes carnivore) coprolites and guano, items of great paleoecological importance during late Quaternary. Archaeologically, Sodmein Cave is one of the rare occupied in late Pleistocene sites in Northeast Africa. Its outstanding cave stratigraphy spans more than 4 m of stratified human occupation debris from the middle Paleolithic up to the Neolithic, with a stratigraphic hiatus between around 25 to 7.5 kyr BP (see Vermeersch 2008; Vermeersch et al. 1994, 1996, 2002). Moreover, the earliest domesticated sheep/goats in Egypt were found in Sodmein Cave and were dated to 7.5 cal kyr BP. The domesticated sheep/goats were diffused to the Western Desert immediately after their first arrival in the Sodmein Cave region during the constant movements of people between the Red Sea coast and the Western Desert.

(4) Collapsed caves of Sheikh Abdalla

Sheikh Abdalla is an oval depression in the Bahariya-Farafra Plateau and includes an extensive unroofed palaeocave system over a distance of 5 km, exposing an extensive network of galleries, separated by chalk walls and hills (Wanas et al. 2009). These ancient galleries contain vast quantities of speleothem and spelean breccias. There is a widespread, but discontinuous, horizon of dark grey epikarst breccia capping all the chalk hills and ridges in the area. The cave infilling at Sheikh Abdalla is represented by four facies of spelean deposition, (1) a coarse basal solution breccia comprising blocks of white chalk, limestone and some chert cemented by red terra rossa, (2) black carbonate-rich sediments and broken speleothem layers rich in organic matter or manganese, (3) laminated, red, fossiliferous sandstone breccias with thin layers of white to pink flowstone deposits and cave pearls, and (4) coarsely crystalline grey calcite speleothem, occasionally forming masses up to 4 m tall, 5 m wide and many meters long.

(5) Pseudokarsts

The term pseudokarst is used to describe a variety of non-dissolutional processes, forms and terrains similar to certain types of karst (Halliday (2007). Pseudokarst shares a considerable range of features, resources and values with karst; these commonly including caves and rock shelters. Unlike karst, integrated subsurface drainage may not be present in pseudokarst. Pseudokarst in rocks with calcareous cement, the major volume of rock not removed by solution but by wind deflation. According to Halliday (2007), the most important types of pseudokarst are rheogenic (developed in basalt flow), badland and piping (in soft clastic sediments), talus, crevice (sea caves), compaction and consequent pseudokarsts.

In Egypt, pseudokarst features are well developed along the exposed Nubian sandstone in southern Egypt, and are represented by columnar caves along the edges of vertical joints and sandstone towers (El-Gammal 2010). Most likely, these pseudokarst features are formed by wind erosion. In Gilf Kebir, pseudokarst features are represented by the Wadi Sura caves. These rock shelters are of special interest as potential analogues of cavernous features on Mars (e.g., El-Baz and Maxwell 1982) and yield important rock art pictures. These pseudokarst caves are formed by wind erosion along curved joints and mass wasting.

In the Eastern Desert, the Tree Shelter, near Quseir, is excavated in sandstone and most likely formed by undermining by fluvial action and mass wasting. It is one of the rare stratified sites (Marinova et al. 2008) which began around 8 cal kyr BP and continued until about 5 cal kyr BP. The archaeological finds show clear connections with the Nile Valley and the Western Desert during the African humid Period. The lower level (ca. 8.1–7.8 kyr BP) contained lithic tools of nomadic hunters. The higher level has numerous hearths (ca. 6.6–5 cal kyr BP) with animal and fish bones and Red Sea mollusks.

Another pseudokarst cave in the Eastern Desert named Wadi Bili Cave. The cave is cut into the calcareous sandstone plateau west of El Gouna (Vermeersch et al. 2005). It is situated at upstream of the northern bank of Wadi Bili gorge (27°23.154′ N and 32°33.451′ E). The cave measures about 20, 12, 3 m in width, depth and height, respectively. At the inner edge, the roof and floor join together i.e. by a curved roof. The cave floor is covered with fine sandstone debris and aeolian sand. The topographic plan assumes an elevation of the wadi floor in front of the cave of 95 m ASL. The frequently collapsed roof creates scree of large boulders

below the cave entrance. It seems that the cave was formed by water action of a fossil water-fall which eroded the horizontal sandstone layers easily and apparently also by salt wedging. Paleolithic remains are very rare. Only a single, possibly middle Paleolithic notched flake was found at depth of 80 cm near the cave entrance (Vermeersch et al. 2005).

In Moghra Depression (North Western Desert), a piping cave attains 250, 50, 10 m, in length, depth and height, respectively. It was excavated in soft sandstone and the ceiling remains being made of hard mudstone. It seems that the structure was formed by horizontal, graded grain-by grain removal of particles by channelized ground-waterflow and to a small extent by mass wasting. Crevice pseudokarst is well developed along the Mediterranean and Red Sea coasts. Bir Masoud in Alexandria is a good example of crevice pseudokarst formed by hydraulic wedging by waves and other forms of marine erosion. It forms tabular fractures extending hundreds of meters inland and these are readily traceable on the surface.

12.3.3.3 Tufa Deposits

The first scientific mention of the tufas of the Kharga Oasis region was made by Zittel (1883). Ball (1900) was the first to describe the tufas as Pleistocene in age and Beadnell (1909) originally recognized the tufas as fossil-spring deposits. The first systematic work on these deposits was carried out by Caton-Thompson (1952). Tufa is freshwater terrestrial carbonate rocks were deposited at positions along alkaline springs, seeps and streams, particularly at rapids and waterfalls (Nicoll et al. 1999). Tufas are derived from the dissolution and re-precipitation of calcium carbonate rocks. They were deposited from supersaturated water as it degassed CO_2 via turbulence and/or biogenic mediation of microbes and plants (Nicoll and Sallam 2017). There are different facies in spring tufas ranging from stepped, cascading waterfalls separated by small pools, to possibly ephemerally flowing small wadis, to marshy floodplains, to occasionally slightly larger lakes (Smith et al. 2004). Tufas always unconformably overlay older bedrock limestone in the Western Desert (Sultan et al. 1997) or Precambrian rocks in the Eastern Desert and Sinai (Hamdan and Brook 2015).

Tufas of the Western Desert are concentrated principally along escarpments and depressions of the Sinn el-Kaddab plateau at Kharga-Dakhla in the north to Kurkur-Dungle in the south. Tufas are absent north and south of these areas; however, a remnant of early Holocene tufas has been recorded at Gebel Uweinat (Marinova et al. 2014). Geologic setting play an important role in the formation of the tufas, where the thickness of the Nubian Sandstone Aquifer in tufa areas extends below 1000 m, while a deep fault system may allow water to rapidly reach the surface (Abotalib et al. 2016). Two types of tufa units have been recorded in the Western Desert, plateau and wadi tufas (Caton-Thompson 1952; Sultan et al. 1997; Smith et al. 2006).

Plateau tufa is the oldest and the topographically highest of the tufas, is typically heavily wind-fluted with a steel blue to black patina and densely recrystallized outer surface. Fresh surfaces of the tufa are white to buff, often resembling limestone. The plateau Tufa was formed by shallow sheets of lime-charged water flowing in undefined channels. It lack of primary structure is a result of diagenesis; however, a few reed casts often exist indicating an arcuate barrage dam (Smith 2004). The date of the plateau tufas is >400 kyr BP (Smith 2006) or >450 kyr BP (Sultan et al. 1997). Crombie et al. (1997) gave dates for the plateau tufas of Kurkur as about 300-450 kyr BP. No absolute dating is available for Dungle plateau tufas but Caton-Thompson (1952) suggested that the plateau tufa may all be Plio-Pleistocene in age.

Wadi Tufa occurs along the escarpment of the Sinn el Kaddab plateau and could be sub-divided into discrete sub-units but which may not be temporally correlated amongst localities (Smith 2004). It generally attains a thickness of 1–2 m and is represented by inclined sheets that follow the old slope of the escarpment or as a thick horizontal strata similar to Plateau Tufa. The color of weathered surfaces of Wadi tufas, range from black to brown to blue-gray; fresh surfaces are generally white to light tan. Much of the tufa is highly porous, with porosity principally resulting from the decay of incorporated plant material (e.g., Crombie et al. 1997; Nicoll et al. 1999). In Kharga Depression, Wadi tufas are subdivided into three units: Wadi Tufas 1, 2, and 3 (oldest to youngest), based on topographic and textural criteria (Smith et al. 2004, 2006). Younger tufa units may either overlie or be incised into older tufa units. Preservation of structure within the Wadi Tufa is usually excellent. Several facies within the Wadi Tufa were recorded, (1) a laminated to thinly bedded clastic tufa, with well preserved fragments of plant stem or leaf casts, (2) cascaded tufa barrage dams, as a combination of organically mediated deposits and flowstone-like, inorganically-precipitated deposits, (3) un-cemented oncoids (2–4 cm in diameter), ranging from roughly spherical to elongate in shape, which accumulated upstream of the dam and (4) inclined escarpment-veneer tufa, precipitated from the waters of springs that emerged relatively high up on the escarpment or from the base of the Thebes Group chalks. In Kharga, Wadi tufas contain middle Stone Age artifacts within a thin (50 cm) silt lens (Caton-Thompson 1952); an isolated, probable Acheulean implement, was found on the surface of an adjacent ridge (Smith et al. 2004). They exhibit dates of 260–219 and 160 kyr BP in Kurkur Oasis (Crombie et al. 1997) with only one more recent date for wadi tufas of Dungle, 22.900 ± 600 BP. In Dakhla they are dated to 220 ± 20, 125 ± 16 and 40 ± 10 kyr BP (Churcher et al. 1999). U/Th dates published for wadi tufas of Kharga as 272,

255, 190-175 and 45 kyr BP (Sultan et al. 1997; Hamdan 2003b). At Matana, east Kharga, two ESR dates on freshwater gastropods yield dates 65.1 ± 4.1 and 27.7 ± 1.9 kyr BP (Blackwell et al. 2012).

Hamdan and Brook (2015) studied the petrography, isotope geochemistry and AMS radiocarbon ages of eight tufas in the Eastern Desert and three tufas in Sinai. The tufas unconformably overly Precambrian basic igneous rocks (basalt, diabase and gabbros).

The ^{14}C ages of carbonate and organic residue in tufas from the Eastern Desert and Sinai suggest three phases of deposition associated with increased rainfall:

~62,000–56,000 cal yr BP; ~31,234–22,474 cal yr BP and ~12,058–6678 cal yr BP. Late Pleistocene tufas (mean $\delta\ ^{18}O$ = 7.74‰ and 7.66‰ VPDB) were deposited by spring waters initially similar in $\delta^{18}O$ to the Sinai Pleistocene ground waters (mean = 8.06‰; maximum = 6.53‰ VSMOW; Abouelmagd et al. 2012, 2014). Pleistocene tufas imply a temperature at deposition of 14.3–21.1 °C for the Sinai tufas and 14.0–20.8 °C for the Eastern Desert tufas (Hamdan and Brook 2015). The Holocene tufas (mean $\delta^{18}O$ = 6.59‰ and 6.63‰ VPDB) were deposited by spring waters initially similar in $\delta^{18}O$ to the Sinai Holocene ground waters (mean = 5.36‰; maximum to 4.84‰ VSMOW; Abouelmagd et al. 2012) and implies a deposition temperature of 21.22 ± 23.7 °C for the Sinai tufas and 21.41 ± 23.89° for the Eastern Desert tufas.

12.3.4 Quaternary Marine Sediments

The Quaternary witnessed a series of low and high sea level fluctuations corresponding to glacial/interglacial climatic cycles, respectively. Marine sediments related to these cycles are represented by raised coral reefs in the Red Sea coast, calcareous coast ridges along the Mediterranean coastal and placer deposits (black sands) on the northern coast of Nile Delta.

12.3.4.1 Quaternary Coral Reefs

The Pleistocene Red Sea reefs were among the first worldwide references concerning raised reefs (Sandford and Arkell 1939). The very limited uplift of the Egyptian coastal plain (at least during late Pleistocene) suggests that the respective altitudes of the late Quaternary marine terraces indicate their respective derived sea-level altitudes. From at least earliest Pleistocene times, the Egyptian coast of the Red Sea has been characterized by the development of fringing and barrier reefs. Owing to glacial-interglacial cycles, the Red Sea appears to have favored reef development during every interglacial high stand of sea-level. The Pleistocene sequences show at least five reefal units above the present sea level (Plaziat et al. 1990). The earlier, undated Pleistocene fringing reefs have been raised moderately, up to 50 m ASL (Plaziat et al. 1990), middle Pleistocene (>290–300 kyr BP) is found at +10 to +15 m ASL. A 200 kyr BP high-sea stand is recorded by a relic terrace at +17 m ASL. The late Pleistocene system (125–138 kyr BP) is very well represented with terraces at about +6 to +8 m ASL. The latest Pleistocene reef terrace (60 kyr BP) has remained near its original altitude (averaging 4 m ASL; Plaziat et al. 1990). The sedimentary facies are similar in modern and Pleistocene reefs, with silciclastic beach facies at the base and carbonate reefal facies at the top (Mansour and Madkour 2015). Reef sequences exhibit different degrees of diagenetic alteration which are reflected by a gradual change of skeletal particles and early-formed cement from aragonite and high Mg-calcite to low Mg-calcite.

12.3.4.2 Mediterranean Coastal Ridges

Quaternary deposits in northern Egypt are represented by elevated offshore bars, lagoonal beds, evaporites and marls (Butzer 1960; Said 1990). The Mediterranean coastal plain west of Alexandria, is characterized by the presence of a number of elongated ridges, also called Kurkar ridges, which run parallel to the coast, separated by longitudinal depressions. The lower three ridges to the shore, the 10, 25, 5 m high ridges (named the coastal, Abu Sir and Maryut bars) can be traced for long distance along the coast. The succeeding ridges, the 60, 80, 90 and 110 m high ridges (Khashm el Eish, Alam el Khadem, Miheirta, Raqaet el Halif and Alam Shaltut), are less conspicuous and do not form continuous ridges (Said 1990).

The ridges are composed of oolitic limestone (Shukri and Philip 1956; Butzer 1960), and they seem to represent successive fossil off shore bars that were formed in the receding Mediterranean during the Pleistocene. However, some literatures interpret these ridges as aeolinite deposits (Butzer 1960; El-Asmar 1994). The depressions between the ridges contain lagoonal deposits, such as evaporites and marls. Three calcareous oolitic ridges with two intervening lagoonal depressions have been recognized in the coastal plain in the Salum area (Selim 1974). They range in age from late Monasterian to Tyrrhenian. The ooids in the oldest (Tyrrhenian) ridges have developed micritic envelopes and are probably recycled detrital grains. The younger deposits (late Monasterian and main Monasterian) have a well-developed oolitic texture and were probably deposited in shallow, agitated marine waters. Oolites dominate the deposits of the first and second ridges, whereas bio-clastics with abundant coralline algae, benthonic foraminifera, mollusks, echinoderms and intra-clasts prevail in the deposits of the third and fourth ridges (Wali et al. 1994). Diagenetic alterations and cementation are concentrated below exposure surfaces (pedogenic calcrete horizons). Wali et al. (1994) believe that the ridges were initiated by the accumulation of

carbonate ooids as marine bars and then lithofied by early diagenetic processes under marine subaqueous conditions. Modification by aeolian processes followed after a phase of sub-aerial exposure and marine regression.

The lack of reliable absolute dating of the Mediterranean coastal ridges makes them of poor scientific importance for global sea level and climatic variation. However, a few absolute dates, using U/Th, OSL and ESR, have been published (El-Asmar 1994; El-Asmar and Wood 2000). The coastal ridge yield OSL dates of 0.6 ± 0.1 and 1.5 ± 0.2 cal kyr BP and ^{14}C dates of 3680 ± 40, 4100 ± 120 and 4355 ± 40 cal BP from top to bottom (El-Asmar and Wood 2000). The oolitic limestone of El-Max-Abu Sir (second ridge) yield U/Th ages of 90 ± 15 kyr BP, 110 ± 5 kyr BP and an OSLage of 104 ± 17 kyr BP. One *Helix* sp. sample collected from the paleosols at the northern flank of the second ridge yielded an OSL date of 67 ± 31 kyr BP. Three samples of the aeolinite of the third ridge gave OSL ages of 191 ± 42, 416 ± 255 and 454 ± 151 kyr BP (El-Asmar 1994). Four samples were studied from the marine beds of the third ridge gave ages of 423 ± 153, 546 ± 352 and 208 ± 59 kyr BP, respectively. One ESR determination on the *Cardium* limestone gave an age of 292 ± 48 kyr BP. The paleosols (Pink limestone) at the top of the Khashm El-Ish (fourth) ridge show a wide range of ages, giving age estimates between 360 ± 140 and 584 ± 317 kyr BP indicating a middle Pleistocene age.

12.3.4.3 Placer Deposits (Black Sands)

Egyptian black sands are beach placers deposited from the Nile stream during flood seasons reaching the Mediterranean Sea at the river mouth. They are heavy, glossy, partly magnetic mixtures of usually fine sand (El-Kammar et al. 2011). The River Nile transports heavy minerals from two sources, mainly from eastern and Equatorial Africa- in the south to the Mediterranean Sea in the North (Shukri 1950). The mineral composition of the Egyptian black sands is represented by six main minerals accompanied by minor minerals. According to their relative frequencies and economic importance, the six main minerals are: ilmenite, magnetite, zircon, monazite, garnet and rutile. Traces of cassiterite and gold as well as some rare earth elements (El-Kammar et al. 2011) in some minerals are also present. Elemental concentrations in Egyptian black sands show an average concentration of natural radionuclides (U and Th) higher than the average world level. However, exposure to natural radionuclides (U and Th) is still within the acceptable limits due to low exposure. However,, the black sands from north of Nile Delta are not recommended for use in building constructions due to the potenmtial for high radioactive doses. Kaiser et al. (2014) used high-resolution airborne gamma ray spectrometry to estimate radioactive elements spatial abundance along the Rosetta coastal zone area. They noticed that both Uranium and Thorium are concentrated in the black sand deposits along the beach. In addition, the areas with the highest concentrations of Uranium and Thorium show the highest level of radiogenic heat production.

Egyptian black sand deposits also occur along the Egyptian northern Mediterranean coast from Rosetta to Rafah. Their contents vary from place to place but beach area of Rosetta contains most of the economic heavy mineral reserves of black sand in Egypt owing to their great extension and high grade (Dabbour 1995). Rosetta black sands contain about 3% of some important economic minerals. The ore shows lateral variations with high concentrations in the West; these decrease gradually to the East. Heavy concentrations of black sands are deposited in a thin mantle near and parallel to the shoreline and thay also existed as naturally formed concentrated lenses. The thickness of the deposited layer range from 0.5 m to more than 40 m (Naim et al. 1993).

The formation of black sand facies comprises several steps: (1) deposition of fluvial Nile sediments rich in heavy minerals along the shore of the Mediterranean-during periods of high interglacial high sea level, (2) sorting of the sediments under the effect of waves and waves induced longshore currents, where the heavier and more stable minerals (opaque, garnet, zircon, tourmaline, rutile and monazite) are concentrated in the surf zone and the lighter and less stable minerals (hornblende, augite and epidote) are transported offshore, (3) during last glacial maximum (LGM) when sea level dropped abruptly and the delta sediments were exposed, wind action led to the formation of coastal dunes. Wind deflation also concentrated heavy minerals in the deflated sediments and in the newly formed coastal dunes. Therefore, the Egyptian black sands are now present either as beach sands or coastal sand dunes. The coastal sand dunes of El Burullus-Baltim area contain economic mineral reserves. These sand dunes extend for about 16 km and have an average with of 700 m. Using the individual mineralogical composition data of the evaluated four zones of this sand dune area, the calculated average economic mineral grade equals 4.87%. The estimated average total economic minerals content is 4.66% and this is distributed as follows: different ilmenite varieties, 3.41%; magnetite, 0.27%; garnet, 0.52%; zircon, 0.31%; rutile, 0.14% and monazite, 0.01% (Moustafa 2007).

El Kammar et al. (2011) compared heavy minerals in source areas (Shukri 1950s samples housed in the geology Museum, Cairo University) and those of black sand from the Rosetta area. They found several changes in morphology and composition of the heavy minerals during the long transportation. Brittle and meta-stable minerals (e.g., barite and pyrite and mica) are entirely lost and never reached to the Nile Delta. Abrasion polishes the surface of the heavy minerals and dissolution of these minerals takes place along

cleavage planes. Grains consisting of polycrystalline mineral clusters such as zircon from the White Nile and titano-magnetite from Atbara usually disintegrate into individual crystals during long transportation. The ultra-stable minerals as zircon and monazite experienced changes in their composition. Heterogeneity in zircon covers all aspects including; color, morphology, size, elongation index, radioactivity and composition. However, radioactivity discriminates the uraniferous zircon of the White Nile from the non-radioactive variety from the Ethiopian province.

12.4 Quaternary Sediments and Landforms Related to Arid Climate

12.4.1 Aeolian Deposits

Aeolian sands occupy a significant position in the geologic history of Egypt in general and in the Quaternary in particular. Generally, aeolian deposits cover about 160,000 km^2 of the Egyptian land representing about 16% of the total surface area of the country. Based on the total area of the dune coverage, the aeolian deposits are represented by six sand seas with >50% sand cover and total area >5000 km^2 (e.g. Great Sand Sea, Abu Moharik, North Sinai) and 10 dune fields with dune coverage less than 50% (e.g. West Delta, South Rayan, Embabi 2017).

The Great Sand Sea attains an area of more than 100 000 km^2 (Besler 2008). It is situated in westernmost Egypt, where its northwestern edge extends across the border into Libya. The sand sea does not lie in a distinct depression, but covers weakly sculptured ground sloping from more than 500 m ASL, in the south to less than 100 m ASL, near Siwa Depression in the north. The dunes of Great Sand Sea are represented by three dune types; linear, transverse and star. Linear dunes are the most common and are represented by two forms; sharp-crested recent linear "seif" ridges (Silk; Besler 2008) and the broad-crested dunes (whalebacks; Bagnold 1931, 1933 or Dra'a Besler 2008). Currently, the former is active while the latter are stabilized. The whalebacks had been active dunes from the end of the middle Paleolithic pluvial to the beginning of the African Humid Period at ca. 10 cal kyr BP (Haynes 1982). They stabilized by combined action of bioturbation, human occupation, pedogenesis, and slope wash vegetation under a semiarid climate from 10 to 6.5 cal kyr BP. The transverse dune type is represented by barchans and barchanoids and is found below the recent still active dunes in the northern part of the Great Sand Sea.

At 800 km long and 50 km width, Ghard Abu Moharik is most outstanding linear sand dune belt in the Western Desert of Egypt, with various dune density and dune types. Only recently, Ghard Abu Moharik was ranked as sand sea (Embabi 2017). The northern and middle parts comprise mainly linear dunes, whereas the southern section in Kharga Depression contains mostly barchans (Hamdan et al. 2016b). From south of Qattara to the Bahariya Depressions, it composed of isolated small-to-large linear dunes consisting of two dune chains: (1) a western chain represented by Ghard Williams and Ghard Ghorabi, at 32 and 71 km long, respectively and heights 30–45 m, and (2) an eastern group of relatively small dunes, called "Abu Moharik Dunes" (Embabi 2017), with lengths 1.5–8.5 km, and heights 5–16 m. In north Kharga plateau, the Ghard predominate with high-density linear dunes in one main chain with a secondary discontinuous belt to the east. The main chain also contains barchans and barchanoid belts, as well as mega-ripples. Inter-dune areas are occupied by transverse dunes, sometimes barchanoid, appearing as sand giant waves. The southern part (Kharga Depression to Egyptian Sudanese border) is characterized by low dune density and the predominance of barchan and barchanoid chains as well as sand sheets. Based on a ratio of the length/width ratio, most of the barchans in the southern part of Ghard Abu Moharik are fat (54%) or pudgy (24%) with length/width ratios of ≥ 1 and 0.75, respectively (Hamdan et al. 2016b).

An extensive dune field extends for about 185 km from the southern part of Wadi El-Rayan to the latitude of the city of Dairut in the Nile floodplain. It seems that the pre-dune topography of the southern part of Wadi El-Rayan controlled the development of this dune field into linear dunes in the northern part, then into barchans on the plateau surface in the southern part (Embabi 2017). Said (1981) named this stretch of aeolian sand dune remains as El Khafoug Formation; inter-fingering with both the Pre-Nile deposits of the middle Pleistocene and the Neo-Nile sediments of the late Pleistocene sediments. The Landsat ETM images and aerial photography both show that the barchan sand dunes are present in the western part of this dune belt extending over a rugged area with a relatively higher relief than the area covered by longitudinal sand dunes (El-Gammal and El-Gammal 2010). Longitudinal sand dunes are located in the eastern part of the dune field covering and surrounded by low land. These dunes are striking in a NW–SE direction (parallel to the prevailing NE wind) and are often composed of barchan dunes. The eastern horns of the barchan dunes are longer than their western ones. Sometimes these horns are coalescing with each other to constitute longitudinal sand dunes (El-Gammal and El-Gammal 2010).

The North Sinai landscape is dominated by the most complex dune system among Egyptian dunes (ca. 13,600 km^2). They are composed of ancient vegetated fixed dunes, overtopped by recent active dunes (see Misak and Attia 1983). Inland, the former are represented by less vegetated fixed dunes and coastal fixed dunes sank in the water of Bardawil lagoon and coastal sabkhas formed during LGM low sea level and were fixed during early Holocene

humid phase. Active dunes are represented by linear, crescent, and transverse dunes. Sand and dune movement represents a major hazard to development projects in the region of Sinai.

In northeast Cairo, the Khanka sand dune belt cover ca. 20% of the area, with numerous linear, transverse and star dunes, reflecting variable wind directions, e.g. NW, W, NE and S (Misak and Draz 1997). Linear and transverse dunes dominate the western and north-western fringes of the dune system. The longitudinal dunes range from 200 to 2000 m long and up to 150 m in width. Aerial photos (1955 and 1977) show annual rate of dune movement of ca. 30 m in the NE. The present annual rate of dune migration is relatively low due to intensive agricultural activities (Misak and Draz 1997).

Coastal dunes spread along the plains of the northern Mediterranean coast. The largest area covered by dunes with highest density extends from El-Borg to Gamasa. Dune types in this field vary between simple barchans with horns pointing southward, most notably in the Mid-Delta sector, to complex and deformed barchans and to small linear dunes. Maximum height is about 20 m in the vicinity of Rosetta and to the east of El-Borg but the most common height is 2–3 m (Embabi 2017).

There are two generations of coastal dunes, stabilized and active dune. Stabilized dunes are characterized by low elevation (4–7 m ASL), and conspicuous cross stratification and dense vegetation cover. They are also characterized by their relatively higher content of fine grain constituents (silt and clay). Optical Simulating Luminescence (OSL) dating for the stabilized dunes yield 2.6 ± 0.6–1.9 ± 0.4 cal Kyr BP (El-Asmar 2000). Remains of former Islamic settlements are found on these ancient dunes at Kom Mastero and El-Borg (Embabi 2017). Active dunes are higher and sharper than the ancient stabilized ones. They are represented by two dune types; longitudinal and barchans. The former are elongate in shape, more or less straight with continuous serratic crest without breaks with two steep sides 1–1.5 km long and 15–30 m height. Barchan dunes occur in two patterns, isolated and complex. Both have axes nearly normal to the wind regime of WNW and NW directions and reach 30 m in height and 50–300 m in length. Inter-dune areas in these recent dunes appear as innumerable small depressions with flat floors, some of which are occupied by temporary or permanent ponds. The ponds are fed by rainwater stored in dune sands that percolates into the inter-dune areas. Most of the area covered by coastal dunes has undergone reclamation since at laest Pharaonic times for a variety of purposes. However, the dunes are now gradually disappearing due to cultivation and urbanization (Embabi 2017).

The first attempt to estimate the rate of movement of Egyptian desert dunes was done by Cornish (1900), who measured a rate of 4.5 m/year for dune crests east of the Nile Delta. Many areas in the Western Desert were the subject of evaluation of sand dune movements by different authors (e.g., Ashri 1973; El-Gammal and Cherif 2006; Hamdan et al. 2016b); they assigned diverse dune rates ranging from 0.5 m/year to as high as 100 m/year. More recently, the mean movement of barchan dunes in the Toshka area varied from about 4 to 7.67 m/year, averaging 6 m/year along a SSW direction (Hamdan et al. 2016b).

The source of aeolian sand in Egypt is explained by three main hypotheses. The aeolian sands have been derived from arenaceous formations (i.e. Moghra Formation) in northern Egypt (Beadnell 1910; Ball 1927) and Nubian sandstone in the south (e.g. El-Baz 1988; El-Baz and Wolfe 1982). Several arguments face the latter source because in Nubian sand exposed in southern Egypt most dunes migrate in a north-to-south direction parallel to the prevailing winds. Said (1998) believed that dune fields of the Egyptian Western Deserts started to accumulate during the last glacial period when northern Africa was arid and the sea-level lower by at least 120 m. The exposed continental shelf which probably extended into the Mediterranean Sea at places for more than 40 km made a ready source for all the sand needed to build the huge dunes of the eastern Sahara. Recent studies, using textural, mineralogical and geochemical proxies (e.g. Hamdan et al. 2015) indicated that the formation of aeolian dunes was a complex multicasual process formed in several alluvial, lacustrine and aeolian environments throughout the Tertiary-Quaternary. The sands were reworked from arenaceous bedrock formations by alluvial processes extending from a south to north direction through radar rivers and inverted wadis (see above), before they were distributed by wind action during arid periods in the early-late Pleistocene and by alluvial and lacustrine processes during the middle Pleistocene and early Holocene. Indeed, aeolian dune sand of Egypt were formed in three cycles (Hamdan et al. 2015; Embabi 2017, with references therein). The first cycle (700–300 kyr BP) occurred during the arid phase of the middle Pleistocene, where Acheulean artifacts at the surfaces of inter-dune areas indicated that the dunes are older than Acheulean time (Haynes 1982). The second cycle (35–10 kyr BP), is without evidence of human occupation (Wendorf et al. 1993) and is characterized by the formation of whaleback dunes in different parts of the Western Desert in different wind regimes during the late Pleistocene glacial period where the winds were strong enough for dra'a formation (Besler 2008). The third and last cycle of dune development of the Great Sand Sea extended from the middle Holocene to the present time.

12.4.2 Wind Erosive Landforms (Yardangs)

In the Western Desert, large-scale aeolian erosional features include: (1) pits and hollows (blowouts), formed by deflation or removal of loose particles, (2) wind gaps, or wind-eroded notches in ridges, (3) wind-sculptured hills such as yardangs.

Yardangs (a Turkmenistan word for an inverted boat) are well developed on the surface of playa sediments due to the intensive hyperaridity that predominate allover Egypt during the late Holocene (Hamdan 2014b). These streamlined erosional ridges have long been known, not only in the Western Desert of Egypt, but also in most of the major deserts of the world (Embabi 2017) where they typically occur in large fields. Synonymy of yardangs in early studies Kharga Depression included "mud lions" or "sitting sphinxes" or simply hummocks (Beadnell 1909). Morphometric studies show that they averaged 2.5 ± 1.3 m in height, 16.9 ± 12.4 m in length, and 4.8 ± 1 m in width. There is no significant correlation ($R = -0.41$) between width and height but the length to width ratio is about 3:1 (Hamdan 1987, 2014a). These positive relationships between length/width indicate that yardangs pass through a cycle of development, whereby their size becomes smaller by time (Embabi 2017). The shape of playa yardangs is as asymmetric streamline or linear with a steep windward face and a gentle lee slope. Irregular or dome-like shapes are common in some fields of playa yardangs in Farafra Depression (Hamdan 2014a). Linear shapes are found in environments with a unidirectional wind regime such as in Kharga and Dakhla (Hamdan 1987). The windward face of many large yardangs is very steep and very rarely, some linear yardangs might acquire certain shapes like the sphinx.. The leeward ends of many yardangs are tapered and are lower in general than the windward side.

The formation of yardangs is apparently a stage in the denudation of playa deposits and may in fact explain the reduction of a playa surface through time. Hamdan (2014a), related the formation of the yardang to an interaction between internal (lithology, sedimentary structures and joints and fractures) and external factors (uni-directional winds, flow system around the yardangs and water action). These factors vary in different areas which in turn produce different yardang shapes. An evolutionary model of different yardang types in Farafra Depression (Hamdan 2014a) where after the main episode of playa formation, it is likely that the playa undergoa sequence of erosional events. The development of yardangs requires strong wind (highly charged with sand) and selective incision of the substrate in order to isolate positive forms between erosional grooves which become troughs, then corridors, as they deepen and widen (Fig. 12.13). Incision progressively focuses air flow, which exploitslithological/structural weaknesses to erode transversely and attack an upwind facing prow. The early development of yardangs produes irregular shapes as well as ambiguous axial trends inherited from relict fluvial dissection or giant desiccation cracks. During subsequent stages, wind blowing parallel to the irregular shaped yardangs, deepen grooves between them by deflation resulting linear ridges. Simultaneously, the ridges are streamlined, primarily by wind abrasion. The winds also rise above the ridges and subsequently descend forming eddies in a leeward direction. This process often creates depressions on the top of the ridges as well as abrading the top in a downwind direction. Deeping of the depressions at the top of the ridges leads to dissection into smaller flat topped yardangs with different shapes (Fig. 12.13). Flat topped domal yardangs are formed in the centre of the playa basin where the lithology is dominated by thick massive playa silt. Continuous wind erosion of the homogenous playa lithology leads to the formation of curved-top yardangs. A perfect domal yardang shape indicates that the erosion proceeded simultaneously on all surfaces by fine particles abrasion and vortices within a complex system of subsidiary air flow. Due to geologic structures, such as joints and calcified root casts, asymmetric domal yardangs are also formed. When wind approaches asymmetric domal yardangs, eddies are generated, with accelerates velocities along flanks of the yardangs. The wind eddies scour the sides of the yardang facing the wind. Since eddies are formed close to the ground surface and to height of ca. 1 m, erosion preceded much faster near the ground. This leads to lowering of the ground around the yardangs and exposes softer playa sand to further wind erosion (Fig. 12.13). As erosion proceeds, the upper hard playa silt becomes overhanging as a result of undermining of the lower softer layer and the yardang changes to a conical shape. At the edge of the playa basin, asymmetric domal yardangs are changed to a sphinx shapeby unidirectional wind and the effects of thin hard massive playa silt.

In a final stage, the yardangs lose their streamline shape and mushroomand cylindrical shapes are developed. Some yardangs may then split into several collapsed blocks while others are separated completely from their base and lean over or a reduced to form small pedestals (stack yardang) as the only indictor of a former yardang. All such remnants are eroded by time and flat surface is formed with residual and coarse sand often with abundant lithic artifacts.

Other yardangs occur on bedrock surfaces in the Dakhla and Kharga plateau and are also known as Kharafish (Brookes 1993). Bedrock yardangs develop in Tertiary limestone that does not contain a large content of chert. The ridges attain few hundred meters wide and few kilometers long and the furrows are shallow and broad. The floor of the furrows is occupied by late Holocene playa sediments associated with an indigenous late Neolithic-Old Kingdom archaeological culture (Sheikh Muftah), at the top of the plateau in front of Dakhla Oasis.

12.4.3 Evaporite Deposits

Arid climatic conditions prevailed in Egypt during the Quaternary as represented by thick evaporite deposits in the Qattara Depression, continental sabkhas in south western

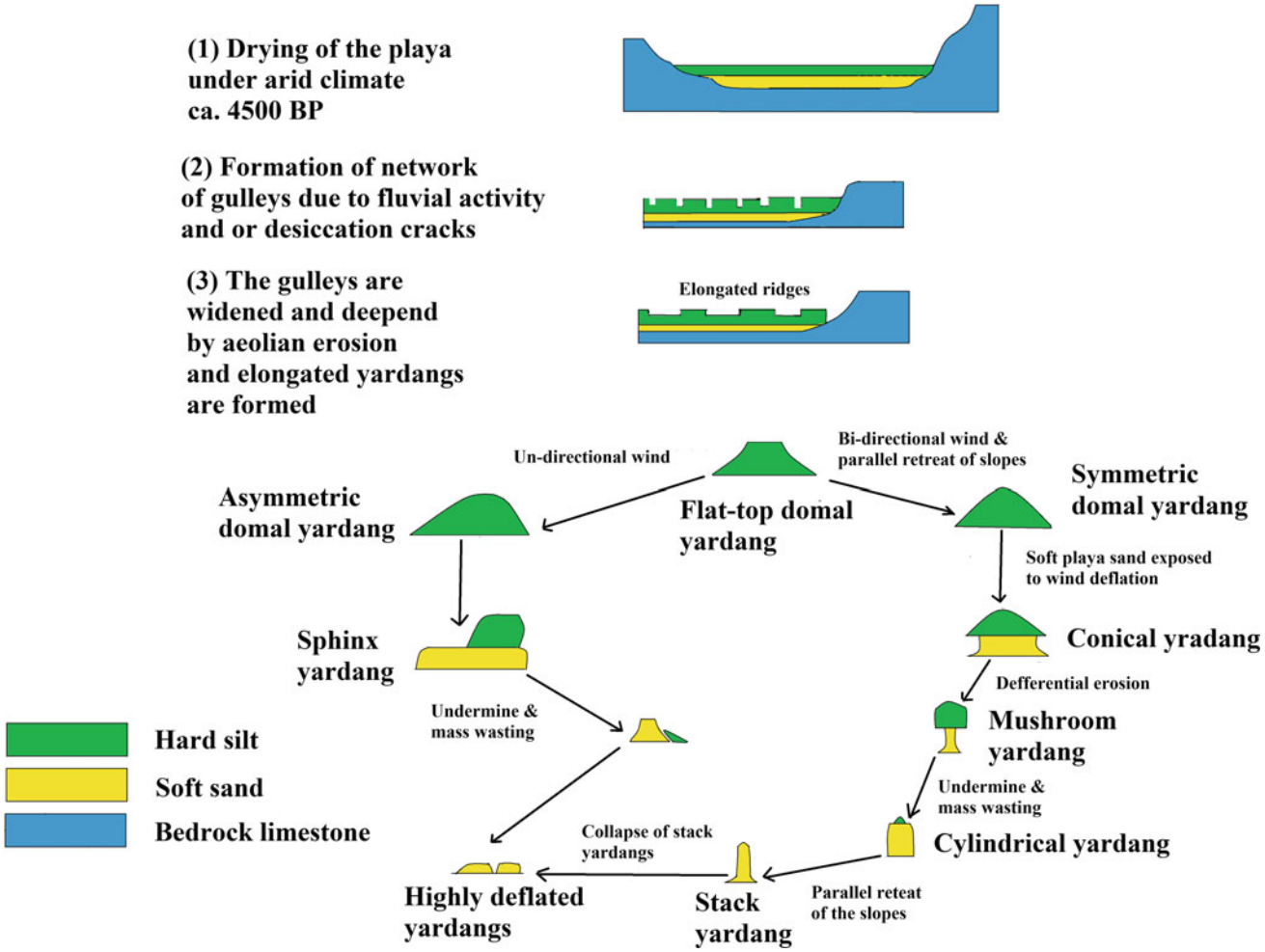

Fig. 12.13 An evolutionary model of yardang formation in the of Farafra Depression (*Source* Hamdan 2014a)

Desert and by hypersaline lakes in Wadi Natrun (El-Bassyony 1995; Attia and Hussein 2015; Taher and Abdel-Motelib 2015). The evaporite sediments of the Qattara Depression are represented by three types (Aref et al. 2002, Aref and Hamdan 2003). Type 1 evaporite sediments are the oldest and represent the earliest record of Quaternary aridity in the depression. They are present as random, isolated or dense, evaporite nodules within the top part of the Moghra clastics and form a dense crust capping a mesa-like plateau (called a salt plateau Ball 1933) at 100 m BSL. Type 2 evaporite sediments are comprise a dry, indurate rough sabkha surface that extends for hundreds of meters around type 1 terraces. It represents a previous stage of groundwater lowering since the sabkha surface has no connection with the present groundwater table. It consists of gypsum/anhydrite or halite crusts, 7–20 cm thick that forms a tepee polygonal structure with margins warped upwards to about 50 cm in height (Aref and Hamdan 2003). Type 3 evaporite sediment is recorded at levels lower than types 1 and 2 sediments, as wet, rough sabkha surface that also extends for hundreds of meters. It represents the last stage of a lowering groundwater table.

Salt weathering was one of the agents responsible for excavation of the Qattara Depression (Aref et al. 2002). Crystallization of halite and/or gypsum generates increased pressure that leads to mechanical disintegration of the bedrock into fine-grained debris. Features related to disintegration include blistering of the rock surface, splitting, spalling and/or granular disintegration. Salt weathering provides fine-grained debris that is easily removed by deflation, which accounts for the topographically lower level of the western part of the depression (134 m below sea level). The disintegration by salt weathering has been in effect since the onset of aridity in northern Egypt in Quaternary time. Howver, initial excavation of the depression started in late Miocene or Pliocene time by fluvial erosion, karstic processes, and mass-wasting and by wind deflation (Aref et al. 2002).

Quaternary continental sabkhas are existed also in Bir El Shab area, south Western Desert, where four sabkha units are recorded (Attia and Hussein 2015). Sabkha 1 consists of sand

and silt with an alum salt crust. Sabkha 2 includes wet silt and sands at its base and an alum and gypsum crust at the top. Sabkha 3 is composed of mudstone intercalated with ferruginous laminae and capped with alum and gypsum crusts associated with black crenulated microbial laminae. Sabkha 4 includes a gypsum crust which usually displays a polygonal fracture and tepee structure. Mineralogically, Bir El-Shab salt complex includes gypsum, natroalunite, tamarugite, nitratine and halite. These minerals indicate evaporation of non-alkaline water (Attia and Hussein 2015). No absolute dating is given to these sabkhas but their geomorphic and stratigraphic settings most likely refer to the Quaternary age.

In Wadi El Natrun, there are seven large alkaline, hypersaline lakes in addition to numerous small ephemeral pools (Taher and Abdel-Motelib 2015). Lake waters have extremely high salt concentrations of 91.0–393.9 g/l, and pH values of 8.5–11 (Taher 1999). Most lakes reach maximum levels in winter between December and March, with lowest levels in summer. Their depths range between 0.5 and 2 m, regulated by seasonal changes in influx seepage and evaporation (Mesbah et al. 2007). The mineral composition is represented by three main types of sodium salt; chlorides, carbonates and sulphates. Sodium chloride (halite, Na Cl), is the most abundant mineral present within these lakes (Shortland 2004). Halite occurs as a crust or found within the layer structure of the mineralogical deposits. Although Wadi Natrun is named after the mineral natron ($Na_2CO_3.10H_2O$), natrun is scarce in the mineralogical record but trona ($NaHCO_3.Na_2CO_3.2H_2O$) is the most common carbonate. Nahcolite ($NaHCO_3$) is also occasionally found within Lake Ruzunia (Attia et al. 1970). Sodium sulphates mineral is also represented by the double crystal salt, burkeite ($Na_2CO_3.2Na_2SO_4$).

The origin of the lakes water remains unclear. Pavlov (1962) suggested a radial inflow of underground waters towards the lakes. Underground flow from the Rosetta branch of the Nile could be another source (Shata and El-Fayoumi 1967; Attia et al. 1970). Chemical and isotopic data of the lake waters hower suggests the source is rainwater that occasionally infiltrates from the shallow alluvial and Eocene limestone aquifers (Sturchio et al. 1998). The Wadi Natrun has been identified as a potential source of both natron and salt from the middle Kingdoms onward and resources from within the wadi are believed to have been utilized in medicine, mummification and in the glass making industry.

12.4.4 Quaternary Paleoclimate, Paleoenvironmental and Archeology of Egypt

Quaternary paleoclimate of Egypt is related to the glacial-interglacial cycles well established in Europe and North America. These cycles are expressed in Egypt as alternating dry (interpluvials) and relatively humid intervals (pluvials) (e.g. Said 1981, 1990, 1993; Hamdan and Brook 2015 and many others). Currently, it is now accepted that there are seven pluvials corresponding to global eustatic events and warm humid phases (Said 1981). The oldest two pluvials (the Edfu and Armant pluvials) are assigned as the early Pleistocene. The position of these two pluvials in the early Pleistocene stratigraphic scheme is not well established, because of the lack of reliable dating and absence of interpluvial sediments (Wysocka et al. 2016). The five subsequent pluvials; Abbasia I, Abbasia II, Sahara I, Sahara II and the Nabata pluvials, are assigned to the middle–late Pleistocene and the early Holocene, respectively (cf. Said 1990).

Generally, the climate of Egypt during early Pleistocene (from ca. 2.84 Ma) was arid and Egyptian lands were proper desert (Said 1981). During this long arid episode, wind was active and modeled the fluvial sediments that had accumulated mainly in basins, e.g. the basin of the Great Sand Sea (Embabi 2017). This period was interrupted with a short pluvial (the Idfu Pluvial), during which a highly competent river (the Protonile) flowed in the Nile Valley (Said 1990). By the end of the early Pleistocene, another short pluvial period occurred, whitnessed by the Armant conglomerate Formation. This Armant Pluvial is separated from the Protonile Pluvial by a short arid phase (Said 1990). Unfortunately, few dates are available for the two early Pleistocene short wet periods; however, there is one early Pleistocene date of 2288 kyr BP from a snail-bearing horizon at Lazy Beach 1, Kharga Depression. This may indicate that the Kharga climate was relatively wet or its water table sat high enough to host hominins during the Matuyama Chron, MIS 87 (Blackwell et al. 2017).

Owing to the extensive tufa and spring deposits in the Western and Eastern Desert, the climate of Egypt during middle Pleistocene is well known (see Smith 2004, 2006; Sultan et al. 1997). Figure 12.13 shows a comparison of the uranium-series ages of lacustrine carbonates accumulated at Western Desert during the middle-late Pleistocene pluvial periods together with the glacial/interglacial curve (Imbrie et al. 1984). The distribution of dates demonstrate the clustering of carbonate deposition not only during most interglacial periods (e.g., during stages 5a, 5c, 5e, 7a, 7c, 7e), but also during glacial stages 6 and 8 (Fig. 12.14). Szabo et al. (1995) cited five pluvial periods: at 320–250, 240–190, 155–120, 90–65 and 10–5 kyr BP, corresponding to interglacial Oxygen Isotope Stages (OIS) 9, 7, 5e, 5c, 5a and 1, respectively. These pluvial periods correlate well with tufa and spring deposits exposed at Kharga (Smith 2004, 2006; Sultan et al. 1997), Dakhla (Blackwell et al. 2017), Kurkur (Crombie et al. 1997; Hamdan 2003b) and in the Eastern Desert (Hamdan 2000b; Hamdan and Brook 2015) as well as with lacustrine deposits (McKenzie 1993). More recently, ESR dates published by Blackwell et al. (2017)

show flourishing ecosystems in Dakhla and Kharga during MIS 5 (74–133 kyr BP), 7 (188–244 kyr BP), 9 (285–338 kyr BP), 11 (364–426 kyr BP), and 17 (659–712 kyr BP), and in shorter episodes in MIS 1 (0–12kyr BP), 2 (12–26 kyr BP), 3 (26–59 kyr BP), 6 (133–188 kyr BP), and 12 (426–475 kyr BP). Indeed, these dates associated with prehistoric sites confirm that enough water existed in the Western Desert to support animal and plant life including herbivoresand likely hominins during much of the mid and late Pleistocene (Blackwell et al. 2017). Generally, most dates of Western Desert tufas and spring deposits fall within the warm, odd numbered MIS periods that correlate with interglacial periods in the Northern Hemisphere (Sultan et al. 1997). Interestingly, wetter conditions also existing from colder periods (e.g. Hamdan and Brook 2015).

In Egypt, the oldest prehistoric sites materials are mainly represented by late Lower Paleolithic occupations on the margins of the Nile Valley and in the Western Desert (Fig. 12.14a). The sites include upper Acheulean Complex (later early Stone Age) artifacts, probably dated to >400 kyr BP, and terminal early Stone Age lithics, probably dated at >300 kyr BP (Brookes 1989, 1993; Kleindienst et al. 2009, 2016). In middle Pleistocene pluvial events, the Western Desert may have received as much precipitation as 50–85 cm/y (Kieniewicz and Smith 2007, 2009). Stable isotopic analysis of tufa sediments indicate that rain water-was delivered from the Atlantic by strong westerlies (e.g. Sultan et al. 1997; Abouelmagd et al. 2012). The existence of fossil freshwater mollusks in palustrine and/or lacustrine sediments may indicate permanent water bodies and even large lakes (Blackwell 2017). During wet periods of the middle Pleistocene, savanna and savanna-woodland environments were common in Egypt (Churcher et al. 1999). Vertebrate and mollusk fossils have been recovered from deposits dated to the Pleistocene and Holocene in the Western Desert (Churcher et al. 1999, 2008; Gautier 1980, 1981, 1984). Middle Pleistocene vertebrate taxa at Dakhla Oasis included African elephant, camel, hippopotamus,

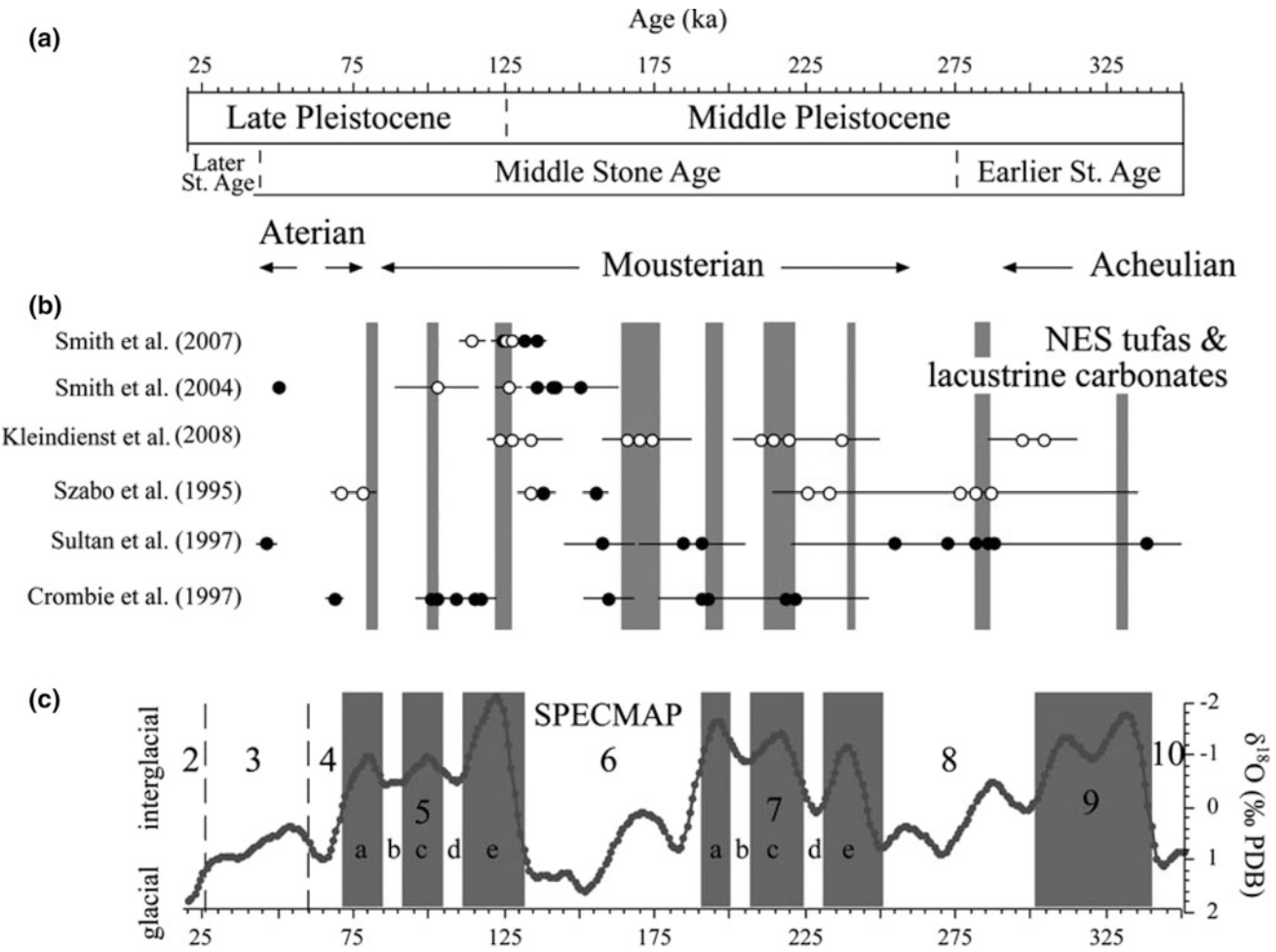

Fig. 12.14 **a** Age range of archaeological industries found in the northeastern Sahara (see text); **b** Uranium-series ages of lacustrine and spring carbonates from the northeastern Sahara. White (black) symbols indicate carbonates with (without) associated archaeological remains; **c** SPECMAP curve (Imbrie et al. 1984) (*Source* Larrasoana, 2012)

warthog, African buffalo, hartebeest, antelope, gazelle, small buck, extinct Cape zebra, wading birds, water fowl a small thrush-sized bird and small catfish (Churcher et al. 1999). The existence of freshwater snails and catfish in areas now proper desert indicate that the water was permanent and fresh which correlates with the presence of hippo, buffalo and zebra species that cannot exist far from potable water. The fauna and flora suggest a lake-shore environment with nearby savannah-woodland similar to the modern East African Valley.

In the Nile Valley, forty vertebrate taxa associated with archaeological sites dated to ca. 15,000 to 10,500 B.C. are known. Fish taxa are represented by Nile catfish, African barbel and Nile perch. The avian fauna includes twenty two species of shore, wading, and divingbirds. The mammalian fauna includes a canid, striped hyaena, *Lepus capensis*, Egyptian bandicoot or pest rat, wild ass, hippopotamus, wild cattle, bubal hartebeest, Dorcas gazelle, rhim or white gazelle and Barbary sheep (Gautier 1981). The remains of these animals collected from prehistoric sites of the Nile Valley are useful in constructing the ancient landscape and environment that prevailed during late Pleistocene. The fauna of the Nile River indicate that woodlands along the river banks and tree savannas and grasslands on the low hills and plains were widespread in the Nile Valley.

In the Eastern Desert, Pleistocene sediments in the Sodmein cave contain an extensive layer of humic material rich in plant micro-remains and Chironomidaeinsects (Marinova et al. 2008). In fact, the immature stages of these insect occur only in aquatic or wet habitats. The plant remains include, *Acacia tortilis* (a tree frequently used to make fire), *Clematis*sp., *Balanites* cf. *aegyptiaca* and Brassicaceae. The plant assemblage confirms conditions much wetter than the actual desert. Faunal analysis shows some remains of dorcas gazelle, rock dassie, a large bovid (buffalo), kudu and an elephantid which also indicate wetter environments in Eastern Desert during late Pleistocene (Marinova et al. 2008).

Between ca. 250–220 kyr BP, the middle Paleolithic began in Egypt with flakes made by the Levallois method (Bard 2007). Middle Paleolithic tools have been found in the Nile Valley, in Egypt and Nubia, but the best preserved sites are in the Western Desert (Fig. 12.14b). In Bir Sahara East and Bir Tarfawi, middle Paleolithic artifacts were found on the beaches of permanent lakes during wet intervals between 175 and 70 kyr BP (Wendorf and Schild 1993). After ca. 70 kyr BP the Western Desert was dry and cool and human habitation was no longer possible except in the oases. In Upper Egypt near Qena, evidence of a late middle Paleolithic culture dating to ca. 70–50 kyr BP has been identified (Van Peer et al. 2010). At the site of Taramsa-1, near the Ptolemaic temple of Hathor at Dendera, the oldest known human skeleton in Egypt has been excavated (Van Peer et al. 2010). From 70 to 12 kyr BP, dry conditions prevailed in Egypt and Saharan hyperarid environmental conditions expanded southward (Swezey 2001). Nile flow was also diminished (Lamb et al. 2007) and lakes dotting the Western and Eastern deserts during the Pleistocene interglacials dried out as dunes became active (e.g., Besler 2008). However, more humid conditions persisted especially around the Kharga and Dakhla Oases where water was available and these served as refuges for both hominins and other fauna (Blackwell et al. 2017).

During the hyperarid phase of the late Pleistocene, when the Sahara dried out, the Nile Valley also turned into a refuge for people and animals. The Western Desert remained largely uninhabitable until after ca. 10 kyr BP, creating a gap in the archaeological evidence of human cultures until after the upper and late Paleolithic. Upper Paleolithic sites in the Nile Valley are also rare (Bard 2007). The oldest known flint mine in the world (ca. 35–30 kyr BP), a source of stone for tools, is located at the site of Nazlet Khater-4 in middle Egypt (Vermeersch et al. 2002) where a grave of a robust *Homo sapiens sapiens* was found with a stone axe placed next to the skull (Vermeersch et al. 2002). Many more sites are known for the late Paleolithic ca. 21–12 kyr BP), than for the Upper Paleolithic (Bard 2007). Late Paleolithic sites are found in Lower Nubia and Upper Egypt, but not further north, where contemporary sites are probably buried under later river alluvium. Archaeological evidence suggests that the subsistence of late Plaeolithic peoples was based on hunting large mammals such as wild cattle and hartebeest, small dorcas gazelle, waterfowl, shellfish, and fish.

After a long late glacial hyperarid period, the entire Sahara, including Egypt, became wetter as tropical rainfall belts shifted northwards (Nicholson and Flohn 1980). Several palaeoclimatic data show that the early to mid-Holocene (10–5 BP) was a relatively humid period in Northern Africa, however, ITCZ effects didn't get further North than about 25° N (e.g. Shanahan et al. 2015). During this phase, often called the African Humid Period (AHP), grasslands covered the Sahara/Sahel region, with many lakes and wetlands (DeMenocal et al. 2000). During the AHP, summer heating of the Northern Hemisphere was maximized, with values of 8% more insolation than today due tocycles in the Earth's orbital parameters. More intense summer insolation deepened the East Saharan atmospheric low which in turn strengthened the summer African Southwest monsoon and brought Atlantic-derived moisture much further north than today (DeMenocal et al. 2000). The sequence of early Holocene playa development of Western Desert begins with an initial episode of wind deflation corresponding to the aeolian sand unit at the base of the early Holocene playa.

The sedimentological characteristics of the lacustrine sediments show an abundance of coarse clasts probably reflecting sedimentation by slope wash and sheet flow as a result of thundershower monsoon rains. Evidence for early

Holocene wet phases in the Eastern Sahara has been adequately documented in many of the modern oases and around the ancient, ephemeral playas in Southern Egypt (Wendorf and Schild 1980; Kröpelein 1987; Hassan et al. 2001). Haynes (1987) suggested that the mountains and surrounding plains in SW Egypt and NW Sudan received from 400 to 600 mm rainfall annually when occupied by Saharan Pastoral Neolithic communities. These poeple depicted their pastoral activities (particularly cattle) in the rock art of the area (Kuper and Kröpelein 2006). The most ancient playa sediments at Gilf Kebir were deposited between ca. 9300 cal. BP and 8200 cal. BP (Linstädter and Kröpelein 2004).

Moreover, stable isotope studies of carbon and oxygen, coupled with paleontological studies of mollusks and microfossils, confirm the widespread occurrence of stable freshwater lakes up to a few tens of meters deep in Dakhla Depression (Kieniewicz and Smith 2009). Also, higher precipitation and intensified monsoonal activity in the African Nile Headwaters led to higher Nile discharge and flooding of the Faiyum Depression (Hassan 1986; Hassan et al. 2012). Early Holocene river activity and surface groundwater recharge are recorded also in western desert of Egypt and northern Sudan (Pachur and Röper 1984; Pachur and Hoelzmann 2000).

The early Holocene humid period was interrupted by colder episodes of increased aridity, as shown by low Nile discharges: the most severe was around 8.2 cal kyr BP which is inferred from a widespread drying and increase in the oxygen isotope signal between 8400 and 8000 BP (Hassan et al. 2012; Hamdan et al. 2016a) and desiccation of the early Holocene play as associated with deposition of thermoclastic rubbles in Farafra Depression (Hassan et al. 2001; Hamdan and Lucarini 2013). The radiocarbon dates in the Bir Kiseiba region may indicate an arid period from 8.2 to 8.1 cal kyr BP (Close 1984), while a hyper-arid interval in the Nabta region occurred around 8.5 cal kyr BP (Nicoll 2004). There is no evidence of occupation in the southern Egyptian Western Desert (Wendorf and Schild 2001). Occupation is instead concentrated in Western oases and the Red Sea Mountains (Moyersons et al. 1999). Along the Nile, human occupation is consistently reported, and for the middle Nile region there is clear evidence of the population clustering along the river and moving south of the Third Cataract (Gatto and Zerboni 2015).

General, after the 8.2 cal kyr BP cooling event, moisture in Egypt generally decreased (Nicoll 2004), the northern playas began to dry as early as 7.7 cal kyr BP (Brookfield 2010). Also, most rainwater-fed playas began to wane around 7 cal kyr BP and became desiccated by 5.5 cal kyr BP. Vegetation diminished, decreasing the number of taxa, and sand was mobilized, forming dunes and sand sheets (Nicoll 2004). Botanical evidence from Egypt indicates that the savannah environment progressively disappearied in the middle Holocene as desert species substituted for more water-dependent plants. Savannah elements but persist but only in isolated ecological niches manly in the Western Desert Oases (Neumann 1989). At Siwa, the interfingering of playa layers with longitudinal dunes suggests a trend of seasonal variability in water availability (Haynes 1982). In south western Egypt around Selima, the level of lakes fluctuated and suffered profound evaporation after 8.9 cal kyr BP (Haynes et al. 1989).

In the middle Holocene, Sahelian vegetation zones were only 300–400 km north of their present range compared to 500–600 km during the early Holocene (Brookfield 2010). With increasing desiccation from 6 cal kyr BP onwards, savannah formations retreated to the south until their present position was reached by about 3.8 cal kyr BP (Neumann 1989). Some climate modeling results and paleoclimate data have indicated that the change from a semi-arid climate with about 250 mm/yr of rainfall to a hyperarid climate with less than 50 mm/year of rainfall occurred over a relatively short period of time, on the order of hundreds of years (DeMenocal et al. 2000).

During late Holocene, aridification started rapidly as the Western Desert lakes dried out and the level of Lake Qarun in the Faiyum dropped by ca. 15 m after 4.5 cal kyr BP (Hamdan and Lucarini 2013; Hamdan et al. 2016a, Hassan et al. 2012); sedimentation turned from freshwater into evaporitic/saline in Lake Qarun (Hamdan et al. 2016a); isotopic data on sediments and mollusks indicate a progressive decrease in the precipitation/evaporation balance (Hassan et al. 2012). These data indicate that the Nile flow diminished significantly (Hassan et al. 2017; Hamdan et al. 2018). In the wider region, pollen data illustrate that many tropical taxa disappeared or were confined to a few refuges (Nicoll 2004). Freshwater was available only in the Nile Valley and those Western Desert oases which inherited water from reservoirs formed in the AHP and occasionally from residual precipitations. According to most evidence, aridification continued up to the onset of present-day environmental conditions

Human occupation of the western Desert of Egypt indicates four distinct phases (Kuper and Kröpelein 2006): the Reoccupation phase (10.5–9 cal kyr BP); the Formation phase (9–7 cal kyr BP) ending abruptly in areas without permanent water; the Regionalization phase (7.3–5.5 cal kyr BP) featuring retreat to highland and Nile refuges; and the Marginalization phase (5.5–3.5 cal kyr BP). All these phases reflect the changing Holocene paleoclimatic and paleoenvironmental conditions in the Western Desert of Egypt. During the Reoccupation phase (10.5–9 cal kyr BP); the northward advance of monsoon rains at 10.5 cal kyr BP transformed the Sahara into a savannah, allowed hunter gatherers to migrateduring northwards into the present desert. During the Formation phase (9–7.3 cal kyr BP), human populations

adapted to multi-resources with domestic livestock of sheep and goats introduced from the Middle East and cattle probably from local domestication. Nabta playa has the earliest documented domestic cattle and goats, and these animals dominate rock art in the Western Desert. Recent studies in the Western Desert, Nile Valley and Faiyum show increase winter rainfall in Egypt during early and middle Holocene (Kröpelein 1987; Hassan et al. 2012; Hamdan and Lucarini 2013).

During the Regionalization phase (7300–5500 BP), populations retreated from increasing desertified land into refuges like the Gilf Kebir and plains further south, where rainfall was still sufficient and increase groundwater sources. By the time of the marginalization phase (5.5–3.5 cal kyr BP), permanent occupation of the desert was restricted to northern Sudan. The Gilf Kebir occupation ceased and a great migration to the Nile Valley occurred (Kuper and Kröpelein (2006). By the beginning of the early Predynastic Period, around 5.2 cal kyr BP, the inhabitants of Upper Egypt depended little on hunting for survival, having adopted an agricultural way of life.

The Pharaonic Empire became well-established along the Nile after 5 cal kyr BP; the western-most desert andoases, such as Abu Ballas in the western desert and Laqiya and Wadi Howar in the Sudan, then played only marginal roles except for mineral exploration and sporadic trade routes to more fertile areas in the west, south and east. Thus, by the beginning of the First Dynasty of Egypt (5.05 cal kyr BP), a united state had formed, with Memphis as probably its largest urban center, judging from the extent of the nearby cemetery fields on both sides of the Nile, at Saqqara (West Bank) and Helwan (East Bank). The development, however, of the requisite social specialization processes and hierarchies had begun much earlier, during the increasing aridity of the predynastic Naqada period at the latest.

Aknowledgments The authors greatly thank Roger Flower (UCL), Georg Brook (Georgia University, USA) and Juergen Wunderlich (Frankfurt Unversity, Germany) for their valuble comments and corrections that help in enhancement very much of the current chapter. They also wish to thank the following authores for their kind permissions to use some illustrations from their publications in this chapter; Barbara Barich (Roma University), Eman Ghoneim (University of North Carolina, USA), B.T. Pennington (University of Southampton, UK), A. Zaki (Ain Shams University, Egypt).

References

Abdelkareem M, El-Baz F (2015) Evidence of drainage reversal in the NE Sahara revealed by space-borne remote sensing data. J Afr Earth Sc 110:245–257

Abdelkareem M, Ghoneim E, El-Baz F, Askalany M (2012) New insight on palaeoriver development in the Nile Basin of the eastern Sahara. J Afr Earth Sc 62:35–40

Abotalib ZA, Mohamed RSA (2013) Surface evidences supporting a probable new concept for the river systems evolution in Egypt: a remote sensing overview. Environ Earth Sci 69:1621–1635

Abotalib AZ, Sultan M, Elkadiri R (2016) Groundwater processes in Saharan Africa: implications for landscape evolution in arid environments. Earth Sci Rev 156:108–136

Abouelmagd A, Sultan M, Milewski A, Kehew AE, Sturchio NC, Soliman F, Krishnamurthy RV, Cutrim E (2012) Toward a better understanding of palaeoclimatic regimes that recharged the fossil aquifers in North Africa: inferences from stable isotope and remote sensing data. Palaeogeogr Palaeoclimatol Palaeoecol 329–330: 137–149

Abouelmagd A, Sultan M, Sturchio NC, Soliman F, Rashed M, Ahmed M, Kehew AE, Milewski A, Chouinard K (2014) Paleoclimate record in the Nubian Sandstone aquifer, Sinai Peninsula, Egypt. Q Res 81:158–167

Abu-Bakr M, Ghoneim E, El-Baz F, Zeneldin M, Zeid S (2013) Use of radar data to unveil the paleolakes and the ancestral course of Wadi El-Arish, Sinai Peninsula, Egypt. Geomorphology 194:34–45

Adamson DA (1982) The integrated Nile. In MAJ Williams, DA Adamson (eds) A land between two niles: quaternary geology and biology in Central Sudan. A.A. Balkema, Rotterdam, pp 221–234

Ahmed S (1993) Collapse and solution red breccia of the Issawia Sharq locality, Nile Valley, Upper Egypt. Egypt J Geol 37(2):187–194

Aigner T (1983) A Pliocene cliff-line around the Giza pyramids plateau, Egypt. Palaeogeogr Palaeoclimatol Palaeoecol 42(3–4):313–322

Aly M, Zebker H, Giardino J, Klein A (2009) Permanent scatterer investigation of land subsidence in Greater Cairo, Egypt. Geophys J Int 178(3):1238–1245

Aly MH, Klein AG, Zebker HA, Giardino JR (2012) Land subsidence in the Nile Delta of Egypt observed by persistent scatterer interferometry. Remote Sens Lett 3(7):621–630

Andres W, Wunderlich J (1992) Environmental conditions for early settlement at Minshat Abu Omar, eastern Nile Delta, Egypt. In: van den Brink ECM (ed) The Nile delta in transition: 4th–3rd Millennium BC. IES, Tel Aviv, pp 157–166

Arduino G (1760) Sopra varie sue Osservazioni fatte in diverse parti del Territorio di Vicenza, ed altrove, appartenenti alla Teoria Terrestre, ed alla Mineralogia. Letter to Prof. Antonio Vallisnieri, dated 30th March, 1759. Nuova Raccolta di Opuscoli Scientifici e Filologici (Venice), v. 6 (1760)

Aref M, El-Khoriby E, Hamdan MA (2002) The role of salt weathering in the origin of Qattara Depression, Western Desert, Egypt. Geomorphology 45:181–195

Aref M, Hamdan MA (2003) Sedimentology and environmental interpretation of the evaporite deposits in the Qattara Depression, Western Desert, Egypt. Sedimentol Egypt 10:193–213

Ashour MM, Embabi NS, Donner J, Abu Zeid KA (2005) Geomorphology and quaternary geology of Abu El-Egl a playa, Western Desert of Egypt. Bull Egypt Geogr Soc 78:1–26

Ashri AH (1973) Themovement of the Sand Dune at Kharga Oasis, Egypt. J Geol 17:37–46

Attia AKM, Hilmy ME, Hegab OA (1970) Mineralogy of the sediments of Wadi el-Natrun lakes. Desert Inst Bull 2:327–357

Attia OE, Hussien KH (2015) Sedimentological characteristics of continental sabkha, south Western Desert, Egypt. Arab J Geosci 8:7973–7991

Bagnold R (1931) Journeys in the Libyan Desert 1929 and 1930. Geogr J 78:13–39

Bagnold R (1933) A further journey through the Libyan Desert. Geogr J 82:103–129

Ball J (1900) Kharga Oasis: its topography and geology. Survey Department, Public Works Ministry, Cairo

Ball J (1927) Problems of the Libyan Desert. Geogr J 70: 21–83, 105–128, 209–224, 512

Ball J (1933) The Qattara depression of the Libyan Desert and the possibility of its utilization for power production. Geogr J 82:289–314
Ball J (1939) Contributions to the geography of Egypt. Survey and Mines Department, Cairo, p 308
Bard KA (2007) Introduction to the archaeology of Ancient Egypt. Blackwell Publishing Ltd. 400 pp
Barich BE (2014) The Wadi Obeiyid Cave 1: the rock art archive. In: Barich BE, Lucarini G, Hamdan AM, Hassan FA (eds) From lake to sand, the archaeology of Farafra Oasis, Western Desert, Egypt. All'Insegna del Giglio, Firenze, pp 385–405
Barich BE, Hassan FA (1987) The Farafra Oasis archaeological project (Western Desert, Egypt). 1987 field campaign, Origini XIII:117–191
Barton RNE, Lane CS, Albert PG, White D, Collcutt SN, Bouzouggar A, Ditchfield P, Farr L, Oh A, Ottolini L, Smith VC, Van Peer P, Kindermann K (2015) The role of cryptotephra in refining the chronology of late Pleistocene human evolution and cultural change in North Africa. Q Sci Rev 118:151–169
Beadnell HJL (1909) An Egyptian Oasis: an account of the Oasis of Kharga in the Libyan Desert, with special reference to its history, physical geography, and water supply. John Murray, London
Beadnell L (1910) The sand dunes of the Libyan Desert. Geogr J 35:379–395
Becker RH, Sultan M (2009) Land subsidence in the Nile Delta: inferences from radar interferometry. Holocene 19(6):949–954
Besler H (2008) The great sand sea in Egypt: formation, dynamics and environmental change—a sediment analytical approach. Elsevier, Amsterdam
Blackwell BAB, Skinner AR, Smith JR, Hill CL, Churcher CS, Kieniewicz JM, Adelsberger KA, Blickstein JIB, Florentin JA, Deely AE, Spillar KV (2017) ESR analyses for herbivore teeth and molluscs from Kharga, Dakhleh, and Bir Tarfawi Oases: Constraining water availability and hominin Paleolithic activity in the Western Desert, Egypt. J Afr Earth Sci 136:216–238
Blackwell BAB, Skinner AR, Mashriqi F, Deely AE, Long RA, Gong JJJ, Kleindienst MR, Smith JR (2012) Challenges in constraining pluvial events and hominin activity: examples of ESR dating molluscs from the Western Desert, Egypt. Q Geochronol 10:430–435
Blankenhorn M (1900) Neues zur Geologie and palaeontologie Aegyptens. II: Das palaeogen (Eozaen und Oligozaen). Z Deutsch Geol Ges 52:403–479
Briere PR (2000) Playa, playa lake, sabkha: proposed definitions for old terms. J Arid Environ 45(1):1–7
Brown RH (1892) The Faiyum and Lake Moeris. Edward Stanford, London, p 110
Brookfield M (2010) The desertification of the Egyptian Sahara during the Holocene (the Last 10,000 years) and its influence on the rise of Egyptian Civilization In: Martini IP, Chesworth W (eds) Landscapes and societies. Springer Science & Business Media B.V. https://doi.org/10.1007/978-90-481-9413-1_6
Brook G, Embabi N, Ashour M, Edwards R, Cheng H, Cowart J, Dabous A (2002) Djara Cave in the Western Desert of Egypt: morphology and evidence of quaternary climatic change. Cave Karst Sci 29:57–66
Brookes IA (1989) Early Holocene basinal sediments of the Dakhla Oasis region, south-central Egypt. Quatern Res 32:139–152
Brookes IA (1993) Geomorphology and quaternary geology of the Dakhla Oasis region, Egypt. Q Sci Rev 12:529–552
Brookes IA (2001) Possible Miocene catastrophic flooding in Egypt's Western Desert. J Afr Earth Sci 32:325–333
Brookes IA (2003) Palaeofluvial estimates from exhumed meander scrolls, Taref Formation (Turonian), Dakhla Region, Western Desert, Egypt. Cretac Res 24(2):97–104
Bubenzer O, Hilgers A (2003) Luminescence dating of Holocene playa sediments of the Egyptian southern plateau Western Desert, Egypt. Q Sci Rev 22(10–13):1077–1084
Bubenzer O, Besler H, Hilgers A (2007) Filling the gap: OSL data expanding 14C chronology of late quaternary environmental change in the Libyan Desert. Q Int 175:41–52
Bunbury J, Jeffreys D (2011) Real and literary landscapes in Ancient Egypt. Camb Archaeol J 21(1), 65bri
Bunbury JM, Graham A, Hunter MA (2008) Stratigraphic landscape analysis: chartering the Holocene movements of the Nile at Karnak through ancient Egyptian times. Geoarchaeology 23:351–373
Bunbury JM, Tavares A, Pennington BT, Gonçalves P (2017) Development of the Memphite floodplain—landscape and settlement symbiosis in the Egyptian capital zone. In: Willems H, Dahms JM (eds) The Nile: natural and cultural landscape in Egypt. Proceedings of the international symposium held at the Johannes Gutenberg-Universität Mainz, 22 and 23 February 2013. Bielefeld: Transcript Verlag, pp 71–96
Butzer KW (1960) On the Pleistocene shorelines of Arab's Gulf. Egypt J Geol 68:626–637
Butzer KW (1964) Environment and archeology: an introduction to Pleistocene geography. Aldine Publishing Company, Chicago
Butzer KW (1980) Pleistocene history of the Nile valley in Egypt and lower Nubia. Sahara Nile 253:280
Butzer KW (1982) Archaeology as human ecology: method and theory for a contextual approach. Cambridge University Press
Butzer KW (1997) Late quaternary problems of the Egyptian Nile: stratigraphy, environments, prehistory. Paléorient 23(2):151–173
Butzer KW, Hansen CL (1968) Desert and river in Nubia. University of Wisconsin Press, 256 pp
Caton-Thompson G (1952) Kharga Oasis in prehistory. Athelon Press, London
Caton-Thompson G, Gardner EW (1929) Recent work on the problem of LakeMoeris'. Geogr J 73:20–60
Caton-Thompson G, Gardner EW (1934) The Desert Faiyum. The Royal Anthropological Institute of Great Britain and Ireland, London
Chen Z, Warne AG, Stanley DJ (1992) Late Quaternary evolution of the northwest Nile Delta between Rosetta and Alexandria. Egypt. J. Coast. Res. 8(3):527–561
Churcher CS, Kleindienst MR, Schwarcz HP (1999) Faunal remains from a middle Pleistocene lacustrine marl in Dakhla oasis, Egypt: palaeoenvironmental reconstructions. Palaeogeogr Palaeoclimatol Palaeoecol 154(4):301–312
Churcher CS, Kleindienst MR, Wiseman MF, McDonald MMA (2008) The quaternary faunas of Dakhla oasis, western desert of Egypt. In: Wiseman MF (ed) The Oasis papers 2: the 2nd international conference of the Dakhla Oasis project. Oxbow Books, Oxford, pp 1–24
Campmas E (2017) Integrating human-animal relationships into new data on aterian complexity: a paradigm shift for the North African middle stone age. Afr Archaeol Rev 34(4):469–491
Close AE (ed) (1984) Cattle-keepers of the Eastern Sahara: the Neolithic of Bır Kiseiba. Southern Methodist University, Dallas, p 452
Coutellier V, Stanley DJ (1987) Late Quaternary stratigraphy and paleogeography of the eastern Nile Delta, Egypt. Mar Geol 77(3–4):257–275
Crombie MK, Arvidson RE, Sturchio NC, Alfy ZE, Zeid KA (1997) Age and isotopic constraints on Pleistocene pluvial episodes in the Western Desert, Egypt. Palaeogeogr Palaeoclimatol Palaeoecol 130:337–355
Cornish V (1900) On desert sand dunes bordering the Nile Delta. Geogr J 43:1–32

Dabbour GA (1995) Estimation of the economic minerals reserves in Rosetta beach sands. Egypt Min 7:153–166
Dabous AA, Osmond JK (2000) U/TH study of speleothems from the Wadi Sannur Cavern Eastern Desert of Egypt. Carbonates Evaporites 15:1–16
DeHeinzelin J (1968) Geological history of the Nile Valley in Nubia. In: Wendorf IF (ed) The Prehistory of Nubia, Southern Methodist University, Dallas, Texas, pp 19–55
Deino AL, Behrensmeyer AK, Brooks AS, Yellen JE, Sharp WD, Potts R (2018) Chronology of the acheulean to middle stone age transition in eastern Africa. Science 360(6384):95–98
DeMenocal P, Ortiz J, Guilderson T et al (2000) Abrupt onset and termination of the African humid period: rapid climate responses to gradual insolation forcing. Q Sci Rev 19:347–361
De Wit HE (1993) The evolution of the Eastern Nile Delta as a factor in the development of human culture. In: Krzyzaniak L, Kobusiewicz M, Alexander J (eds) Environmental change and human culture in the Nile Basin and Northern Africa until the 2nd Millennium B.C. Poznan Archaeological Museum, Poznan, pp 305–320
De Wit HE, Van Stralen L (1988) Preliminary results of the 1987 palaeogeographical survey. In: van den Brink ECM (ed) The Archaeology of the Nile Delta: problems and priorities. Netherlands Foundation for Archaeological Research in Egypt, Amsterdam, pp 135–139
Donner J, Ashour MM, Brook GA, Embabi NS (2015) The quaternary history of the Western Desert of Egypt as recorded in the Abu El-Egl playa. Bull Soc Geog d'Egypte 88:1–18
Ebinger C (2005) Continental break-up: the East African perspective. Astron Geophys 46:2.16–12.21
El-Aref MM (1993) Paleokkarst surfaces in the Neogene succession of Wadi Essel-Wadi Sharm El ahari area, Egyptian Red Sea coast as indication of uplifting and expouse. Geol Soc Egypt Spec. Publ. no. 1:205–231
El-Aref MM, Lotfy Z (1985) Genetic karst significance of the iron ore deposits of El Bahariya Oasis, western Desert. Egypt. Ann Geol Surv Egypt 15:1–30
El-Aref MM, Refai E (1987) Paleokarst processes in the Eocene limestones of the Pyramids Plateau, Giza, Egypt. J Afr Earth Sci 6:367–377
El-Aref MM, Awadalah F, Ahmed S (1986) Karst landforms development and related sediments in the Miocene rocks of the Red Sea coastal zone, Egypt. Geologische Rundschau 75(3):781–790
El-Aref MM, Abou Khadrah A, Lotfi Z (1987) Karst topography and karstification processes in the Eocene limestone plateau of El Bahariya Oasis, Western Desert, Egypt. Z Geomorph N F 31:45–64
El-Aref MM, Saleh MH, Salama AM (2017a) Geomorphological classification and zonation of the exposed karst landforms in Bahariya—Farafra region, Western Desert Egypt. Int J Sci Res (IJSR) 6(5):956–965
El-Aref MM, Hammed MS, Salama AM (2017b) Inventory and assessment of the geomorphosites of Bahariya—Farafra territory, Western Desert, Egypt. Int J Sci Basic Appl Res 128–143
El-Asmar HM (1994) Aeolianite sedimentation along the northwestern coast of Egypt; Evidence for middle to late Quaternary aridity. Q Sci Rev 13:699–708
El-Asmar HA (2000) Geoenvironmental studies on the coastal area between Gamasa and Baltim, North of the Nile Delta. Z Geomorph N F, 44(1):59–73
El-Asmar HM, Wood P (2000) Quaternary shoreline development: the northwestern coast of Egypt. Q Sci Rev 19:1137–1149
El-Awady HMS (2009) Application of the geophysical survey for environmental and archaeological purposes, Central Western Part of the Nile Delta, Egypt. Unpublished MSc Thesis. University of Mansoura
El-Bassyony AA (1995) Sabkhas of Qattara Depression, Western Desert, Egypt—a survey. Sedimentol Egypt 3:13–26
El-Baz F (1988) Origin and evolution of the desert. Interdisc Sci Rev 13:331–347
El-Baz F, Maxwell T (eds) (1982) Desert landforms of Southwest Egypt: a basis for comparison with Mars. NASA, Washington, DC
El-Baz F, Wolfe RW (1982) Wind patterns in the Western Desert. In: El-Baz F, Maxwell TA (eds) Desert landforms of Southeast Egypt: a basis for comparison with Mars. NASA, CR-3611, pp 119–139
El-Baz F, Robinson C, Maxwell TA, Hemida IH (1998) Palao-channels of the great selima sand sheet in the Eastern Sahara and implications to ground water. Palaoecol Afr 26
El-Gammal EA (2010) New findings on the Karst in Nubia sandstone Southern Egypt. Nat Sci 8(8):125–129
El-Gammal EA, Cherif OH (2006) Use of remote sensing for the study of the hazards of Ghard Abu Muharik Sand Dune Field, Western Desert, Egypt. In: The 2nd international conference on water resources and arid environment. NARS, Cairo, pp 1–20
El-Gammal EA, El-Gammal AA (2010) Hazard impact and genetic development of sand dunes west of Samalut, Egypt. Egypt J Remote Sens Space Sci 13:137–151
El-Kammar AA, Ragab AA, Moustafa MI (2011) Geochemistry of economic heavy minerals from Rosetta Black Sand of Egypt. JAKU Earth Sci 22(2):69–97
El-Shahat A, Ayyad SN, Abdalla MA (1997) Pliocene facies and fossil contents of Qaret El-Muluk formation at Wadi El-Natrun Depression, western desert, Egypt. Facies 37(1):211–223
El-Shahat A, Ghazala H, Wilson P, Belal Z (2005) Lithofacies of the upper quaternary sequence of San el-Hagar area, Gharbiya Governorate, Nile Delta, Egypt. Mansoura J Geol Geophys 32:97–120
El-Sharkawi MA, El-Aref MM, Abdel Motelib A (1990) Manganese deposits in a Carboniferous palaeokarst profile, Um Bogmaregion, west-central Sinai, Egypt. Mineral Deposita 25:34–43
Embabi NS (2017) Landscapes and landforms of Egypt: landforms and evolution. World Geomorphol Landsc 336 pp. https://doi.org/10.1007/978-3-319-65661-8
Embabi NS (1999) Playas of the Western Desert, Egypt. Ann Acad Sci Fennicae, Geologica-Geographica 160:5–47
Fairbanks RG (1989) A 17,000-year glacio-eustatic sea level record: influence of glacial melting rates on the Younger Dryas event and deep-ocean circulation. Nature 342:637–642
Fielding L, Najman Y, Millar I, Butterworth P, Ando S, Padoan M, Barfod D, Kneller B (2017) A detrital record of the Nile River and its catchment. J Geol Soc 174:301–317
Fielding L, Najman Y, Millar I, Butterworth P, Garzanti E, Vezzoli G, Barfod D, Kneller B (2018) The initiation and evolution of the River Nile. Earth Planet Sci Lett 489:166–178
Flower RJ, Stickley C, Rose NL, Peglar S, Fathi AA, Appleby PG (2006). Environmental change at the desert margin: an assessment of recent paleolimnological records in Lake Qarun, middle Egypt. J Paleolimnol 35(1):1–24
Flower RJ, Keatings K, Hamdan M, Hassan FA, Boyle JF, Yamada K, Yasuda Y (2012) The structure and significance of early Holocene laminated sediments in the Faiyum Depression (Egypt) with special reference to diatoms. Diatom Res 27:127–140
Flower RJ, Keatings K, Hamdan M, Hassan FA (2013) StephanodiscusEhr. Speciesfrom holocene sediments in the Faiyum Depression (middle Egypt). Phytotaxa 127(1):66–80
Gatto MC, Zerboni A (2015) Holocene supra-regional environmental changes as trigger for major socio-cultural processes in Northeastern Africa and the Sahara. Afr Archaeol Rev 32:301–333
Gautier A (1980) Contributions to the archeozoology of Egypt. In: Wendorf F, Schild R (eds) Prehistory of the Eastern Sahara. Academic Press, New York, pp 317–344

Gautier A (1981) Non-marine molluscs and vertebrate remains from Upper Pleistocene deposits and middle Paleolithic sites at Bir Sahara and Bir Tarfawi, Western Desert, Egypt. In: Schild R, Wendorf F (eds) The prehistory of an Egyptian Oasis: a report of the combined prehistoric expedition to Bir Sahara and Bir Tarfawi, Western Desert, Egypt. Polska Academia Nauk, Warsaw, pp 126–145

Gautier A (1984) Quaternary mammals and archaeozoology of Egypt and the Sudan: a survey. In: Krzyzaniak L, Kobusiewicz M (eds) Origin and early development of food producing cultures in north-eastern Africa. Poznan Archaeological Museum, Poznan, pp 43–56

Ghoneim E, Robinson C, El-Baz F (2007) Radar topography data reveal drainage relics in the Eastern Sahara. Inter J Remote Sens 28:1759–1772

Giegengack RF (1968) Late Pleistocene history of the Nile Valley in Egyptian Nubia. Unpublished PhD thesis. Yale University

Giegengack R, Zaki A (2017). Inverted topographic features, now submerged beneath the water of Lake Nasser, document a morphostratigraphic sequence of high amplitude late-Pleistocene climate oscillation in Egyptian Nubia. J Afr Earth Sci 1–12

Gladfelter BG (1977) Geoarchaeology: the geomorphologist andarchaeology. Am Antiq 42(4):519–538

Gladfelter BG (1988) Late Pleistocene lakes within the mountains of southern Sinai: observations at the Tarfat Oasis. Bull Societe de Gtographie d'Egypte Tomes LXI/LXII, 29–49

Gladfelter BG (1990) The geomorphic situation of upper paleolithic sites in Wadi El Sheikh, Southern Sinai. Geoarchaeol Int J 127–141

Gladfelter BG (1992) Soil properties of sediments in Wadi Feiran, Sinai: a geoarchaeological interpretation. In Holliday VT (ed) Soil in archaeology, Smithonian Univ. Press 169–192

Goldberg P (1984) Late Quaternary history of Qadesh Barnea, northeastern Sinai. Zeit Geomorph 28:193–217

Goodman S, Hobbs J, Brewer D (1992) Nimir Cave: morphology and fauna of a cave in the Egyptian Eastern Desert. Paleoecol Afr 23:73–90

Goudie AS (2005) The drainage of Africa since the Cretaceous. Geomorphology 67:437–456

Gunn J (ed) (2004) Encyclopedia of Caves and Karst Science. Taylor and Francis Books, Inc. 1940 pp

Gunnell GF, Winkler AJ, Miller ER, Head JJ, Abdel El-Barkooky AN, Gawad M, Sanders WJ, Gingerich PD (2016) Small vertebrates from Khasm El-Raqaba, late middle Miocene, Eastern Desert, Egypt. Hist Biol 28(1–2):159–171

Günay G, Ekmekci M, Bayari CS, Kurttaş T, El-Bedewy F (1997) Sannur Cave: a crescent shaped cave in Egypt. In: Günay G, Johnson AI (eds) Karst: waters and environmental impacts. Balkema, Rotterdam

Halliday WR (2003) Caves and karsts of Northeast Africa. Int J Speleol 32(1/4):19–32

Halliday WR (2007) Pseudokarst in the 21st century. J Cave Karst Stud 69(1):103–113

Hamdan MA (1987) Geomorphology and quaternary geology of Umm El-Dabadib Area, Kharga Oasis. Dissertation, Ms thesis, Cairo University

Hamdan MA (1993) Pliocene and quaternary sediments and their relationship to the geological evolution of River Nile at lower Egypt. PhD thesis, Cairo University

Hamdan MA (2000a) Subsurface late Pleistocene Nile floodplain sediments of Saqqara area: palaeoenvironmental interpretations. J Sedimentol Egypt 8:243–254

Hamdan MA (2000b) Quaternary travertines of Wadis Abu Had-dib area Eastern Desert, Egypt: Paleoenvironment through field, sedimentology, age, and isotopic study. Sedimentol Egypt 8:49–62

Hamdan MA (2003a) Late quaternary geology and geoarchaeology of Kafr Hassan Dawood, east delta. In: Hawass Z, Pinch Brock L (eds) Egyptology at the Dawn of the twenty-first century: proceedings of the eighth international congress of Egyptologists, Cairo, 2000, vol 1. The American University in Cairo Press, Cairo, pp 221–228

Hamdan MA (2003b) Stable isotope and geochemistry of some travertine deposits of southern Egypt and their paleoclimatic and paleoenvironmental implications: sedimentology of Egypt 11:43–61

Hamdan MA, Lucarini G (2013) Holocene paleoenvironmental, paleoclimatic and geoarchaeological significance of the Sheikh El-Obeiyid area (Farafra Oasis, Egypt). Q Int 302:154–168

Hamdan MA (2014a) Sedimentological characteristics and geomorphic evolution of the Holocene playa of Wadi Obeiyid. In: Barich BE, Lucarini G, Hamdan AM, Hassan FA (eds) From lake to sand, the archaeology of Farafra Oasis, Western Desert, Egypt. All'Insegna del Giglio, Firenze, pp 81–91

Hamdan MA (2014b) Geology of the Holocene playa sediments of Hidden Valley, Wadi Obeiyid, Farafra. In: Barich BE, Lucarini G, Hamdan AM, Hassan FA (eds) From lake to sand, the archaeology of Farafra Oasis, Western Desert, Egypt. All'Insegna del Giglio, Firenze, pp 151–166

Hamdan MA, Hassan FA, Mahmoud A (2014c) The Wadi Obeiyid Cave 1—geological features. In: Barich BE, Lucarini G, Hamdan AM, Hassan FA (eds) From lake to sand, the archaeology of Farafra Oasis, Western Desert, Egypt. All'Insegna del Giglio, Firenze, pp 377–384

Hamdan MA, Brook GA (2015) Timing and characteristics of Late Pleistocene and Holocene wetter periods in the Eastern Desert and Sinai of Egypt, based on 14C dating and stable isotope analysis of spring tufa deposits. Quatern Sci Rev, 130:168–188

Hamdan MA, Abu Refaat AA, Anwar E, Shallaly NA (2015) Source of the aeolian dune sand of Toshka area, southeastern Western Desert, Egypt. Aeolian Res 17:275–289

Hamdan A, Ibrahim MIA, Shiha MA, Flower RJ, Hassan FA, Eltelet SAM (2016a) An exploratory early and middle Holocene sedimentary record with palynoforms and diatoms from Faiyum lake, Egypt. Q Int 410:30–42

Hamdan MA, Refaat AA, Abdel Wahed M (2016b) Morphologic characteristics and migration rate assessment of barchans dunes in the Southeastern Western Desert of Egypt. Geomorphology 257:57–74

Hamdan MA, Hassan FA, Flower RJ, Leroy SAG, Shallaly NA, Flynn A (2019) Source of Nile sediments in the floodplain at Saqqara inferred from mineralogical, geochemical, and pollen data, and their palaeoclimatic and geoarchaeological significance. Q Int. 501, 272-288

Hassan FA (1976) Prehistoric studies of the Siwa Oasis Region, 1975 season. Nyame Akuma 9:18–34

Hassan FA (1979a) Geoarchaeology: the geologist and archaeology. Am Antiq 44(2):267–270

Hassan FA (1979b) Archaeological explorations at Baharriya Oasis and the West Delta, Egypt. Curr Anthropol 20:806

Hassan FA (1986) Holocene lakes and prehistoric settlements of the Western Faiyum, Egypt. J Archaeol Sci 13:483–501

Hassan FA (1997) The dynamics of a riverine civilization: a geoarchaeological perspective on the Nile Valley. World Archaeol 29(2):51–74

Hassan FA (2007a) Extreme Nile floods and famines in Medieval Egypt (AD 930-1500) and their climatic implications. Q Int 173–174:101–112

Hassan FA (2007b) Droughts, famine and the collapse of the Old Kingdom: Rereading lpuwer. In: Hawass Z, Richards J (eds) The archaeology and art of ancient Egypt: essays in honor of David B.

O'Connor. Annales du Service des Antiquit_es de L'Egypte Cahier, vol 36, pp 357–377
Hassan FA (2010) Climate change, Nile floods and riparia. In: Hermon E (ed) Riparia dans l'empire romain pour la d_efinition du concept. BAR International S2066, Oxford, pp 131–152
Hassan FA, Hamdan MA (2008). The Faiyum Oasis—climate change and water management in ancient Egypt. In: Hassan (ed) Traditional water techniques: cultural heritage for a sustainable future. 6th Framework Programme, ShadufProject, pp 117–147
Hassan FA, Barich B, Mahmoud M, Hamdan MA (2001) Holocene playa deposits of Farafra Oasis, Egypt, and their palaeoclimatic and geoarchaeological significance. Geoarchaeol Int J 16(1): 29–44
Hassan FA, Hamdan MA, Flower RJ, Keatings K (2012) The oxygen and carbon isotopic records in Holocene freshwater mollusc shells from the Faiyum palaeolakes, Egypt: their palaeoenvironmental and palaeoclimatic implications. Q Int 266:175–187
Hassan FA, Hamdan MA, Mahmoud A (2014) Desert and Oasis: geomorphology and geomorphic evolution. In: Barich BE, Lucarini G, Hamdan AM, Hassan, FA (eds) From lake to sand, the archaeology of Farafra Oasis, Western Desert, Egypt. All'Insegna del Giglio, Firenze, pp 63–78
Hassan FA, Hamdan MA, Flower RJ, Shallely NA, Ebrahem E (2017) Holocene alluvial history and archaeological significance of the Nile floodplain in the Saqqara-Memphis region, Egypt. Q Sci Rev 176:51–70
Haynes CV (1980) Geological evidence of pluvial climates in the Nabta area of the Western Desert, Egypt. In: Wendorf F, Schild R (eds) Prehistory of the Eastern Sahara. Academic Press, New York, pp 353–371
Haynes CV (1982) Great Sand Sea and Selima sand sheet. Geomorphol Desertification Sci 217:629–632
Haynes CV (1987) Holocene migrations of the Sudano-Sahelian wetting front, Arba'in Desert, Eastern Sahara. In: Close A (ed) Prehistory of arid North Africa. Essays in honour of Fred Wendorf. Southern Methodist University Press, Dallas, pp 69–84
Haynes CV, Eyles CH, Pavlish LA, Ritchie JUC, Rybak M (1989) Holocene palaeoecology of the eastern Sahara: Selima oasis. Q Sci Rev 8:109–136
Hawass Z (1997) The discovery of the harbors of Khufu and Khafre at Giza. In: Berger C, Mathieu B (eds) Etudes sur l'Ancien Empire et la nécropole de Saqqara dédiées a Jean-Philippe Lauer. Orientalia Monspeliensia IX, Montpellier, pp 245–256
Hill CL, Schild R (2017) Pleistocene deposits in the southern Egyptian Sahara: lithostratigraphic relationships of sediments and landscape dynamics at Bir Tarfawi. Stud Q 34:23–38
Hillier JK, Bunbury JM, Graham A (2006) Monuments on a migrating Nile. J Archaeol Sci 34(7):1011–1015
Hobbs JJ, Goodman SM (1995) Leopard-hunting scenes in dated Rock Art from the Northern Eastern Desert of Egypt. Sahara 7: 7–16, réponses de Béatrix Midant-Reynes, idem: 124–126 et d'Alfred Muzzolini, idem: 126–127
Hoelzmann P (2002) Lacustrine sediments as key indicators of climate change during the late quaternary in Western Nubia (Eastern Sahara). Geo-Sciences in Northern Africa 375–388
Hsu KJ, Ryan WBF, Cita MB (1973) Late Miocene desiccation of the Mediterranean. Nature 242:239–243
Imbrie J, Hays JD, Martinson DG, Mclntyre A, Mix AC, Morley JJ (1984) The orbital theory of Pleistocene climate: Su pport from a revised chronology of the marine 6180 record. In Berger A, Imbrie J, Hays J, Kukla G, Saltzman B (eds) Milankovitch and climate, part 1. Plenum Reidel, Dordrecht, pp 269–305
Issar KS, Bruins S (1983) Some climatological conditions in the deserts of Sinai and the Negv during the latest Pleistocene. Paleogeogr Paleoclimatol Paleoecol 44:63–77
Issawi B (1971) Geology of Darb El-Arbain, Western Desert. Ann Geol Surv Egypt 1:53–92
Issawi B, McCauley JF (1992) The Cenozoic rivers of Egypt: the Nile problem. In: Adams B, Friedman R (eds) The followers of Horus. Oxbow Press, Oxford, pp 1–18
Issawi B, McCauley J (1993) The Cenozoic landscape of Egypt and its river systems. Ann Geol Surv Egypt 19:357–384
Issawi B, Osman R (2008) Egypt during the Cenozoic: geological history of the Nile river. Bull Tethys Geol Soc Cairo 3:43–62
Jeffreys DG (2008) Archaeological implications of the moving Nile. Egypt Archaeol 32:6–7
Jeffreys DG, Tavares A (1994) The historic landscape of early Dynastic Memphis. Mitteilungen des Deutschen Archäologischen Instituts, Abteilung Kairo 50:143–173
Jelínek R, Eckert S, Zeug G, Krausmann E (2009) Tsunami vulnerability and risk analysis applied to the City of Alexandria, Egypt. EUR—Scientific and Technical Research series, 40 pp
Kaiser MF, Aziz AM, Ghieth BM (2014) Environmental hazards and distribution of radioactive black sand along the Rosetta coastal zone in Egypt using airborne spectrometric and remote sensing data. J Environ Radioact 137:71–78
Kieniewicz JM, Smith JR (2007) Hydrologic and climatic implications of stable isotope and minor element analyses of authigenic calcite silts and gastropod shells from a mid-Pleistocene pluvial lake, Western Desert, Egypt. Q Res 68:341–344
Kieniewicz JM, Smith JR (2009) Paleoenvironmental reconstruction and water balance of a mid-Pleistocene pluvial lake, Dakhleh Oasis, Egypt. Bull Geol Soc Am 121:1154–1171
Kindermann K, Van Peer P, Henselowsky F (2018) At the lakeshore—An early Nubian Complex site linked with lacustrine sediments (Eastern Desert, Egypt). Q Int 485:131–139
Kindermann K, Bubenzer O, Nussbaum S, Riemer H, Darius F, Pöllath N, Smettan U (2006) Palaeoenvironment and Holocene land-use of Djara, Western Desert of Egypt. Q Sci Rev 25:1619–1637
Kleindienst MR, Smith JR, Adelsberger KA (2009) The Kharga oasis prehistory project (KOPP), 2008 field season: Part I geoarchaeology and pleistocene prehistory. Nyame Akuma 71:18–30
Kleindienst MR, Blackwell BAB, Skinner AR, Churcher CS, Kieniewicz JM, Smith JR, Wise NL, Long RA, Deely AE, Blickstein JIB, Chen KKL, Huang A, Kim MKD (2016) Assessing long-term habitability at an eastern Sahara oasis: ESR dating of molluscs and herbivore teeth at Dakhleh Oasis, Egypt. Q Int 408:106–120
Knetsch G (1954) Allgemein-geologische Beobachtungen aus Ägypten 1951–1953. Neues Jb Geol u Paläontol Abh 99:287–297
Kozlowski JK (ed) (1983) Qasr el-Sagha 1980. Contributions to the Holocene Geology, the predynastic and dynastic settlements in the Northern Fayum Desert Warschau-Krakow: UniversitasIagellonica
Kröpelein S (1987) Palaeoclimatic evidence from early to mid-Holocene playas in the Gilf—Kebir, southwest Egypt. Palaeoecol Afr 18:189–208
Kröpelein S (1993) Geomorphology, landscape evolution and paleoclimates of Southwest Egypt. Catena Suppl 26:31–65
Krom MD, Stanley DJ, Cliff RA, Woodward JC (2002) Nile River sediment fluctuations over the past 7000 yr and their key role in sapropel development. Geology 30(1):71–74
Kuper, R. 1996. Between the oases and the Nile—Djara: Rohlfs' Cave in the Western Desert. Interregional Contacts in the later Prehistory of Northeastern Africa. Poznan Archaeological Museum, Poznan, pp 81–91
Kuper R, Kröpelein S (2006) Climate-controlled Holocene occupation in the Sahara: motor of African evolution. Science 313:803–807
Kusky T, El-Baz F (2000) Neotectonics and fluvial geomorphology of the northern Sinai Peninsula. J Afr Earth Sci 31:213–235

Lamb HF, Bates CR, Coombes PV, Marshall MH, Umer M, Davies SJ, Dejen E (2007) Late Pleistocene desiccation of Lake Tana, source of the Blue Nile. Q Sci Rev 26:287–299

Larrasoan JC (2012) A Northeast Saharan perspective on environmental variability in North Africa and its implications for modern human origins. In: Hublin J-J, McPherron SP (eds) Modern origins: a North African perspective, vertebrate paleobiology and paleoanthropology. Springer Science + Business Media B.V., pp 19–34

Little OH (1936) Recent geological workin the Fayum and in the adjoining portion of the Nile Valley. Bull Institut d'Egypte 18:201–240

Linstädter J, Kröpelein S (2004) Wadi Bakht revisited: Holocene climate change and prehistoric occupation in the Gilf Kebir region of the Eastern Sahara, SW Egypt. Geoarchaeology 19:753–778

Lutley KL, Bunbury J (2008) The Nile on the move. Egypt Archaeol 35:261–292

Macgregor DS (2012) The development of the Nile drainage system: integration of onshore and offshore evidence. Petrol Geosci 18 (4):417–431

Mansour AM, Madkour HA (2015) Raised coral reefs and sediments in the coastal area of the Red Sea. In: Rasul NMA, Stewart ICF (eds) The Red Sea, Springer earth system sciences. Springer, Berlin, Heidelberg

Marks L, Salem A, Welc F, Nitychoruk J, Chen Z, Blaauw M, Zalat A, Majecka A, Szymanek M, Chodyka M, Tołoczko-Pasek A, Sun Q, Zhao X, Jiang J (2018) Holocene lake sediments from the Faiyum Oasis in Egypt: a record of environmental and climate change. Boreas 47(1):62–79

Marinova E, Linseele V, Vermeersch PM (2008) Holocene environment and subsistence patterns near the Tree Shelter, Red Sea Mountains, Egypt. Q Res 70:392–397

Marinova M Nele, Meckler A, McKay CP (2014) Holocene freshwater carbonate structures in the hyper-arid Gebel Uweinat region of the Sahara Desert (Southwestern Egypt). J Afr Earth Sci 89:50–55

Marriner N, Flaux C, Morhange C, Kaniewski D (2012) Nile Delta's sinking past: quantifiable links with Holocene compaction and climate-driven changes in sediment supply. Geology 40(12):1083–1086

Mourik A, Bijkerk J, Cascella A, Hüsing S, Hilgen F, Lourens L, Turco E (2010) Astronomical tuning of the La Vedova High Cliff Section (Ancona, Italy)—implications of the middle Miocene climate transition for Mediterranean sapro-pel formation. Earth Planet Sci Lett 297:249–261

Maxwell T (1980) Geomorphology of the Gilf Kebir. In: El-Baz et al (eds) Journey to the Gilf Kebir and Uwienat, Southwest Egypt (1978). Geogr J 146:76–83

Maxwell TA, Issawi B, Haynes CV (2010) Evidences for Pleistocene lakes in the Toshkka region, south Egypt. Geology 38:1135–1138

McCauley J, Schaber G, Breed C, Grolier M, Haynes C, Issawi B, Elachi C, Blom R (1982) Subsurface valleys and geoarcheology of the Eastern Sahara revealed by shuttle radar. Science 218:1004–1020

McCauley J, Breed M, Schaber G, Haynes V, Issawi B, El-Kilani A (1986) Palaeodrainages of the Eastern Sahara, The radar rivers revisited (SIR-A/B Implications for a Mid-Tertiary Trans-African Drainage System). IEE Trans Geo Sci Remote Sens GE 24:624–648

McHugh W, McCauley J, Haynes C, Breed C, Schaber G (1988) Paleorivers and geoarchaeology in the Southern Egyptian Sahara. Geoarchaeology 3:1–40

McKenzie J (1993) Pluvial conditions in the eastern Sahara following the penultimate deglaciation: implications for changes in atmospheric circulation patterns with global warming. Palaeogeogr Palaeoclimatol Palaeoecol 103:95–105

McDougall I, Morton WH, Williams MAJ (1975) Age and rates of denudation of Trap Series basalts at Blue Nile gorge, Ethiopia. Nature 254:207–209

Mein P, Pickford M (2010) Vallesian rodents from Sheikh Abdallah, Western Desert, Egypt. Hist Biol 22(1–3):224–259

Mesbah NM, Abou-El-Ela SH, Wiegel J (2007) Novel and unexpected prokaryptic diversity in water and sediments of the alkaline, Hypersaline Lakes of the Wadi An Natrun, Egypt. MicrobialEcology 55(2):369

Moustafa MI (2007) Separation flowsheet for high-purity concentrates of some economic minerals from El Burullus-Baltim sand dunes area, North Coast, Egypt. In: The 5th international conference on the geology of Africa, vol 1, pp 107–124

Motts WS (1969) Geology and hydrology of selected playas in Western United States. Air Force Cambridge Research Lab Report AFCRL-69–0214, 286 pp

Naim G, El Melegy ET,. El Azab A (1993) Black sand assessment. The Egyptian Geological Survey, 67 pp

Neumann K (1989) Holocene vegetation of the Eastern Sahara: charcoal from prehistoric sites. Afr Archaeol Rev 7:97–116

Nicholson SE, Flohn H (1980) African environmental and climatic changes and the general atmospheric circulation in late Pleistocene and Holocene. Clim Change 2:313–348

Nicoll K (2004) Recent environmental change and prehistorichuman activity in Egypt and northern Sudan. Q Sci Rev 23:561–580

Nicoll K, Sallam ES (2017) Paleospring tufa deposition in the Kurkur Oasis region and implications for tributary integration with the River Nile in southern Egypt. J Afr Earth Sc 136:239–251

Nicoll K, Giegengack R, Kleindienst M (1999) Petrogenesis of artifact-bearing fossil-spring tufa deposits from Kharga Oasis, Egypt. Geoarchaeol Int J 14:849–863

Misak RF, Attia S (1983) On the sand dunes of in Sinai Peninsula. Egypt J Geol 27:115–131

Misak RF, Draz MY (1997) Sand drift control of selected coastal and desert dunes in Egypt: case studies. J Arid Environ 35:17–28

Moeyersons J, Vermeersch PM, van Peer P, Thomas DSG, Singhvi AK (2002) Dry cave deposits and their palaeoenvironmental significance during the last 115 Ka, Sodmein Cave, Red Sea Mountains, Egypt. Q Sci Rev 21(7):837–851

Mostafa A (2013) Paleokarst shafts in the Western Desert of Egypt: a unique landscape. Acta Carsologica 42(1):49–60

Osinski GR, Schwarcz HP, Smith JR, Kleindienst MR, Haldemann AFC, Churcher CS (2007) Evidence for a ~200–100 ka meteorite impact in the Western Desert of Egypt. Earth Planet Sci Lett 253:378–388

Osinski GR, Kieniewicz J, Smith JR, Boslough MB, Eccleston M, Schwarcz HP, Kleindienst MR, Haldeman AFC, Churcher CS (2008) The Dakhleh glass: product of an impact airburst or cratering event in the western desert of Egypt. Meteorit Planet Sci 43 (12):2089–2107

Pachur H, Röper H (1984) The Libyan "Western Desert" and Northern Sudan during the late Pleistocene and Holocene. In: Klitzsch E, Said R, Schrank E (eds) Research in Egypt and Sudan, Band 50, Results of the Special Research Project in Arid Areas, Period 1981–1984, Berliner geowissenschaftlicheAbhandlungen, Reihe A, Band, vol 50, pp 249–284

Pachur H-J, Hoelzmann P (2000) Late Quaternary palaeoecology and palaeoclimates of the eastern Sahara. J Afr Earth Sci 30:929–939

Pavlov M (1962) Preliminary report on the ground water beneath the Wadi El-Natrun and adjacent areas. Report to General Desert Development Organization of U.A.R. Desert Institute, Cairo

Pik R, Marty B, Carignan J, Lave J (2003) Stability of the Upper Nile drainage net-work (Ethiopia) deduced from (U–Th)/He thermochronometry: implications for uplift and erosion of the Afar plume dome. Earth Planet Sci Lett 215:73–88

Rapp GR, Hill CL (2006) Geoarchaeology: the earth-science approach to archaeological interpretation. Yale University Press

Pennington BT, Bunbury J, Hovius N (2016) Emergence of civilization, changes in fluvio-deltaic style, and nutrient redistribution forced by Holocene sea-level rise. Geoarchaeol Int J 31(3):194–210
Pennington BT, Sturt F, Wilson P, Rowland J, Brown AG (2017) The fluvial evolution of the Holocene Nile Delta. Q Sci Rev 170:212–231
Philip G, El-Aref MM, Darwish M, Ewais E (1991) Paleoerosion surfaces and karst manifestations including " Egyptian Alabaster" in Gabal Homret Schaibun- Gabal Sannur area, east of the Nile valley, Egypt. Egypt J Geol 34:41–79
Pickford M, Wanas H, Soliman H (2006) Indications for a humid climate in the Western Desert of Egypt 11–10 Myr ago: evidence from Galagidae (Primates, Mammalia). Palaeoecology 5:935–943
Plaziat JC, Montenat C, Orszag-Sperber F, Philobbos E, Purser BH (1990) Geodynamic significance of continental sedimentation during initiation of the NW Sea rift (Egypt). In: Kogbe S, Lang J (eds) Continental sediments in Africa. J Afr Earth Sci, Oxford, 10 (1–2):355–360
Raboul H (1833) Géologie de la Période Quaternaire et Introduction à l'Histoire Ancienne. F.G. Levrault, Paris 222 pp
Rifai RI (2007) Reconstruction of the middle pleistocene climate of South Mediterranean using the Wadi Sannur speleothem, Eastern Desert, Egypt. Carbonates Evaporites 22(1):73–85
Rizzini A, Vezzani F, Cococcetta V, Milad G (1978) Stratigraphy and sedimentation of a Neogene-Quaternary section in the Nile Delta area. Mar Geol 27(3–4):327–348
Renne PR, Schwarcz HP, Kleindienst MR, Osinski GR, Donovan JJ (2010) Age of the Dakhleh impact event and implications for middle stone age archeology in the western desert of Egypt. Earth Planet Sci Lett 291:201–206
Rohling EJ, Marino G, Grant KM (2015) Mediterranean climate and oceanography, and the periodic development of anoxic events (sapropels). Earth-Sci Rev 143:62–97
Rowland JM, Hamdan MA (2012) The Holocene evolution of the Quesna turtleback: geological evolution and archaeological relationships within the Nile Delta. In: Kabacinski J, Chłodnicki M, Kobusiewicz M (eds) Prehistory of Northeastern Africa: new ideas and discoveries. Poznan Archaeological Museum, Poznan, pp 11–24
Said R (1981) The geological evolution of the River Nile. Springer, New York, p 151
Said R (1990) Quaternary. In: Said R (ed) The geology of Egypt, Chapter 25. A A Balkema, Rotterdam
Said R (1993) The River Nile: geology, hydrology and utilization. Pergamon Press, Oxford, p 320
Said R (1998) Sand accumulation and groundwater in the eastern Sahara: A rebuttal to El-Baz F (Episodes, vol 21, no 3). Episodes 21, 287–289
Schweinfurth G (1886) Reise in das Depressions-gebietimUmkreise des FajumimJanuar 1886'. Zeitschrifr der GesellschuftfirErdkundezu Berlin 21:96–149
Selim AA (1974) Origin and lithification of the Pleistocene carbonates of the Salum area, western coastal plain of Egypt. J Sediment Petrol 44:70–78
Sandford KS (1934) Paleolithic man and the Nile Valley in upper and middle Egypt. Chicago University Press, Oriental Publication, vol 3, pp 1–131
Sandford KS, Arkell J (1929) Paleolithic man and the Nile-Fayum Divide. Chicago University Press, Oriental Institute Publication, 1
Sandford KS, Arkell WJ (1939) Paleolithic man and the Nile Valley in Lower Egypt with some notes upon a part of the Red Sea Littoral: a study of the regions during Pliocene and Pleistocene Times. University of Chicago Press, Chicago
Schaber G, McCauley J, Breed C (1997) The use of maltifrequency and polarimetric SIR-C/X-SAR data in the geologic studies of Bir Safsaf. Egypt Remote Sens Environ 59:337–363
Schild R, Wendorf F (1989) The late Pleistocene Nile in Wadi Kubbaniya. In: Wendorf F, Schild R, Close AE (eds) The prehistory of Wadi Kubbaniya, vol 2. Southern Methodist University Press, Dallas, pp 15–100
Shahin M (1985) Hydrology of the Nile Basin. Elsevier, Amsterdam, p 575
Shanahan TM, McKyry KA, Hughen JT, Overpeck B, Otto-Bliesner CW, Heil J King, Scholz CA, Peck J (2015) The time-transgressive termination of the African Humid period. Nat Geosci 8(2):140–144
Shata A, El-Fayoumy I (1967) Geomorphological and morphopedological aspects of the region west of the Nile Delta with special reference to Wadi el Natrun area. Bull Desert Inst 17:1–28
Shortland AJ (2004) Evaporites of the Wadi Natrun: seasonal and annual variation and its implication for Ancient exploitation. Archaeometry 46:497–516
Shukri NM (1950) The mineralogy of some Nile sediments. Q J Geol Soc 105:511–534; 106:466–467
Shukri NM, Philip G, Said R (1956) The geology of the Mediterranean coast between Rosetta and Bardia, part II: Pleistocene sediments Geomorphology and Microfacies. lnst Egypt Bull 37:395–433
Smith JR (2012) Spatial and temporal variation in the nature of Pleistocene pluvial phase environments across North Africa. In: Hublin JJ, McPherron SP (eds) Modern origins: a North African perspective. Springer, New York, pp 35–48
Smith JR, Giegengack R, Schwarcz HP, McDonald MMA, Kleindienst MR, Hawkins AL, Churcher CS (2004) Reconstructing pluvial environments and human occupation through study of the stratigraphy and geochronology of fossil-spring tufas, Kharga Oasis, Egypt. Geoarchaeol Int J (Toronto, Ontario), 19(5):407–439
Smith JR, Kieniewicz JM, Adelsberger KA, HeilChapdelaine V (2006) Reconstructing Pleistocene pluvial phase environments, Western Desert, Egypt, from the geochemistry of authigenic water-lain deposits. Geochimica et Cosmochimica Acta, 70(18), supplement 1, p. A599
Sneh A (1982) Drainage systems of the quaternary in Northern Sinai with emphasis on Wadi El-Arish. Z Geomorph 26:129–185
Sneh A, Weissbrod T, Ehrlich E, Horowitz A, Moshkovitz S, Rosenfeld A (1986) Holocene evolution of the northeast corner of the Nile Delta. Q Res 26:194–206
Stanley DJ (1988) Subsidence in the northeastern Nile Delta: rapid rates, possible causes, and consequences. Science 240:497–500
Stanley DJ (1990) Recent subsidence and northeast tilting of the Nile Delta. Mar Geol 94(1–2):147–154
Stanley JD (2012) New geoarchaeological approaches to assess relative sea-level rise on recently submerged Egyptian and Italian coastal margins. Società Geologica d'Italia
Stanley DJ, Maldonado A (1977) Nile Cone: late quaternary stratigraphy and sediment dispersal. Nature 266:129–135
Stanley JD, Toscano MA (2009) Ancient archaeological sites buried and submerged along Egypt's Nile Delta Coast: Gauges of Holocene delta margin subsidence. J Coastal Res 25(1):158–170; 83
Stanley DJ, Warne AG (1993a) Nile Delta: recent geological evolution and human impact. Science 260(5108):628–634
Stanley DJ, Warne AG (1993b) Sea level and initiation of Predynastic culture in the Nile Delta. Nature 363(6428):435–438
Stanley DJ, Warne AG (1994) Worldwide initiation of Holocene marine deltas by deceleration of sea-level rise. Science 265 (5169):228–231
Stanley DJ, Warne AG, Davis HR, Bernasconi MP, Chen Z (1992) Nile Delta: the late Quaternary north-central Nile Delta from Manzala to Burullus Lagoons. Egypt Natl Geogr Res Explor 8(1):22–51
Sturchio N, Sultan M, El-Alfy Z, Taher AG, El-Maghraby A, El-Anabaawy M (1998) Geochemistry and origin of ground water in the newly reclaimed agricultural lands, western Nile Delta, Egypt: preliminary isotopic results. In: Proceedings 4th international conference geology of the Arab World. Cairo University, Egypt

Sultan M, Sturchio N, Hassan FA, Hamdan MAR, Mahmood AM, Alfy ZE, Stein T (1997) Precipitation source inferred from stable isotopic composition of Pleistocene groundwater and carbonate deposits in the Western Desert of Egypt. Q Res 48:29–37

Swezey C (2001) Eolian sediment responses to late Quaternary climate changes: temporal and spatial patterns in the Sahara. Palaeogeogr Palaeoclim Palaeoecol 167:119–155

Szabo BJ, Haynes CV, Maxwell TA (1995) Ages of quaternary pluvials episodes determined by Uranium-Series and radiocarbon dating of lacustrine deposits of Eastern Sahara. Palaeogeogr Palaeoclimatol Palaeoecol 113:227–242

Taher AG (1999) Inland saline lakes of Wadi El Natrun Depression, Egypt. Int J Salt Lake Res 8:149–169

Taher AG, Abdel-Motelib A (2015) New insights into microbially induced sedimentary structures in alkaline hypersaline El Beida Lake, Wadi El Natrun, Egypt. Geo-Mar Lett 35(5):341–353

Timmermann A, Friedrich T (2016) Late Pleistocene climate drivers of early human migration. Nature 538(7623):92

Tousson O (1922) Mémoire sur les ancienne branches du Nil. Memoire Institut d'Égypte 4:212

Van Neer W (1993) Fish remains from the Last Interglacial at Bir Tarfawi(Eastern Sahara, Egypt). In: Wendorf F, Schild R, Close A (eds) Egypt during the last interglacial, Plenum New York, pp 144–154

Van Peer P, Vermeersch PM, Paulissen E (2010) Taramsa 1: Chert quarrying, lithic technology and human burial at the Palaeolithic site of Taramsa 1, Upper Egypt. Leuven University Press, Leuven

Vermeersch PM (2008) A holocene prehistoric sequence in the Egyptian Red Sea area: the tree shelter. Egyptian Prehistory Monographs, 4

Vermeersch PM, Van Neer W (2015) Nile behaviour and late Palaeolithic humans in Upper Egypt during the late Pleistocene. Q Sci Rev 130:155–167

Vermeersch PM, Van Peer P, Moeyersons J, Van Neer W (1994) Sodmein Cave Site, Red Mountains (Egypt). Sahara 6:32–40

Vermeersch PM, Van Peer P, Moeyersons J, Van Neer W (1996) Neolithic occupation of the Sodmein Area, Red Sea Mountains, Egypt. In: Pwiti G, Soper R (eds) Aspects of African archaeology, papers from the 10th congress of the PanAfrican Association for prehistory and related studies. University of Zimbabwe publications, Harare, pp 411–419

Vermeersch PM, Paulissen E, Vanderbeken T (2002) Nazlet Khater 4. An Upper Palaeolithic underground chert mine. In PM Vermeersch (ed) Paleolithic quarrying sites in Upper and Middle Egypt. Egyptian Prehistoy Monograph, Leuvenm, vol 4, pp 211–271

Vermeersch PM, Van Peer P, Rots V, Paulussen R (2005) A survey of the Bili cave and its surroundings in the Red Sea mountains, El Gouna, Egypt. J Afr Archaeol 3:267–276

Vignard E (1923) Une nouvelle industrie lithique: le "S_ebilien". Bull Inst Fr Archeol Orient 22:1–76

Underwood CJ, King C, Steurbaut E (2013) Eocene initiation of Nile drainage due to East African uplift. Palaeogeogr Palaeoclimatol Palaeoecol 392:138–145

Wali AM, Brookfield ME, Schreiber BC (1994) The depositional and diagenetic evolution of the coastal ridges of northwestern Egypt. Sed Geol 90:113–136

Wanas HA, Pickford Mein MP, Soliman H, Segalen L (2009) Late Miocene karst system at Sheikh Abdallah, between Bahariya and Farafra, Western Desert, Egypt: implications for palaeoclimate and geomorphology. Geologica Acta 7(4):475–487

Warne AG, Stanley DJ (1993) Archaeology to refine Holocene subsidence rates along the Nile Delta margin, Egypt. Geology 21:715–718

Waters CN, Zalasiewicz J, Smmerhayes C (2016) The Anthropocene is functionally and stratigraphically distinct from the Holocene. Science 351:6269

Wendorf F, Schild R (1976) Prehistory of the Nile Valley. Academic Press, New York

Wendorf F, Schild R (1980) Prehistory of the Eastern Sahara. Academic Press, 414 pp

Wendorf F, Schild R (eds) (2001) Holocene settlements of the Egyptian Sahara, vol 1. The archaeology of Nabta playa. Kluwer Academic/Plenum, New York

Wendorf F, Schild R (1986) The geological setting. In: Close AE (ed) The prehistory of Wadi Kubbaniya, volume I: The Wadi Kubbaniya skeleton: a late Paleolithic Burial from Southern Egypt, Southern Methodist University Press, Dallas, Texas, pp 7–32

Wendorf F, Schild R (Assemblers), Close AE (eds) (1989) Prehistory of Wadi Kubbaniya III, Southern Methodist University Press, Dallas, Texas

Wendorf F, Schild R, Close A (eds) (1993) Egypt during the late interglacial. Plenum, New York, p 596

Williams MAJ, Williams FM, Duller GAT, Munro RN, El Tom OAM, Barrows TT, Macklin MG, Woodward JC, Talbot MR, Haberlah D, Fluin J (2010) Late Quaternary floods and droughts in the Nile valley, Sudan: new evidence from optically stimulated luminescence and AMS radiocarbon dating. Q Sci Rev 29:1116–1137

Williams MAJ, Duller GAT, Williams FM, Woodward JC, Macklin MG, El Tom OAM, Munro RN, El Hajaz Y, Barrows TT (2015) Causal links between Nile floods and eastern Mediterranean sapropel formation during the past 250 kyr confirmed by OSL and radiocarbon dating of Blue and White Nile sediments. Q Sci Rev 130:89–108

Woodward JC, Macklin MG, Krom MD, Williams MAJ (2007) The Nile: evolution, quaternary river environments and material fluxes. In: Gupta A (ed) Large rivers: geomorphology and management. Wiley and Sons, Ltd

Wysocka A, Welc F, Czarniecka U (2016) Sedimentary environment of the early Pleistocene gravels of the edfu formation from the Saqqara archaeological site (Egypt)—preliminary results. Studia Quat 33 (1):69–78

Youssef AM, El-Shater A, El-Khashab MH, El-Haddad BA (2018) Karst induced geo-hazards in Egypt: case study slope stability problems along some selected desert highways. In Wasowski J et al (eds) Engineering geology and geological engineering for sustainable use of the earth's resources, urbanization and infrastructure protection from geohazards, sustainable civil infrastructures. Springer International Publishing AG, pp 149–164

Zaki A, Giegengack R (2016) Inverted topography in the southeastern part of the Western Desert of Egypt. J Afr Earth Sci 121:56–61

Zaki AS, Pain CF, Edgett KS, Giegengack R (2018) Inverted stream channels in the Western Desert of Egypt: synergistic remote, field observations and laboratory analysis on Earth with applications to Mars. Icarus 309:105–124

Zittel K (1883) Beitrae zur Geologie und Palaeontologie der Libyschen Wuste. Fischer, Cassel